Development of Novel Quantitative Methods for Monitoring Neurodegenerative Phenotypes in Niemann-Pick Disease Type C Mice



Hsin Tsung Chen

Wolfson College

University of Oxford

A thesis submitted for the degree of

Doctor of Philosophy

Acknowledgements

I would like to express my greatest gratitude to my supervisor, Prof. Frances Platt, for giving me the opportunity four years ago to work in her lab at the Department of Pharmacology, at the University of Oxford. I would like to thank her for all her support and trust to innovate and complete my new behavioural assessment methods. I would also like to thank Prof. Mario Cortina Borja at University College London for his guidance, support and inspiration with statistics and programming (R). He taught me analytic thinking to analyse data rigorously. My thanks also go out to everyone in Fran's lab, particularly Ecem, Reuben and Maria. Many other members of the Platt lab have helped me over the years including Allie, Carla, Kerri, Dave, David, Claire, Danielle and Yuzhe and for all their invaluable help.

I would particularly like to thank the Wu family in Taiwan, whose children Yixin Wu and Yinuo Wu were both diagnosed with the Niemann-Pick Type C disease. I thank the children as well as their parents Jinhui Wu and Lilin Zhou for befriending me and allowing me to spend time with the children, which ultimately led me to research lysosomal storage disorders. They are the source of my inspiration, empathy and compassion and my main motivation behind my commitment to Niemann-Pick Disease type C research.

I would also like to thank multiple Niemann-Pick family associations, especially Niemann-Pick UK (NPUK), NPSuisse and Niemann-Pick Research Foundation (NPRF), and the Taiwanese government for sponsoring my studies.

My love goes out to my wife Daisy and my family for their support and encouragement. Finally, I would like to thank my God for all the opportunities, directions, resources, and lovely people I have encountered during my PhD as without them this project would not exist.

Hsin Tsung Chen
Wolfson College, Oxford
06 January 2023

Abstract

A hallmark of neurodegenerative diseases, such as the rare monogenic lysosomal storage disease, Niemann-Pick disease type C (NPC), is motor dysfunction. Therefore, gait analysis is frequently used in pre-clinical and clinical studies. The Catwalk system is an automated instrument that collects gait data from rodents. The system captures data on 495 variables. However, there is currently no standard process to identify disease relevant variables or indeed analyse these variables. Therefore, researchers report only a subset of Catwalk data based on assumptions, hypotheses, or the level of statistical significance. Thus, highly relevant variables might be overlooked, and this might lead to misleading or ill-informed conclusions to be drawn. In addition, any disease model that results in reduced body weight (e.g., *Npc1* $^{-/-}$ mice) results in weak paw print signals in the Catwalk system, which will affect the quality and quantity of the data. In this thesis, I have therefore innovated a new standard process, the Evidence Based Gait Analysis Method, that not only optimises the quality and the quantity of the data but also provides a systematic unbiased basis for selecting relevant variables. Cerebellar ataxia is a key feature in *Npc1* $^{-/-}$ mice and results from the loss of Purkinje cells in the cerebellum. The Catwalk system can detect this trait as it generates paw-oriented variables. However, these variables are insufficient to describe the whole picture of the ataxia these mice display, particularly the angle of deviation from movement in a straight trajectory. Thus, an additional walking path method was developed to complement the gait analysis method. The walking path was tracked using DeepLabCut (DLC), a deep learning algorithm, using videos recorded by the Catwalk system. The paths were analysed in four aspects, namely velocity, X-direction, Y-direction, and angular rotation. This can capture the walking phenotype of mice and the interpretation of the result is therefore straightforward. Together, these two new methods offer for the first time a detailed evaluation of gait performance underpinned by robust statistical evidence and so is a potential game changer in this field. I have applied this new and innovative approach to analysing changes in gait in two mouse models of NPC disease either untreated or treated with single or combination therapies and the data generated allow us for the first time to study in detail the differential responses of the disease to different treatments. We anticipate that this will form the basis for the rational selection of optimal combination therapies for clinical application in the future.

Contents

List of Figures vii

List of Tables x

List of Abbreviations xii

1 Introduction 1

1.1 Lysosomes . . . 2
1.2 Lysosomal storage disorders . . . 3
1.3 Niemann-Pick diseases . . . 4
1.4 NPC disease models . . . 7
1.5 *Npc1*$^{-/-}$ murine models . . . 7
1.5.1 *Npc1*^{nih} mouse model . . . 8
1.5.2 *Npc1*^{nmf164} mouse model . . . 9
1.6 Treatments . . . 10
1.6.1 Miglustat . . . 10
1.6.2 Arimoclomol . . . 11
1.6.3 Acetyl-DL-leucine . . . 13
1.7 Behavioural assessment: gait analysis . . . 14
1.8 Literature review of gait analysis using the Catwalk system . . . 14
1.9 Thesis outline . . . 16

2 Evidence Based Gait Analysis Method 18

2.1 Introduction . . . 18
2.2 Materials and Methods . . . 20
2.2.1 Animal Models (*Npc1*^{nih} and *Npc1*^{nmf164}) . . . 20
2.2.2 Evidence Based Gait Analysis Method (EBGAM) . . . 21
2.2.3 The definition of variables and statistics . . . 31
2.3 Results . . . 32
2.3.1 The summary of the data set . . . 32

2.3.2 Impacts of disease progression on gait . . . 34
2.3.3 The results of Evidence Based Variable Analysis (EBVA) . . 38
2.4 Discussion . . . 47
2.4.1 Neuropathology and motor behaviours . . . 47
2.4.2 The Evidence Based Gait Analysis Method (EBGAM) . . . 47
2.4.3 The characterization of NPC models by Evidence Based Variable Analysis . . . 48

3 Catwalk data analysis of *Npc1*$^{-/-}$ mice treated with miglustat, the HSP70 inducing drug (arimoclomol) or a combination of both 51
3.1 Introduction . . . 52
3.2 Materials and Methods . . . 53
3.2.1 Animal model . . . 53
3.2.2 Treatments . . . 53
3.2.3 The Evidence Based Gait Analysis Method . . . 54
3.2.4 Data presentation . . . 55
3.2.5 Statistical analysis environment . . . 55
3.2.6 The definition of variables and statistics . . . 55
3.3 Results . . . 55
3.3.1 The summary of the data set . . . 55
3.3.2 The results of Evidence Based Variable Analysis . . . 57
3.3.3 Treatments results . . . 61
3.3.4 The summary of treatments . . . 72
3.3.5 Improvement Scores . . . 75
3.4 Discussion . . . 78
3.4.1 The results of EBVA . . . 78
3.4.2 The effects of treatments . . . 79

4 Catwalk data analysis of Acetyl-DL-leucine (Tanganil) study 82
4.1 Introduction . . . 82
4.2 Materials and Methods . . . 84
4.2.1 Animal Model . . . 84
4.2.2 Treatments . . . 84
4.2.3 The Evidence Based Gait Analysis Method . . . 84
4.3 Results . . . 85
4.3.1 The summary of data set . . . 85

4.3.2 The results of Evidence Based Variable Analysis 85
4.3.3 Comparison of data from wild type and *Npc1*^{nih} cohorts . . . 89
4.3.4 Treatments results 95
4.4 Discussion 100
4.4.1 The results of EBVA across chapters 100
4.4.2 The limitation of the Catwalk system 101

5 Walking path analysis **103**
5.1 Introduction 103
5.2 Materials and Methods 105
5.2.1 Animal model 105
5.2.2 Treatments 105
5.2.3 Walking path analysis (WPA) 105
5.3 Results 119
5.3.1 Summary of the data set 119
5.3.2 The reference points of a mouse 120
5.3.3 The velocity 121
5.3.4 X direction variables 122
5.3.5 Y direction variables 124
5.3.6 Rotating angle variables 125
5.3.7 The summary of treatments 128
5.4 Discussion 129

6 General Discussion and Future Plans **131**
6.1 Future directions 135

Appendices

A Appendix **137**
A.1 The definition of variables and statistics 137
A.2 The categories of variables in the Catwalk system 145

References **148**

List of Figures

1.1 Schematic diagram of a lysosome. 3
1.2 Schematic diagram of the NPC1 protein. 5
1.3 Progression of systemic and neurological symptoms in Niemann-Pick Type C disease. 6
1.4 Mechanism of action of miglustat 11
1.5 Mechanism of action of arimoclomol 13

2.1 Evidence Based Gait Analysis Method (EBGAM) 22
2.2 The Catwalk device. 23
2.3 An example of study verification as part of the data cleaning process 24
2.4 Example of data segmentation. 25
2.5 Examples of threshold adjustment. 26
2.6 Example of paw print adjustments. 26
2.7 Example of paw signal optimization. 27
2.8 The categories of variables in the Catwalk data. 28
2.9 Coordination-related variable summarization. 30
2.10 The results of unpaired t-test in the model of *Npc1*^{nih}. 35
2.11 The results of unpaired t-test in the model of *Npc1*^{nmf164}. 36
2.12 The relevant physical-related variables in the model of *Npc1*^{nih}. . . . 40
2.13 The relevant physical-related variables in the model of *Npc1* ^{nmf164}. . 41
2.14 The relevant coordination-related variables were found to be modified in the *Npc1*^{nih} model. 43
2.15 The relevant coordination-related variables were found to be modified in the *Npc1*^{nmf164} model. 44

3.1 The relevant physical-related variables were found to be modified in the *Npc1*^{nih} model in (A) paw-wise and (B) non-paw-wise variables in the arimoclomol study. 58
3.2 The relevant coordination-related variables were found to be modified in the *Npc1*^{nih} model in the arimoclomol study. 60

3.3 Heatmap of the results from one-way ANOVA and post hoc analysis in paw-wise variables in *Npc1^{nih}* with miglustat therapy. 64
3.4 Heatmap of the results from one-way ANOVA and post hoc analysis in paw-wise variables in *Npc1^{nih}* with arimoclomol therapy. 65
3.5 Heatmap of the results from one-way ANOVA and post hoc analysis in paw-wise variables in *Npc1^{nih}* with combination therapy. 66
3.6 Heatmap of the results from one-way ANOVA and post hoc analysis in non-paw-wise variables in *Npc1^{nih}*. 67
3.7 Heatmap of the results from one-way ANOVA and post hoc analysis in Coordination-related variables. 71
3.8 The behavioural scores of physical-related variables. 76
3.9 The behavioural scores of coordination-related variables. 77

4.1 The relevant physical-related variables were found to be modified in the *Npc1^{nih}* model in (A) paw-wise and (B) non-paw-wise variables. 87
4.2 The relevant coordination-related variables found to be modified in the *Npc1^{nih}* model. 89
4.3 Venn diagram of relevant variables across chapters. 91
4.4 The overlapping physical-related variables in (A) paw-wise and (B) non-paw-wise variables in the model of *Npc1^{nih}*. 93
4.5 The overlapping Coordination-related variables in the model of *Npc1^{nih}*. 94
4.6 Heatmap of the results from one-way ANOVA and post hoc analysis in (A) paws-wise and (B) non-paw-wise variables (B) variable. . . . 97
4.7 Heatmap of the results from one-way ANOVA and post hoc analysis in Coordination-related variables. 99

5.1 Walking Path Analysis (WPA). 106
5.2 Summary of DLC training process in the protocol. 107
5.3 Example of anatomical labels. 107
5.4 The loss function curve in DeepLabCut training. 108
5.5 Example of non-walking behaviour in a run. 109
5.6 Example of removing stationary behaviours in a run. 110
5.7 Examples of the walking path of a wild-type mouse. 111
5.8 Summary of variables in walking path analysis. 112
5.9 X-coordinate against time. 113
5.10 Y-coordinate against time. 115
5.11 Y-coordinate against time with cycle and amplitude. 116

5.12 Example of rotating angle (θ). 117
5.13 Rotating angle against time with cycle and amplitude variables. . . 118
5.14 The results of group comparison in velocity. 121
5.15 Plots of X coordinate against time. 122
5.16 The results of group comparison in X direction variables. 123
5.17 The results of group comparison in Y direction variables. 124
5.18 The results of group comparison in Y direction cycle and amplitude. 125
5.19 The results of group comparison in rotating angle variables. 126
5.20 The results of group comparison in rotating angle cycle and amplitude variables between studies. 127

A.1 Three main categories of step sequences. 138
A.2 Example of RH->LH Phase Dispersions and Couplings. 140
A.3 Example of stance variables. 144

List of Tables

1.1 Niemann-Pick diseases summary. 4
1.2 Summary of *Npc1* murine models. 8

2.1 Study plan summary. 20
2.2 The summary of $Npc1^{nih}$ data set. 32
2.3 The summary of $Npc1^{nmf164}$ data set. 33
2.4 The number of trials in groups between models. 33
2.5 The number and percentage of variables show significant differences between WT and Hom untreated groups in $Npc1^{nih}$ model 37
2.6 The number and percentage of variables show significant differences between WT and Hom untreated groups in $Npc1^{mnf164}$ model 38
2.8 The EBVA results of physical-related variables between models. . . 42
2.9 The number and percentage of coordination-related variables selected by EBVA in both models. 45
2.10 The EBVA results of coordination-related variables between models. 46

3.1 The data summary of the arimoclomol study. 56
3.2 The number of trials between groups. 56
3.3 The number of relevant physical-related variables selected by EBVA. 57
3.4 The number of relevant coordination-related variables selected by EBVA before summarization. 59
3.5 The number of relevant coordination-related variables selected by EBVA after summarization. 59
3.6 The summary of the number and percentage of variables showing either improvement or deterioration effects between treated groups in physical-related variables. 61
3.7 The summary of the number and percentage of variables showing either improvement or deterioration effects between treated groups in coordination-related variables before summarization. 68

3.8 The summary of the number and percentage of variables showing either improvement or deterioration effects between treated groups in coordination-related variables after summarization. 69
3.9 The summary results of physical-related variables between therapies. 73
3.10 The summary results of coordination-related variables between therapies. 74

4.1 The number of trials between groups. 85
4.2 The number and percentage of relevant physical-related variables selected by EBVA. 86
4.3 The number of relevant coordination-related variables selected by EBVA before summarization. 88
4.4 The number of relevant coordination-related variables selected by EBVA after coordination-related variable summarization. 88
4.5 The number of trials and time points between Chapters 2 and 4. . . 90
4.6 The number of relevant variables and the percentage of overlapping variables in *Npc1*^{nih} mouse model selected by EBVA between Chapter 2 and Chapter 4. 92
4.7 The top 10 overlapped variables in *Npc1*^{nih} mouse model across chapters. 95
4.8 Summary of the number and percentage of physical-related variables shown improvement and deterioration effects relative to*Npc1* null mice at 8 weeks of age. 96
4.9 Summary of the number and percentage of coordination-related variables shown either improvement or deterioration effects relative to*Npc1* null mice at 8 weeks of age after variable summarization. . . 98

5.1 The number of trials/mice and runs used for each group at 8 weeks of age. 119
5.2 The number of significant variables between WT and Hom groups in different body points of mice. 120
5.3 The summary of WPA results between groups. 128

6.1 Summary of the advantages of the novel methods innovated in this thesis. 134

A.1 The catergories of variables. 145
A.2 continued to Table A.1 146
A.3 continued to Table A.1 147

List of Abbreviations

NPA . . . . . Niemann-Pick disease Type A

NPB . . . . . Niemann-Pick disease Type B

NPC . . . . . Niemann-Pick disease Type C

ALS . . . . . Amyotrophic lateral sclerosis

ADM . . . . . Acid sphingomyelinase

CLEAR . . . . Coordinated Lysosomal Expression and Regulation

TFEB . . . . . The transcription factor EB

LAL . . . . . Lysosomal acid lipases

VSGP . . . . . Vertical supranuclear gaze palsy

MaLR . . . . . Mammalian apparent LTR-retrotransposon

sIBM . . . . . Sporadic inclusion body myositis

ANOVA . . . . Analysis of variance

Tukey HSD . Tukey Honestly Significant Difference

SFI . . . . . Sciatic Functional Index

IDA . . . . . Initial data analysis

SD . . . . . Standard deviation

CV . . . . . Coefficient of variation

HSP70 . . . . . Heat shock protein 70

HSPs . . . . . Heat shock proteins

NPCCSS . . . Niemann-Pick Type C Clinical Severity Scale

Mig . . . . . Miglustat

Arim . . . . . Arimoclomol

Comb . . . . . The combination of miglustat and arimoclomol

DLC . . . . . DeepLabCut

ADLL . . . . . Acetyl-DL-leucine

ADL . . . . . Acetyl-D-leucine

ALL . . . . . Acetyl-L-leucine

WPA . . . . . Walking Path Analysis

EBGAM . . . Evidence Base Gait Analysis Method

EBVA . . . . . Evidence Base Variable Analysis

GSL . . . . . Glycosphingolipid

IV . . . . . Irrelevant variable

AD . . . . . Absent data

FP . . . . . Front paw

HP . . . . . Hind paw

RF . . . . . Right front paw

RH . . . . . Right hind paw

LF . . . . . Left front paw

LH . . . . . Left hind paw

1 Introduction

Contents

1.1 Lysosomes 2
1.2 Lysosomal storage disorders 3
1.3 Niemann-Pick diseases 4
1.4 NPC disease models 7
1.5 *Npc1*$^{-/-}$ murine models 7
1.5.1 *Npc1*^{nih} mouse model 8
1.5.2 *Npc1*^{nmf164} mouse model 9
1.6 Treatments 10
1.6.1 Miglustat 10
1.6.2 Arimoclomol 11
1.6.3 Acetyl-DL-leucine 13
1.7 Behavioural assessment: gait analysis 14
1.8 Literature review of gait analysis using the Catwalk system 14
1.9 Thesis outline 16

1.1 Lysosomes

The lysosome is a specialized acidic cellular organelle responsible for the catabolism of endogenous and exogenous macromolecules and the recycling of their monomeric elements [1]. It contains multiple enzymes that act on different biochemical classes of macromolecules. For example, Lysosomal Acid Lipases (LAL) hydrolyse and endogenous lipids in lysosome from endocytosis or autophagy [2, 3], sulfatases catalyse the hydrolysis of glycosaminoglycans and sulphated hormones [4, 5] and nucleases degrade RNA and DNA from RNautophagy or DNautophagy [6] (Fig. 1.1). This organelle is involved in multiple additional key cellular functions including nutrient sensing, energy metabolism, the response to stimuli, calcium signalling and lipid homeostasis [1, 7, 8]. Lysosomes fuse with autophagosomes and the autophagic pathway is regulated by the Coordinated Lysosomal Expression and Regulation (CLEAR) gene network [9] regulated in turn by the transcription factor EB (TFEB) and TFE3, which also regulates lysosome biogenesis and function [10]. Lysosomes are highly dynamic and form contact sites with other organelles, such as mitochondria and the endoplasmic reticulum (ER) [11]. These contact sites regulate cellular signalling and homeostasis [12–14]. There are more than 300 membrane proteins within the limiting membrane of the lysosome. Some membrane proteins are to maintain lysosomal function, such as pH balance and inter-organelle trafficking, however, most of their functions remain unknown [15, 16]. There are some ion channels identified to maintain the ion balance, including Ca^{2+}, Na^{+}, K^{+}, Zn^{2+}, H^{+} and Fe^{2+} channels in the lysosome [8] (Fig. 1.1).

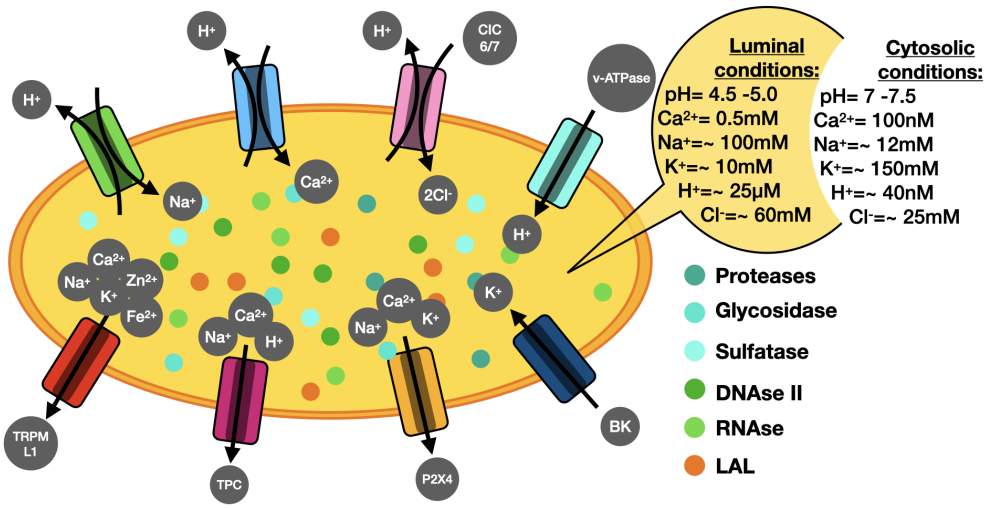


Figure 1.1: Schematic diagram of a lysosome. Modified from reference[8]
The lysosome contains soluble hydrolytic enzymes, including proteases, lysosomal acid lipase (LAL), glycosidases, sulfatases, and Nucleases (DNAse II and RNAse). Lysosomal ion channels and transporters include vATPase, vocuolar H^+-ATPase(proton pump),chloride channel (ClC), K^+ channels (BK), $Ca^{2+}/Na^+/K^+/Zn^{2+}/Fe^{2+}$ non-selective cation channels (TRPML: transient receptor potential cation channel), P2X4 channel, TPC (two-pore channel), Na^+/H^+ excahngers and Ca^{2+}/H^+ exchanger.

1.2 Lysosomal storage disorders

Lysosomal storage disorders (LSDs) are a group of over seventy inherited metabolic disorders. Since the lysosome is the catabolic and recycling centre of the cell [1], the dysfunction of lysosomes results in the accumulation of undegraded macromolecules [17]. The so-called 'storage' macromolecules vary between LSDs depending on the specific defective protein. Most LSDs result from inherited defects in lysosomal enzymes. For example, the mutations in the *HEXB* gene cause dysfunction of β-hexosaminidase resulting in Sandhoff disease and subsequently leading to GM2 ganglioside accumulation [18]. This lipid storage contributes to a multimorbidity condition with multiple organs developing pathology, most notably the brain.

1.3 Niemann-Pick diseases

The Niemann-Pick diseases are a subgroup of lysosomal storage diseases (LSDs). They were first described by Albert Niemann and Ludwig Pick [19]. There are three main subgroups, namely Niemann-Pick disease Type A (NPA), Niemann-Pick disease Type B (NPB) and Niemann-Pick disease Type C (NPC) [20] (Table 1.1). NPA and NPB are caused by a mutation in the *SMPD1* gene that encodes the lysosomal hydrolase, acid sphingomyelinase (ASM) leading to the storage of sphingomyelin [21]. The difference between NPA and NPB is the levels of residual ASM activity. NPB has higher residual enzyme levels than NPA. NPA patients, therefore, suffer early onset severe pathology, including hepatosplenomegaly, progressive neurodegeneration, and premature death. The manifestations in NPB patients are milder and do not involve the brain. These patients can survive into late adulthood[22]. An enzyme replacement therapy for acid sphingomyelinase diseases (NPA and NPB) has shown great promise in clinical trials [23] and has recently been approved in some countries, such as Japan, the EU, and the USA [24].

Names	Gene mutation	Lipids that accumulate	Primary phenotype
NPA	*SMPD1* (< 1% enzyme activity)	Sphingomyelin	Neurological and peripheral
NPB	*SMPD1* (< 10% enzyme activity)	Sphingomyelin	Peripheral organ enlargement
NPC	*NPC1* or *NPC2*	Unesterified Cholesterol and sphingolipids	Neurological and peripheral

Table 1.1: Niemann-Pick diseases summary.
Modified from referenc [22]
NPA : Niemann-Pick Type A; NPB : Niemann-Pick Type B;
NPC : Niemann-Pick Type C

NPC was historically classified with the Niemann-Pick diseases as it also involves the storage of sphingomyelin. However, it is not a lysosomal enzyme deficiency and has a more complex pathophysiological basis. This thesis focuses exclusively on NPC. It is caused by a mutation in either the *NPC1* or *NPC2* genes. The majority of NPC patients have an *NPC1* mutation (95%) and only 5% of patients result

from an *NPC2* mutation [25, 26]. The *NPC1* and *NPC2* genes encode the NPC1 and NPC2 proteins respectively. The NPC2 protein is a soluble cholesterol-binding protein in the lumen of late endosomes and lysosomes and comprises 132 amino acids [26, 27]. The NPC1 protein is a large transmembrane protein with 1,278 amino acids located in the limiting membrane of late endocytic compartments [26]. A schematic representation of NPC1 protein is in Fig. 1.2.

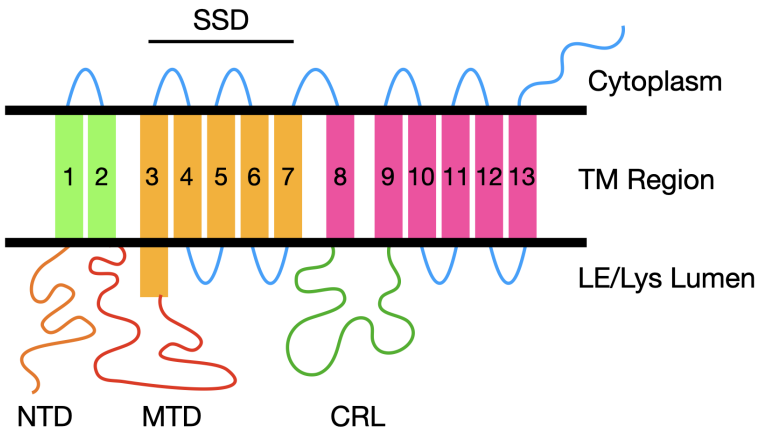


Figure 1.2: Schematic diagram of the NPC1 protein. Modified from reference [28]. NTD: N-terminal domain; MLD: middle luminal domain; SSD: sterol-sensing domain; CRL: Cysteine-rich loop.

There are two potential theories about NPC1 protein function. The first is that NPC1 is a cholesterol transport protein that effluxes low-density lipoprotein-derived cholesterol out of the lysosome in cooperation with the NPC2 protein [29]. The other theory is that the NPC1 protein is a cholesterol-regulated transporter of multiple lipids [30]. Mutations in both genes lead to an identical clinical disorder and involve the accumulation of multiple classes of lipids, including unesterified cholesterol, glycosphingolipids, sphingomyelin, and sphingosine [31]. NPC is variable in terms of age of onset, lifespan, and symptoms [26]. NPC involves systemic and neurological pathology (summarized in Fig. 1.3).

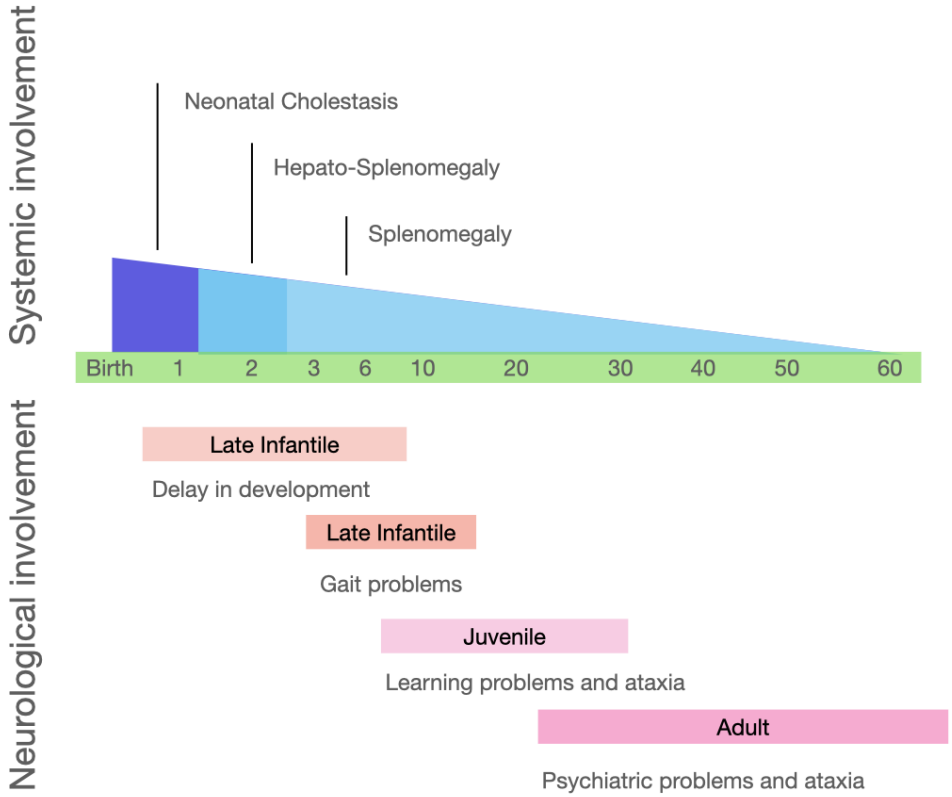


Figure 1.3: Progression of systemic and neurological symptoms in Niemann-Pick Type C disease. Modified from reference[32]

Patients with early clinical onset have a more rapid rate of disease progression relative to the later onset forms and can present in the neonatal period with cholestatic jaundice due to transient liver disease (Fig. 1.3) [20]. The systemic symptoms are not found in every diagnosed patient, but neurological symptoms develop in all NPC patients. NPC patients have vertical supranuclear gaze palsy (VSGP) [33], ataxia, dystonia, and seizures [34]. These symptoms greatly reduce the quality of life for patients and their families. Patients can also have psychiatric symptoms and experience gradual progression to cognitive decline and dementia [35]. Histopathology reveals that NPC patients develop hallmarks associated with Alzheimer's disease (plaques and tangles) regionally distributed in areas of highest lipid storage [36].

1.4 NPC disease models

NPC models are essential tools for studying the pathophysiology of NPC and for evaluating therapies. They recapitulate key features of the human NPC and have been used for discovering disease mechanisms and for developing treatments. The disease models for a study depend on the aims of the study and the results should be able to extrapolate to humans [37]. Most NPC models are of *Npc1* deficiency. There are non-mammalian and mammalian models. Non-mammalian models include plants [38], yeast [39], nematodes [40], fruit fly [41] and zebrafish [42, 43]. These models are used to investigate disease pathways, molecular mechanisms and NPC1 protein interactions [37]. As the genetic manipulation of these models is relatively simple, they are preferred models for drug discovery [44]. There are limited mammalian models used in NPC research, including murine [44], feline [45], canine [46] and bovine [47]. The number of NPC publications using mouse models is the greatest among other models, such as cat, yeast, worm, and fly models [37]. Moreover, there are advantages to the use of the mouse model, including short generation time, well-established genetic manipulation, and wide availability [48]. This thesis focuses on NPC murine models, which will be described in the following sections.

1.5 *Npc1*$^{-/-}$ murine models

At present, there are a number of *Npc1* mouse models with either spontaneous or engineered *Npc1* mutations (Table 1.2). The mutational differences between the mouse models lead to specific characteristics in each model. According to the activity of the Npc1 protein in these models, they can be roughly classified as a complete lack of Npc1 function and partial Npc1 function [37].

Names	Mutation	Features
$Npc1^{nih}$	MaLR retrotransposon insertion	Similar to infantile onset form of the human disease
$Npc1^{spm}$	c.2911 + 3A>C	Similar to infantile onset form of the human disease
$Npc1^{pf/pf}$	c.604C>G; c.607-608TT>GC	Similar to infantile onset form of the human disease
$Npc1^{nmf164}$	c.3163A>G	Adult onset form NPC patients
$Npc1^{I1601T}$	c.3179T>C	The most common human *NPC* mutation.
$Npc1^{imagine}$	c.1554- 1009G>A	Similar to $Npc1^{nih}$
$Npc1^{pioneer}$	c.1920delG	Similar to $Npc1^{nih}$
$Npc1^{em1pa}$	CRISPR-Cas	Specific mutation
$Npc1^{tm1.1Apl}$	Cre/loxP	Cell-specific

Table 1.2: Summary of *Npc1* murine models. Modified from reference[44]

The models of $Npc1^{nih}$[49, 50], $Npc1^{spm}$ [51] and $Npc1^{pf}$ [52] have no functional Npc1 protein and have early onset disease. They are characterized by hepatomegaly, low body weight, and motor impairment. Although $Npc1^{nih}$ in this class is the standard model in the field, there is only a small fraction (about 5%) of patients with truncation mutations [53]. On the other hand, there are approximately 20% of NPC patients with partial loss of NPC1 function [26, 44]. In this category, there are the $Npc1^{nmf164}$, and $Npc1^{I106T}$ models. The mice from these two models have slower disease progression, less severe symptoms, and a longer life span than the model of $Npc1^{nih}$. $Npc1^{Imagine/Imagine}$, $Npc1^{Pioneer/Pioneer}$ and $Npc1^{Imagine/Pioneer}$ models carrying specific human NPC mutation were reported in 2017 [54]. The onset and progression of the disease are similar to early onset models. With advances in genome editing tools, $Npc1^{em1pav}$ was generated by CRISPR-Cas to investigate the impacts of specific mutations [55]. The $Npc1^{tm1.1Apl}$ mice created by the Cre/loxP technique are used to determine the cell-specific effects of elimination of *Npc1*, such from Purkinje cells [56–58]. In this thesis, we evaluate potential treatments on behavioural aspects, focusing on gait analysis. We used two murine models, $Npc1^{nih}$ (representing the acute form of NPC) and $Npc1^{nmf164}$ (similar to the juvenile form of the disease). In the following sections, these two models will be introduced.

1.5.1 $Npc1^{nih}$ mouse model

Currently, the $Npc1^{nih}$ mouse on a BALB/c background is the standard model in the field [44]. This model is a spontaneous mutant that arose in the 1980s in a BALB/c

colony at the NIH. It has a neurodegenerative course and reduced activity of sphingomyelinase and glucocerebrosidase with cholesterol and sphingolipid storage, locomotor impairment and weight loss [50, 59]. It was initially thought to be a model of Gaucher disease and then later Niemann-Pick A [19] but after further research it was revealed to have elevated free unesterified cholesterol in the null mice [60]. In 1997, Loftus identified the mutant mice as an NPC model by an integrated human-mouse positional candidate approach [49]. The *Npc1* gene is mutated with an 824bp insertion of retrotransposon sequence, the mammalian apparent LTR-retrotransposon (MaLR) [49]. The mutation results in NPC1 protein truncation before the Sterol-Sensing domain and 11 of the 13 transmembrane domains [49]. It generally recapitulates well the human neuropathology and has the same cellular abnormalities reported in patients' tissues, such as accumulation of free cholesterol, glucosylceramide, lactosylceramide, sphingomyelin, sphingosine, and gangliosides (GM2 and GM3) in various organs [44]. Disease progression is similar to infantile-onset disease in humans with an early onset of clinical signs and rapid progression. The average lifespan is 74 days [61]. There are discernible behavioural changes including ataxic gait and tremor present by 5-6 weeks of age and motor dysfunction becomes apparent at 7-8 weeks of age as a progressive cerebellar ataxia [61, 62].

1.5.2 *Npc1^{nmf164}* mouse model

This model was engineered by the Jackson Laboratory [61]. The *Npc1^{nmf164}* mice have a point mutation resulting in a D1005G mutation in the cysteine-rich luminal loop of the NPC1 protein, where about one-third of human NPC1 mutations are located [26, 53]. The mutant NPC1 protein is misfolded, highly unstable, and prematurely degraded in the endoplasmic reticulum [63, 64]. The phenotypes of *Npc1^{nmf164}* are similar to *Npc1^{nih}* mice but in general *Npc1^{nmf164}* mice have less severe symptoms and slower diseases progression than is observed in *Npc1^{nih}* mice [61]. The different severity of disease progression is related to the partial loss of functional NPC1 protein compared to the null model [65]. The average life span of *Npc1^{nmf164}* on a C57BL/6J background is 112 days and weight loss are observed around 9-10

weeks of age, compared to 6-7 weeks of age in *Npc1^{nih}* on a BALB/c background [61]. The motor function decline begins at 11 weeks of age in the inverted cling cage lid test [61]. The disease progression resembles human juvenile onset NPC with slower progression and longer life span than the *Npc1^{nih}* model [44, 61].

1.6 Treatments

Although there is no cure for NPC, stabilizing or slowing disease progression can be achieved. Currently, the only approved therapy is a substrate reduction therapy drug, miglustat [66]. Miglustat treatment improves neurologic manifestations in NPC and improves life span [67]. Other small molecule therapies have also been evaluated in clinical trials, including 2-hydroxypropyl-beta-cyclodextrin (ClinicalTrial.gov identifierNCT03471143/NCT04860960/NCT03893071/NCT02534844), acetyl-L-leucine (ClinicalTrial.gov identifier: NCT05163288/NCT03759639) and arimoclomol (ClinicalTrial.gov identifier: NCT02612129). In this thesis, miglustat, arimoclomol and acetyl-DL-leucine have been studied.

1.6.1 Miglustat

N-butyldeoxynojirimycin (miglustat, Zavesca™) is currently the only licensed treatment for NPC [66]. Miglustat is a small iminosugar drug that reversibly inhibits ceramide glucosyltransferase that catalyses the first step in glycosphingolipid (GSL) biosynthesis (see Fig. 1.4) [68]. It crosses the blood-brain barrier which enables it to treat neurological diseases in the brain [69]. There are studies showing the benefits of miglustat in the reduction of GSL accumulation in neurons, delayed neurological diseases progression and increased life span in NPC animal models [70–72]. In clinical use, the therapeutic benefits of miglustat on neurological signs become stable after 6 - 12 months of treatment [73]. This slowing in the rate of progression can be observed in ambulation, fine motor skills, language, and swallowing. About 70% of NPC patients on continuous miglustat treatment had improved or stable disease in at least 3 out of 4 disable scales (ambulation, manipulation, language and

swallowing) and extension of life span by 10 years over 8 years of observation [74]. The major side effects of miglustat, which is the most common reason for stopping treatment [75], are gastrointestinal disturbances, including diarrhoea and flatulence. Miglustat inhibits the digestion of starch [76, 77] and the undigested saccharides create a significant osmotic gradient within the gastrointestinal (GI) tract [77]. The high osmotic gradient attracts water and electrolytes into the small intestine and causes diarrhoea [78]. Eighty per cent of NPC patients taking miglustat experience mild to moderate weight loss in the first 6 months of treatment [75]. Taking anti-propulsive medication (loperamide), dietary modification (low-carbohydrate diet) and probiotics are suggested to ameliorate GI discomforts during miglustat treatment [75]. Despite this, compliance in NPC is good as these symptoms typically resolve within one month of commencing treatment.

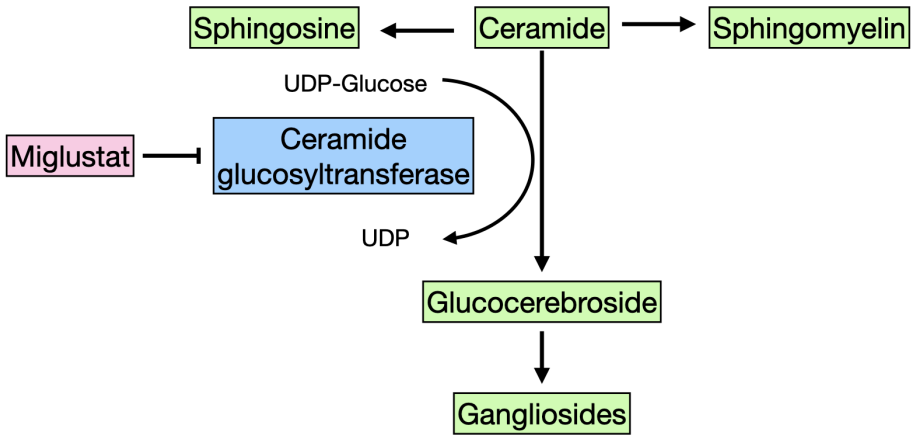


Figure 1.4: Mechanism of action of miglustat. Modified from reference[79].

1.6.2 Arimoclomol

Arimoclomol is an orally available small molecule that can cross the blood-brain barrier [80]. It can amplify heat shock proteins (HSPs) in response to cellular stress and directly facilitate lysosomal function by correcting misfolding of the NPC1

protein [81–83] and stabilising the lysosomal limiting membrane [84]. The HSPs are the natural cellular defense to cellular stress and prevent protein misfolding and lysosomal membrane permeabilisation [64, 84, 85]. Heat shock protein 70 (HSP70) is critical in the correct processing and folding of the NPC1 protein [64, 83, 86]. Arimoclomol can increase the level of HSP70 by stabilizing the interaction of Heat Shock Factor 1 with Heat Shock Elements, which regulate HSPs production. The NPC1 protein is synthesized and folded in the ER [22, 63, 64] and transported to the Golgi [87]. Eventually, the functional NPC1 protein becomes resident in the limiting membrane of lysosomes [87]. However, misfolded NPC1 protein is exported out of the ER and degraded [63, 88]. Arimoclomol induces HSP70 production and helps NPC1 to correctly fold in the ER (see Fig. 1.5). Moreover, most *NPC1* mutations are missense ($70-80\%$), which leads to misfolding and premature degradation of the NPC protein [89, 90]. The activation of HSP can correct the folding of the NPC1 protein, especially HSP70 [64, 83]. It has been proven to be safe in other neurodegenerative diseases, such as amyotrophic lateral sclerosis (ALS) [91] and sporadic inclusion body myositis (sIBM) [92]. Recently, a phase II/III clinical trial (ClinicalTrials.gov identifier: NCT02612129) showed NPC patients treated with arimocloml and migulstat had a 65% reduction of annual disease progression in the 5-domain NPC Clinical Severity Scale (NPCCSS) [93]. The 5-domain NPCCSS measures patients' walking (ambulation), speech, swallow, fine motor skills and cognition [94]. From the clinical trial, arimoclomol can delay NPC progression in patients, mainly in motor skills. The motor benefits of arimoclomol were also observed in the NPC murine model (BALB/cNctr-*Npc1*^{nih}/J) at 7 weeks of age [83]. Therefore, the combination of miglustat and arimoclomol was evaluated in gait analysis in this thesis.

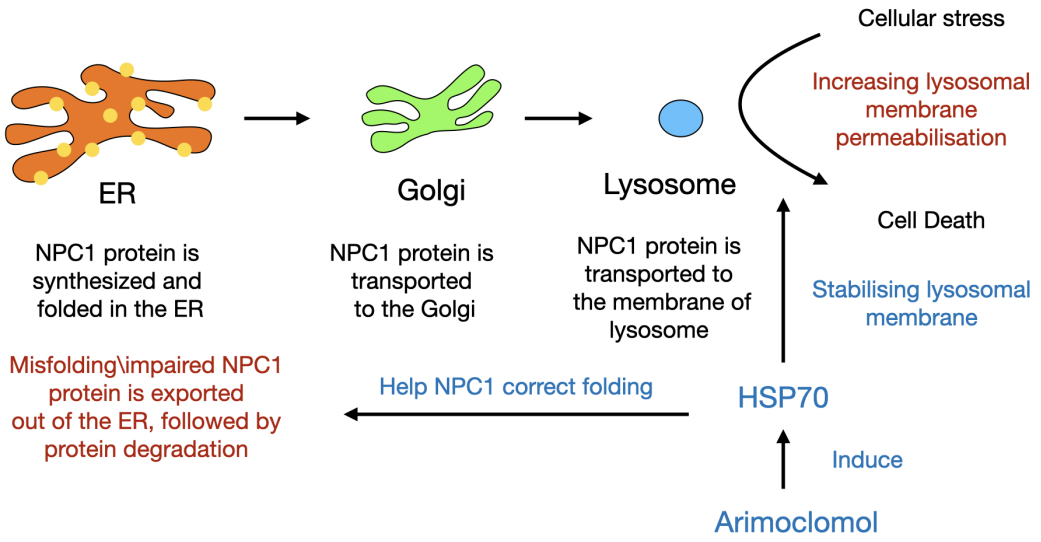


Figure 1.5: Mechanism of action of arimoclomol

1.6.3 Acetyl-DL-leucine

Acetyl-DL-leucine (ADLL) has been an oral treatment for acute vertigo since 1957 in France. It is an acetylated derivative of Leucine (a natural essential amino acid) under the trade name Tanganil^{TM} [95]. ADLL is a racemate with equal mixture of Acetyl-D-leucine (ADL) and Acetyl-L-leucine (ALL). There are case studies in short- and long-term treatment with ADLL in NPC patients showing neuroprotective, disease-modifying effect and improvements in ataxia with no serious side effects [96–98]. Ataxia was also reduced in NPC murine model (BALB/cNctr-*Npc1*^{nih}/J) in symptomatic- and pre-symptomatic- treatment studies with ADLL, and the treatment of ALL showed significant improvements in Y coordinate displacement at both short- and long-term studies [98]. Other pre-clinical studies also suggest ALL is the active element in the racemate [99]. Although the exact mechanism of action of ALL is still unclear, one potential mechanism, explaining its neuroprotective effect, is that it can activate cerebral glucose metabolism in the cerebellum enhancing cerebellar activity [98]. A recent phase II clinical trial (ClinicalTrail.gov identifier: NCT03759639) in NPC patients also reported the effectiveness and safety of ALL, including improvements of gait,

stance, upper extremity function and fine motor skills [100]. Acetyl leucine analogue treatments were therefore also evaluated in this thesis.

1.7 Behavioural assessment: gait analysis

The loss of Purkinje cells in *Npc1*^{nih} is observed in the cerebellum, except in lobules IX and X of the posterior lobe vermis [101]. The symptom of ataxia in *Npc1* null was suggested to result from Purkinje cell death [56]. Therefore, analysing gait in murine models of NPC is an appropriate behavioural assessment to evaluate the symptomatic and neuroprotective effects of treatment.

1.8 Literature review of gait analysis using the Catwalk system

Measuring gait has been a widely used assessment of locomotion in various fields, including in response to peripheral nerve injury, spinal cord injury [102, 103] and in neurodegenerative diseases (Parkinson and Huntington diseases) [104, 105] and stroke [106, 107]. Sperry [108] was one of the pioneering researchers who described the motor features of rodents in the 1940s. Several decades later, de Medinaceli et al. [109] in 1982 began to quantify the functional performance of the affected hind paw using a Sciatic Functional Index (SFI). Later, Basso et al. [110] in 1995 introduced the Basso Beattie Bresnahan scale. A major technological advance was the development of automated gait systems suitable for rodents, e.g. the Catwalk system developed in 1995 by Hammer [111, 112]. The Catwalk system provides not only static variables (such as stride length and base of support) but also dynamic (e.g., swing speed and stance) and coordination variables (such as phase dispersion) [113]. It also offers an objective method with minimum human involvement to analyse gait performance which was evaluated by experienced researchers previously. Although there is a myriad of variables generated by the Catwalk system, researchers only report on a subset of these variables, typically focusing on those that vary to the greatest extent in a disease/treatment. The selection of variables is based on

previous studies or hypothesis-driven assumptions [114]. For example, Kappos et al. [115] reviewed 46 publications from 2006 to 2013 on functional nerve recovery studies across different rodent models and suggested that the most frequently used variables, such Swing and Stride Length, should be used in future studies. On the other hand, Kyriakou et al. [116] compared the results from the Catwalk in three rodent models (one wild type, two ataxia models) and concluded that there was no fixed standard set of variables when studying ataxia in rodent models. Instead, the selection of variables from the Catwalk system should depend on the individual animal model. This highlights the importance of variable selection to generate a unique profile of variables in a specific model when using the Catwalk system. In 2018, Crowley et al. [117] and Zimprich et al. [118] evaluated variables by correlating validated scales using linear regression and principal component analysis respectively. There was no standardized procedure when it comes to the Catwalk data until a study by Timotius et al. [114] in 2019. In her study, she applied the concept of Initial Data Analysis (IDA) [119] which consisted of three steps (data cleaning, data screening and data reporting) and presented the relevance of variables in heat maps [114]. The data processed by IDA has minimal noise and is standardized. The presentation of heat maps helps the readers to get an overview of relevant variables at a glance.

However, there are still many gaps to fill in the current methodologies of the Catwalk analysis in neurodegenerative diseases rodent models. Firstly, there is no systematic variable analysis considering the trend of changes over time. Studies focus on one-time point and the trend is neglected. This is particularly important as many diseases including LSDs are progressive diseases. The trend over time can reveal the time of onset of symptoms and also the onset and duration of the effects of potential treatments. Secondly, the Standard Deviation of variables is ignored in current studies. The variation of variables indicates the level of stability of variables. With disease progression, the variation becomes wider, and it is an important additional aspect of motor function decline that needs capturing. Thirdly, there is no well-established data cleaning process. Although the Catwalk system can automatically record and generate variables, the quality of a given run is not

guaranteed by setting run criteria in the system. The run criteria setting determines whether a run is compliant or not by the duration of a run and speed variation. The system depends on the run criteria to ensure the quality of the data, but it is unfortunately inadequate. Timotius et al. [114] pointed out the importance of data cleaning and gave a procedure for data cleaning in a run. The *Npc1*^{nih} mouse model central to this thesis requires more steps for data cleaning to obtain good quality data due to the poor paw signal caused by the low body weight of the *Npc1*^{nih} mice. Fourthly, there is no data summary generated to help interpret the results. For example, Phase Dispersions and Couplings indicate the coordination between two paws. The various paw combinations in reports can cause confusion.

To solve these problems, I have developed and rigorously validated a standardized procedure to evaluate all variables generated by the Catwalk system. I have shown its utility in two models of NPC and found it can detect the differential effects of small molecule therapeutics, both as monotherapies and when used in combination.

1.9 Thesis outline

This thesis develops a standard process, the Evidence Base Gait Analysis Method (EBGAM), to analyse the Catwalk data and use the machine learning to capture another aspect of gait. Two studies demonstrated the power of these methods and offered details of gait behaviours in response to different treatments.

In Chapter 2, an Evidence Base Gait Analysis Method (EBGAM) is introduced and used to characterizes two *NPC* $^{-/-}$ murine models, *Npc1*^{nih} and *Npc1*^{nmf164} mice.

In Chapter 3, the gait data of an arimoclomol combination therapy is analysed by EBGAM. The study included three treatment arms and gait was measured at multiple time points. The results show the treatment effects on physical-related or coordination-related variables. This is the first time these insights into the effects of treatments have been elucidated.

In Chapter 4, proven treatments, Mig and acetyl leucines, were used to validate Catwalk analysis with EBGAM. However, limitations were found with the methodol-

ogy as Catwalk analysis with EBGAM was unable to identify the positive impacts of acetyl leucines on ataxia. This is due to the intrinsic nature of the Catwalk system.

In Chapter 5, walking path analysis (WPA) with DeepLabCut (DLC) was therefore introduced and validated using the same study data analysed in Chapter 4. The results of WPA can show the significant ataxia improvements with Mig and ALL treatments. Therefore, a more comprehensive picture of ataxia might be drawn by utilising WPA alongside Catwalk analysis with EBGAM.

2

Evidence Based Gait Analysis Method

Contents

2.1 Introduction 18
2.2 Materials and Methods 20
2.2.1 Animal Models (*Npc1*^{nih} and *Npc1*^{nmf164}) 20
2.2.2 Evidence Based Gait Analysis Method (EBGAM) . . . 21
2.2.3 The definition of variables and statistics 31
2.3 Results 32
2.3.1 The summary of the data set 32
2.3.2 Impacts of disease progression on gait 34
2.3.3 The results of Evidence Based Variable Analysis (EBVA) 38
2.4 Discussion 47
2.4.1 Neuropathology and motor behaviours 47
2.4.2 The Evidence Based Gait Analysis Method (EBGAM) . 47
2.4.3 The characterization of NPC models by Evidence Based Variable Analysis 48

2.1 Introduction

This chapter focus on selecting relevant variables from the Catwalk system in two NPC1 rodent models focusing on gait features using a standardized procedure we have innovated termed Evidence Based Gait Analysis Methodology (EBGAM).

In this thesis, gait was analysed using the Catwalk system developed by Noldus

Information Technology [111, 112]. This system is widely used and generates a total of 495 variables of which 245 (138 physical-related and 107 coordination-related) out of 495 variables describe the gait during the movement of a rodent. Although the Catwalk system can provide detailed information through the variables generated on how the rodent walks, the system lacks a standardised procedure to systematically assess the myriad of variables it measures. At present, researchers typically select variables based on hypothesis-driven assumptions, prior observational experience, or the magnitude of change [114]. For example, researchers evaluated a drug-induced diabetic rat model using pre-defined variables [120], which were frequently used in previous studies [115]. The results arising based on these subjective assumptions likely cause misleading conclusions to be drawn, for example ignoring the negative effects of treatments. Thus, in this study we have developed EBGAM to objectively identify relevant variables in two Niemann-Pick type C1 ($NPC^{+/-}$) mutant mouse models. These are $Npc1^{nih}$ and $Npc1^{nmf164}$ mice resembling late infantile and juvenile-onset forms of human NPC1 respectively [44]. The variables selected by EBGAM are the features affected by disease progression.

Characterising animal models objectively is essential when evaluating novel interventions. With the power of EBGAM, the onset and key features of gait between NPC models can be determined. Here, the results provide the first statistical gait characterization of $Npc1^{nih}$ and $Npc1^{nmf164}$. The gait symptoms of the $Npc1^{nih}$ model begin at 6 weeks of age and become more apparent at 8 weeks of age, which are consistent with visual observations [121]. In contrast, the $Npc1^{nmf164}$ develops gait symptoms later at 12 weeks of age. These results offer robust evidence of $Npc1^{nih}$ and $Npc1^{nmf164}$ represent late infantile and juvenile forms of human NPC1 respectively. All the data from the Catwalk system are analysed using a standardised procedure including data collection, data cleaning, data preparation, data analysis and data presentation. The reliability of the results heavily depends on the quality of the analysis at each step. The data cleaning is an important step, especially in the gait data of $Npc1^{nih}$ and is often overlooked in the literature.

The paw signals are often undetectable in the *Npc1*^{nih} model at 8 weeks of age due to the low body weight of the mice.

In this chapter, a standardized method of gait analysis has been developed, validated, and applied to the analysis of two untreated mouse models of NPC1.

2.2 Materials and Methods

2.2.1 Animal Models (*Npc1*^{nih} and *Npc1*^{nmf164})

The two animal studies, *Npc1*^{nih} (section 1.5.1) and *Npc1*^{nmf164} (section 1.5.2), were performed by Dr Ecem Kaya and Dr Maria Fernandez-Suarez respectively in the Platt Laboratory at the Pharmacology Department at the University of Oxford. The gait data were collected by Mr Dave Smith using the Catwalk system. Gait was measured at 6, 7 and 8 weeks of age in *Npc1*^{nih} mice and at 8, 10, 12 and 15 weeks of age in *Npc1*^{nmf164} mice. There were 12 mice recruited in WT and Hom groups of the *Npc1*^{nih} model. In the *Npc1*^{nmf164} model, there were 4 and 5 mice in WT and Hom groups respectively. Table 2.1 shows the number of mice in each group between models and the time points when gait data were collected.

Models	Genotype	No. mice	Age of weeks					
			6wks	7wks	8wks	10wks	12wks	15wks
Npc1^{nih}	WT	12						
	Hom	12						
Npc1^{nmf164}	WT	4						
	Hom	5						

Table 2.1: Study plan summary.
This table shows the number of mice (NO mice column) in each group between models and the time points when gait data were collected. The colour indicates whether gait data were collected (blue) or not (white).

All mice were bred in ICV cages and housed under non-sterile conditions with food and water available *ad libitum*. All experiments were conducted under the Animal Scientific Procedures Act 1986 approved by the UK Home Office. Mice were culled at the humane endpoint, defined as a loss of 1 gram of body weight within 24 hours when the mice can no longer feed and drink efficiently due to advanced neurodegeneration/ataxia.

2.2.2 Evidence Based Gait Analysis Method (EBGAM)

The workflow of the Evidence Based Gait Analysis Method (EBGAM) is summarized in Fig. 2.1. This begins with gait data collection using the Catwalk system by an experienced animal handling technician. The collected data then undergoes data noise minimization in the data cleaning process where both the quality and quantity of the data are optimised, for example, through data segmentation, threshold adjustment and step combination. Before data analysis, the data requires adaptation to a format suitable for analytical tools. In this thesis, the data was adapted for the R programming platform. Subsequently, the data were analysed.

In this chapter, the primary aim is to apply this methodology to study the similarities and differences between two animal models of NPC1. Therefore, the data were first analysed by unpaired t-tests at weekly intervals and subsequently, all variables were analysed by EBVA.

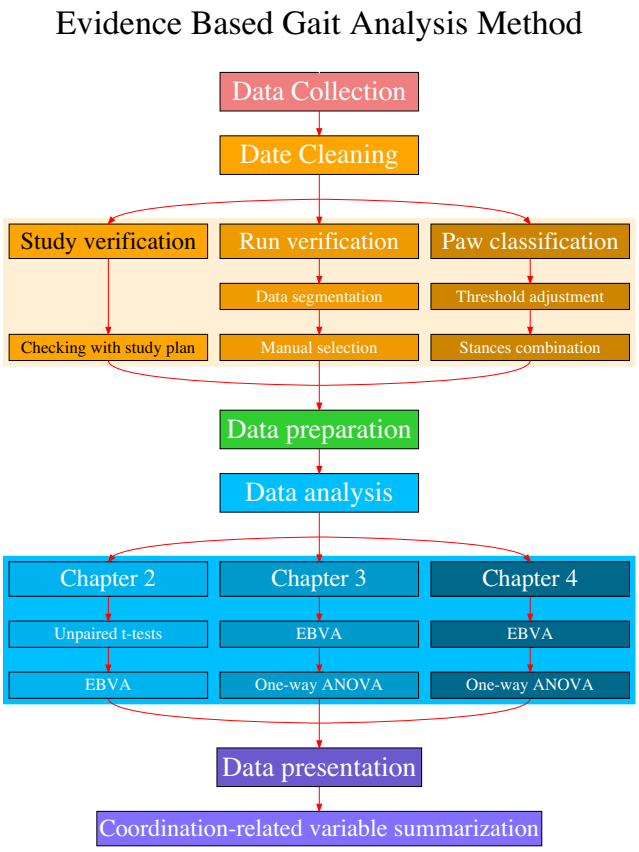


Figure 2.1: Evidence Based Gait Analysis Method (EBGAM).
There are 5 main steps, namely data collection, data cleaning, data preparation, data analysis and data presentation.

Data Collection in the Catwalk system

Gait data were collected using Catwalk XT 9.1 equipment and the 495 variables were generated by the Catwalk XT 10.6 software in the Trial statistics setting. All experimental mice walked freely along the walkway without any rewards. There was no habituation to the Catwalk device performed before the experiments. The Catwalk device is equipped with an enclosed plexiglass walkway (see Fig. 2.2). In the dark room, the green light is illuminated when a paw touches the floor. These green paws, body silhouettes and red background were recorded with a high-speed camera underneath the walkway with a sample rate of 100 frames per second. At least five runs were collected from each mouse at a specific time point and collectively, these runs constitute a trial.

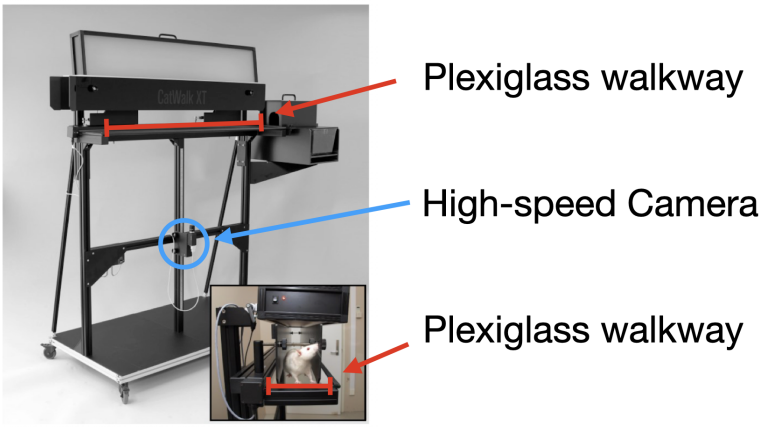


Figure 2.2: The Catwalk device.

Data Cleaning

There are three main steps in the data cleaning process including study verification, run verification and paw classification.

Study verification In the study verification step, the description of mice in the data from the Catwalk system, such as Date of Birth (DOB) are verified by merging the dataset from the Catwalk and the study plan. The study plan stores the experimental design with a unique mouse ID, any treatment and DOB. Mouse ID was the primary parameter used for verification in each data set as human error is inevitable when typing DOB and groups into the Catwalk system. Mouse misplaced in the study from other studies were removed. Age was calculated from Date (the date of gait measured) and DOB. The study verification is shown in Fig. 2.3.

In Fig. 2.3, the left two tables (Table 1 and Table 2) are from the Catwalk system (Table 1) and study plan (Table 2). They are merged by the primary key (Mouse ID) into Table 3 in the middle. Table 4 on the right is the cleaned data. The colours represent different types of data, and the intensity of the colours shows the origin of data from the Catwalk data or study plan. The red circles indicate a human error in the Catwalk data that needs correcting.

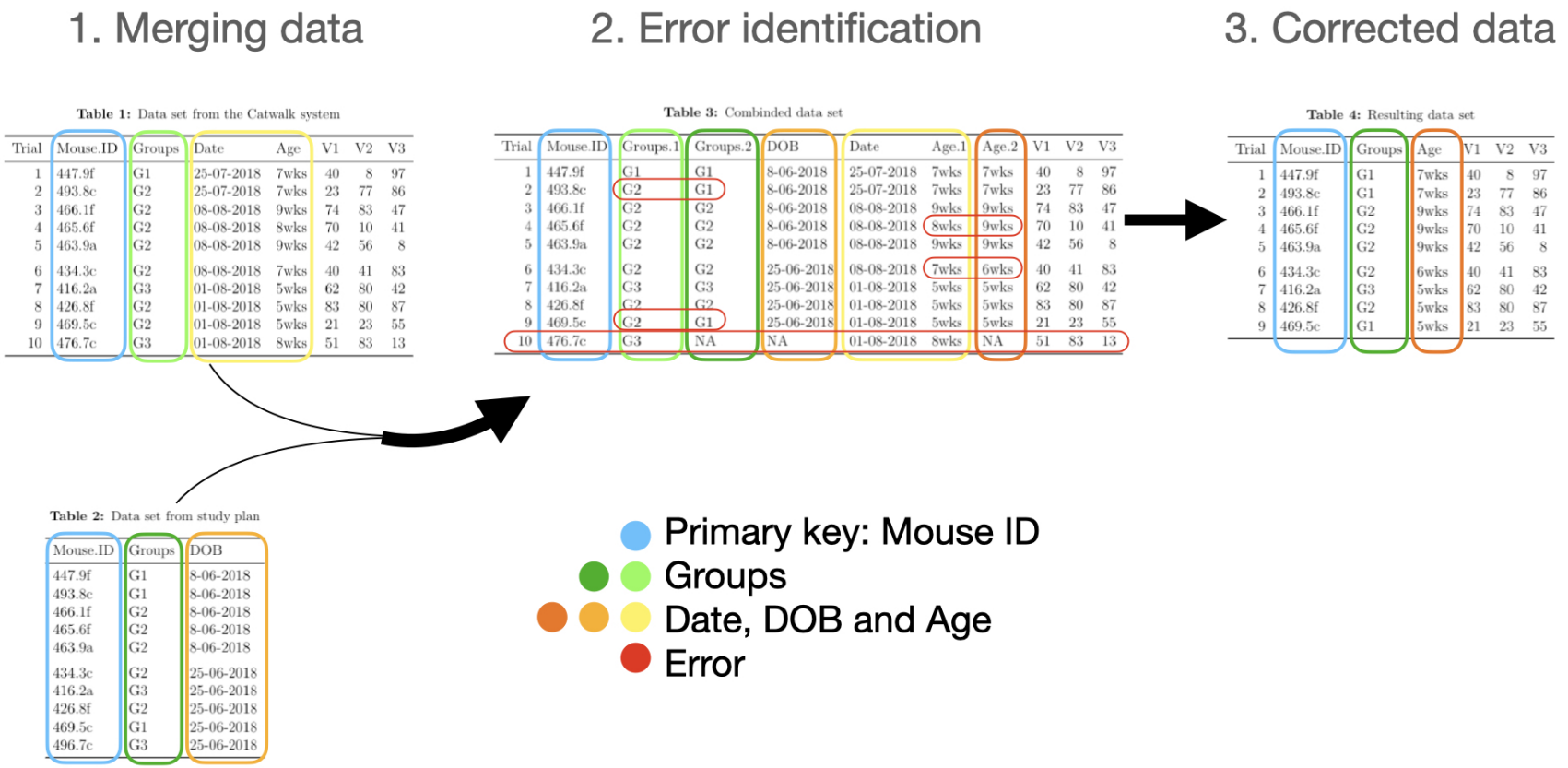


Table 1: Data set from the Catwalk system

Trial	Mouse.ID	Groups	Date	Age	V1	V2	V3
1	447.9f	G1	25-07-2018	7wks	40	8	97
2	493.8c	G2	25-07-2018	7wks	23	77	86
3	466.1f	G2	08-08-2018	9wks	74	83	47
4	465.6f	G2	08-08-2018	8wks	70	10	41
5	463.9a	G2	08-08-2018	9wks	42	56	8
6	434.3c	G2	08-08-2018	7wks	40	41	83
7	416.2a	G3	01-08-2018	5wks	62	80	42
8	426.8f	G2	01-08-2018	5wks	83	80	87
9	469.5c	G2	01-08-2018	5wks	21	23	55
10	476.7c	G3	01-08-2018	8wks	51	83	13

Table 2: Data set from study plan

Mouse.ID	Groups	DOB
447.9f	G1	8-06-2018
493.8c	G1	8-06-2018
466.1f	G2	8-06-2018
465.6f	G2	8-06-2018
463.9a	G2	8-06-2018
434.3c	G2	25-06-2018
416.2a	G3	25-06-2018
426.8f	G2	25-06-2018
469.5c	G1	25-06-2018
496.7c	G3	25-06-2018

Table 3: Combinded data set

Trial	Mouse.ID	Groups.1	Groups.2	DOB	Date	Age.1	Age.2	V1	V2	V3
1	447.9f	G1	G1	8-06-2018	25-07-2018	7wks	7wks	40	8	97
2	493.8c	G2	G1	8-06-2018	25-07-2018	7wks	7wks	23	77	86
3	466.1f	G2	G2	8-06-2018	08-08-2018	9wks	9wks	74	83	47
4	465.6f	G2	G2	8-06-2018	08-08-2018	8wks	9wks	70	10	41
5	463.9a	G2	G2	8-06-2018	08-08-2018	9wks	9wks	42	56	8
6	434.3c	G2	G2	25-06-2018	08-08-2018	7wks	6wks	40	41	83
7	416.2a	G3	G3	25-06-2018	01-08-2018	5wks	5wks	62	80	42
8	426.8f	G2	G2	25-06-2018	01-08-2018	5wks	5wks	83	80	87
9	469.5c	G2	G1	25-06-2018	01-08-2018	5wks	5wks	21	23	55
10	476.7c	G3	NA	NA	01-08-2018	8wks	NA	51	83	13

Table 4: Resulting data set

Trial	Mouse.ID	Groups	Age	V1	V2	V3
1	447.9f	G1	7wks	40	8	97
2	493.8c	G1	7wks	23	77	86
3	466.1f	G2	9wks	74	83	47
4	465.6f	G2	9wks	70	10	41
5	463.9a	G2	9wks	42	56	8
6	434.3c	G2	6wks	40	41	83
7	416.2a	G3	5wks	62	80	42
8	426.8f	G2	5wks	83	80	87
9	469.5c	G1	5wks	21	23	55

Figure 2.3: An example of study verification as part of the data cleaning process

Run verification The gait data includes walking behaviour and non-walking behaviours (e.g., such as exploring, turning, and sniffing). This step of the process aims to identify and remove non-walking behaviours. According to the CatWalk XT version 10.6 manual, the Catwalk system can automatically determine and excluded non-walking segments in a run, its function is called 'Data Segmentation'. Data Segmentation is set by a range of speeds of the mouse, its variation, and minimum consecutive steps. Based on the experience/experimental observation, the speed ranges between $120cm/s$ and $10cm/s$, speed variation limits to 60% and 10 is the minimum consecutive steps in a run. Speed variation is defined as a percentage of the speed of individual steps as a proportion of average speed. Fig. 2.4 shows an example of Data Segmentation in the system. The length of coloured bars in the timing view reflects the duration of the paw touching the floor. The red bars indicate a long duration, which occurs in non-walking behaviours. The nearby steps (dark blue) were also affected by non-walking behaviours either having a speed below $10cm/s$ or exceeding the speed variation of 60%. Thus, these steps were removed from the system. The resulting timing view was validated by manual review and the missed non-walking behaviour by the Data Segmentation was manually removed.



Figure 2.4: Example of data segmentation.
Timing view shows the duration of a paw contacting the ground. The colours represent individual paws: blue: RF, fuchsia: RH, yellow: LF and green; LH. The red colour indicates the stationary steps, which occur in non-walking behaviours. The blue steps were affected by non-walking behaviours having either slow-speed or high-speed variables. The red and blue steps were identified and removed by the Catwalk system.

Run classification In paw classification, the paws were classified into the right front (blue), right hind (fuchsia), left front (yellow) and left hind(green). Mice

with severe motor dysfunction and light body weight (e.g., NPC models) require threshold adjustment and stance combination before performing paw classification. Fig. 2.5 shows an example of threshold adjustment. The default threshold is 0.12. By increasing or decreasing the threshold to get the optimal paw signal.

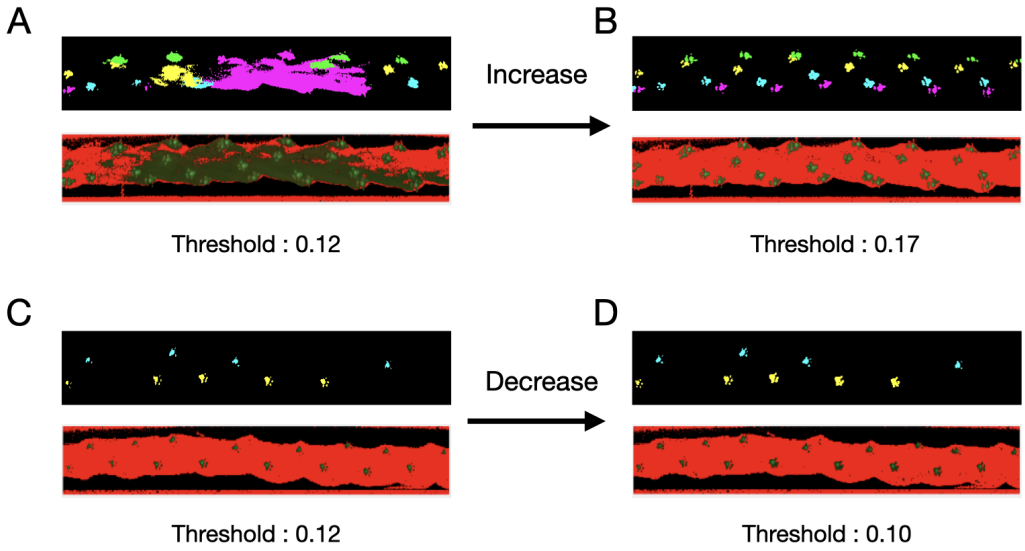


Figure 2.5: Examples of threshold adjustment.
The left-hand panels (A and C) show the paw prints before threshold adjustment and the right-hand panels (B and D) after adjustment. A shows an example of a run with noisy signals and the threshold was increased to better resolve the paw prints in B. C shows an example of a run with weak signals that requires decreasing the threshold to identify the paw prints in D.

Fig. 2.6 displays an example of a stance combination. In the timing view in Fig. 2.6, the red circle highlights segmented stances, which were manually combined into one.

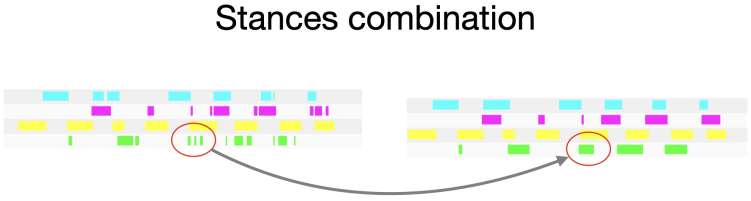


Figure 2.6: Example of paw print adjustments.
The stances in the red circles were manually combined into one stance.

Fig. 2.7 shows an example of paw signal optimization. In the data, signal optimization consists of two steps explained previously. In the first step, the paw signals were optimized by decreasing the threshold. This is shown by the fuchsia stance below. If all stances in a run can be merged, like the example in the fuchsia stance, the second step, stance combination is not necessary. However, the signal of the green stance in the red circle was still weak, showing divided stances, after threshold adjustment. Hence, step two is necessary for this instance to achieve signal optimization.

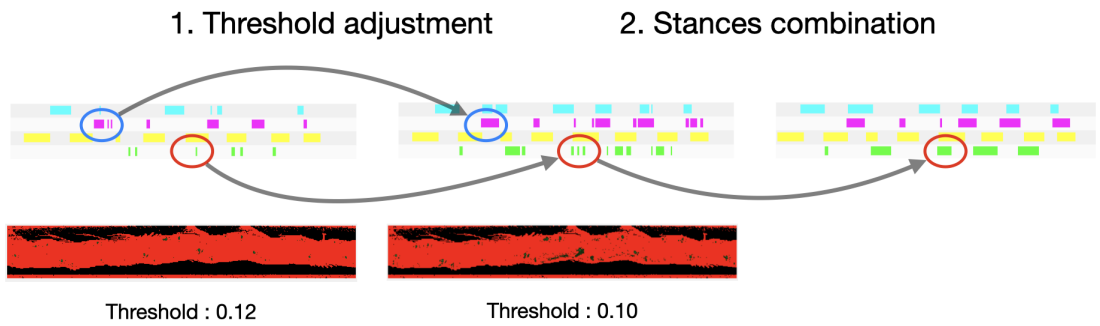


Figure 2.7: Example of paw signal optimization.
There are two steps, namely threshold adjustment and stance combination. The stance in the blue circle only requires threshold adjustment and the red circle needs threshold adjustment and stance combination.

Data preparation

The next step is data preparation, which organizes the data set exported from the Catwalk system and converts it to a format for data analysis in R programming platform. A total of 495 variables were regrouped and shown in Fig 2.8. There are six categories, namely description, physical-related, coordination-related, intensity-related, indices and other variables.

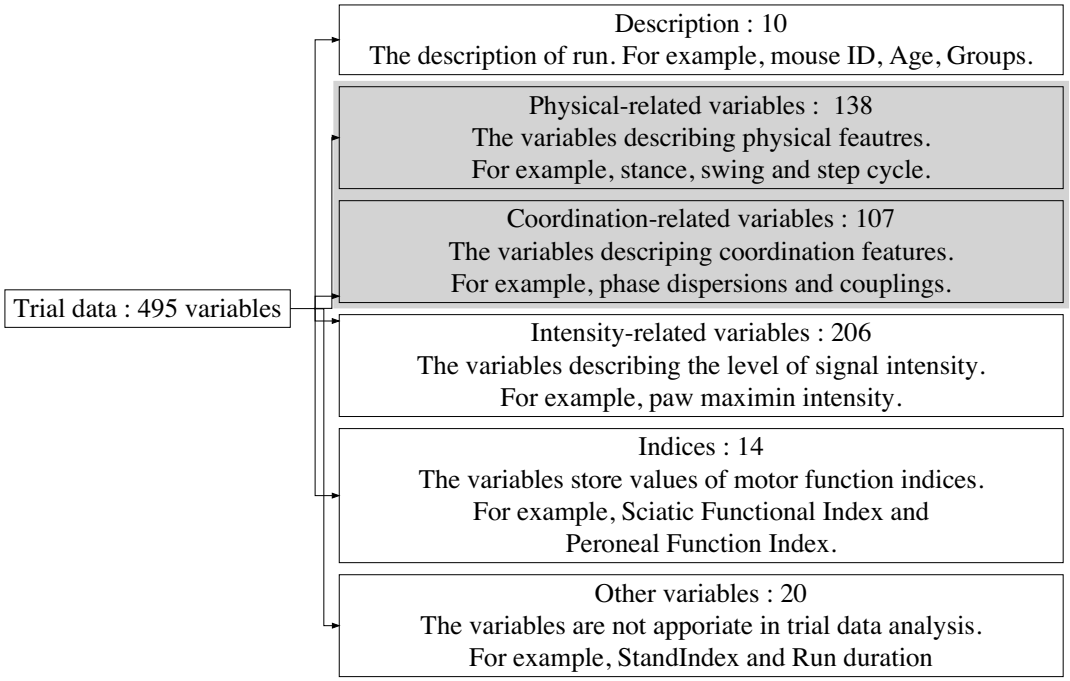


Figure 2.8: The categories of variables in the Catwalk data.
A total of 245 variables in physical-related and coordination-related are analysed in the following procedure.

The flow chart shows the number of variables and the representative variables in each group. The groups with grey backgrounds were analysed in the following section. The variables in intensity-related and other variable groups were excluded as threshold adjustment and data segmentation changed the values of variables in these groups. For example, an increasing threshold also increases the intensity of

paws. Therefore, the values of paw intensity are not comparable between runs as the threshold is not consistent. Other variables, such as Run Duration, describe the duration of a whole run, including non-walking behaviours. Since the data segmentation excludes non-walking behaviours, these variables are not eligible to include in the data set. The indices, such as Sciatic Functional Index, are used to evaluate functional recovery from nerve injury [122], which is not relevant to this thesis, therefore these 14 indices were also removed. The following analysis is focused on physical-related and coordination-related variables with a total of 245 variables. The variables in each category and their definitions are included in Appendix (see section A.1 and Table A.1). After grouping the variables, the data set was analysed using the R programming language.

Data presentation

Heatmaps of the p values The resulting p values from the data analysis section are presented as heat maps according to the significance levels of the data.

Coordination-related variable summary In order to interpret the results of coordination-related variables, further summarization is required in Fig. 2.9. There are 107 coordination-related variables analysed by EBVA. They are in three subgroups, namely Support, Step Sequence, and Inter-paw interaction. When presenting the results of the EBVA, the total of 90 variables in Phase Dispersions and Couplings with mean, SD, Cstat mean, Cstat SD and Cstat R were summarized into 24 inter-paw interaction variables. For example, PD/Couplings RF-LH in mean, Cstat mean, and Cstat R describes the Diagonal interaction. The lowest p values in these variables were selected (mean). PD/Couplings RF-LH in SD and Cstat SD indicate a variation of the Diagonal inter-paw interactions. The details of Cstat (circular statistics) and inter-paw labelling can be found in the Appendix (see section A.1).

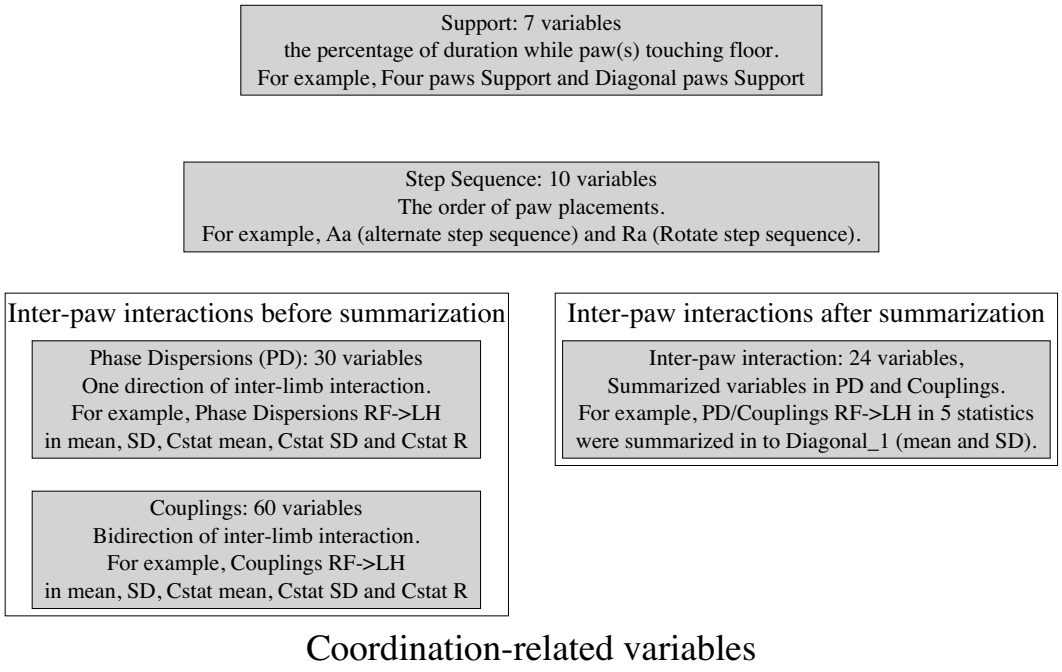


Figure 2.9: Coordination-related variable summarization.
Phases Dispersions (PD) and Couplings with mean, SD, Cstat mean, Cstat SD and Cstat R were summarized into inter-paw interaction mean and SD. The total number of coordination-related variables was reduced from 107 to 41.

Data analysis

In this section, the aim is to characterize two NPC mouse models in terms of their gait performance. It includes two analyses. The group comparison analyses disease progression and Evidence Based Variable Analysis (EBVA) highlights the relevant variables in each mouse model.

Unpaired t-test at each time point In a total of 245 variables in physical-related and coordination-related groups between the WT and Hom groups in the two mouse models were analysed using an unpaired t-test. The significance level was defined as $p \leq 0.05$. The results showed the progression of the disease in

the two models. The features of gait generated from the Catwalk system will be referred to as "variables" in this thesis.

Evidence Based Variable Analysis (EBVA) This analysis aims to narrow down the number of variables relevant to the disease models from the 245 variables derived from the Catwalk exported files and to identify the variables that are functionally relevant to the disease in the two NPC mouse models. Evidence Based Variable Analysis consists of the mixed effects ANOVA and Tukey Honestly Significant Difference (Tukey HSD) post hoc analysis. The mixed effects ANOVA is a mix of two-way ANOVA and ANOVA accounting for repeated measurements. Two factors (Age and Group) are used in the two-way ANOVA and the mouse ID is the random effect in the measured ANOVA. This model will point out whether a variable is affected by disease progression with consideration of individual differences. The resulting variables undergo pairwise comparison using Tukey HSD post hoc analysis. The significance level is defined as $p \leq 0.05$.

Statistical analysis environment Data analysis was performed in the R programming language (4.1.2 version) in the aarch64-apple-darwin20 platform [123]. The thesis was written in Rmarkdown used Oxforddown as a template [124].

2.2.3 The definition of variables and statistics

See Appendix A.1

2.3 Results

2.3.1 The summary of the data set

The process of analysing Catwalk data using the method I have developed will be referred to as the Evidence Based Gait Analysis methodology (EBGAM) from this point on in the thesis.

Table 2.2 and Table 2.3 show the data sets after the data cleaning process. A trial consists of at least 5 runs from a mouse at each time point. In Table 2.2 is the *Npc1*^{nih} mouse model with 12 WT mice and 13 Hom mice and the gait was collected at 6, 7 and 8 weeks of age. Table 2.3 includes the *Npc1*^{nmf164} mouse model with 4 WT mice and 5 Hom mice. This model lives significantly longer than *Npc1*^{nih} mice. Therefore, gait was measured at 8, 10, 12 and 15 weeks of age. The cells of the table include AD meaning absent data. The absent data was frequently caused by mice reluctant to walk or immobile mice.

ID	Group	Age	Trial	Age	Trial	Age	Trial
339.5f	Hom	6	Trial0283	7	AD	8	Trial0062
356.5a	Hom	6	AD	7	AD	8	Trial0223
361.4e	Hom	6	Trial0219	7	Trial0254	8	Trial0288
368.3a	Hom	6	Trial0165	7	AD	8	AD
386.4a	Hom	6	Trial0160	7	Trial0184	8	Trial0205
403.3b	Hom	6	Trial0158	7	Trial0180	8	Trial0202
444.2e	Hom	6	Trial0206	7	AD	8	Trial0271
446.2e	Hom	6	Trial0215	7	Trial0251	8	Trial0281
455.1h	Hom	6	Trial0255	7	Trial0282	8	Trial0031
456.1a	Hom	6	Trial0159	7	Trial0181	8	Trial0204
457.1c	Hom	6	Trial0171	7	AD	8	AD
458.1e	Hom	6	Trial0207	7	Trial0243	8	Trial0272
460.1a	Hom	6	Trial0172	7	Trial0193	8	AD
403.3a	WT	6	Trial0156	7	Trial0179	8	Trial0201
425.3c	WT	6	Trial0212	7	Trial0248	8	Trial0277
428.2d	WT	6	Trial0043	7	Trial0068	8	Trial0099
428.2e	WT	6	Trial0044	7	Trial0069	8	Trial0100
435.4c	WT	6	Trial0214	7	Trial0250	8	Trial0280
444.2b	WT	6	Trial0208	7	Trial0244	8	Trial0273
444.2f	WT	6	Trial0210	7	Trial0246	8	Trial0274
446.2a	WT	6	Trial0213	7	Trial0249	8	Trial0279
451.2f	WT	6	Trial0042	7	Trial0073	8	Trial0096
456.1b	WT	6	Trial0157	7	Trial0182	8	Trial0203
458.1d	WT	6	Trial0209	7	Trial0245	8	Trial0275
458.1g	WT	6	Trial0211	7	Trial0247	8	Trial0276

Table 2.2: The summary of *Npc1*^{nih} data set.
AD: absent data.

ID	Group	Age	Trial	Age	Trial	Age	Trial	Age	Trial
12.1k	Hom	8	Trial0002	10	Trial0008	12	Trial0014	15	Trial0020
12.1l	Hom	8	Trial0003	10	Trial0009	12	Trial0015	15	Trial0021
25.2g	Hom	8	AD	10	Trial0045	12	Trial0052	15	Trial0060
26.1f	Hom	8	Trial0025	10	Trial0032	12	AD	15	Trial0048
26.1h	Hom	8	Trial0026	10	Trial0033	12	AD	15	Trial0049
12.1i	WT	8	Trial0001	10	Trial0007	12	Trial0013	15	Trial0019
27.1g	WT	8	AD	10	Trial0046	12	Trial0053	15	Trial0061
27.1h	WT	8	AD	10	Trial0047	12	Trial0054	15	Trial0062
29.1e	WT	8	Trial0027	10	Trial0034	12	AD	15	Trial0050

Table 2.3: The summary of *Npc1^{nmf164}* data set.
AD: absent data.

The number of trials was summarized in Table 2.4. The data set of the *Npc1^{nih}* models was complete for all WT mouse data over the time course, but 9 trials were missing in the Hom group, mainly at 7 weeks of age. There were 6 trials in total missing from the *Npc1^{nmf164}* model study, mainly at 8 and 12 weeks of age. The Trial column indicates the trial number in an experiment from the Catwalk system.

			No. trials					
Models	Genotype	No. mice	6wks	7wks	8wks	10wks	12wks	15wks
Npc1^{nih}	Hom	12	11	7	9			
	WT	12	12	12	12			
Npc1^{nmf164}	Hom	5			4	5	3	5
	WT	4			2	4	3	4

Table 2.4: The number of trials in groups between models.
The underline of the number of trials indicates whether having missing trials in groups.

In the following analysis process, the data sets included as many trials as possible to improve the power of analysis. Firstly, disease progression within the experimental time frame was obtained in terms of gait features analysed using an unpaired t-test. Secondly, the variables were evaluated using the Evidence Based Gait Analysis methodology (EBVA). The EBVA identify the relevant variables in each model. This is the first time an evidence-based variable profile of these two mouse models has been generated.

2.3.2 Impacts of disease progression on gait

The t-tests compared WT and Hom groups across the 245 variables (physical-related and coordination-related variables) at 6, 7, and 8 weeks of age. The results are summarized in heap maps (see Fig 2.10 and Fig 2.11. From both figures, the Y-axis lists the variables from physical-related (upper figure) to coordination-related (lower figure) features. The X-axis includes two statistics (Mean and SD) of variables. The colours in the cell of the plots represent the different significance levels ranging from light blue ($p \leq 0.05$) to dark blue ($p \leq 0.0001$), while white means no significant difference. Some variables only mean were calculated in the Catwalk system. For example, there are only mean statistics in step sequence variables. These variables with only mean statistics are mainly in coordination-related groups. The cells in grey in Fig. 2.10 and Fig. 2.11 are the variables without SD statistics.

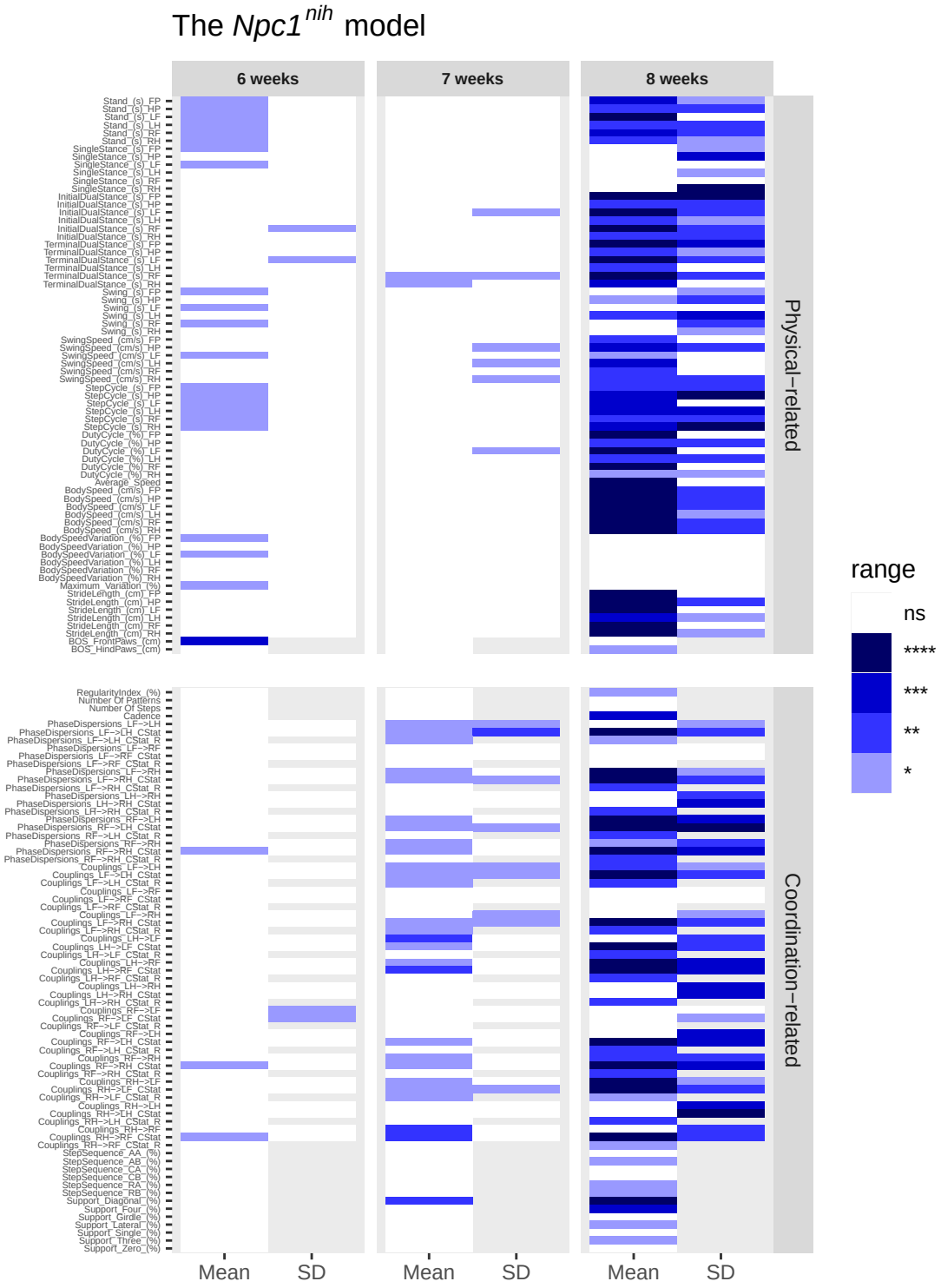


Figure 2.10: The results of unpaired t-test in the model of $Npc1^{nih}$.
Physical-related variables are shown in the upper figure, and the lower figure demonstrates variables related to coordination. Significance levels: ns: not significant; *=$p \leq 0.05$; **=$p \leq 0.01$; ***=$p \leq 0.001$; ****=$p \leq 0.0001$.

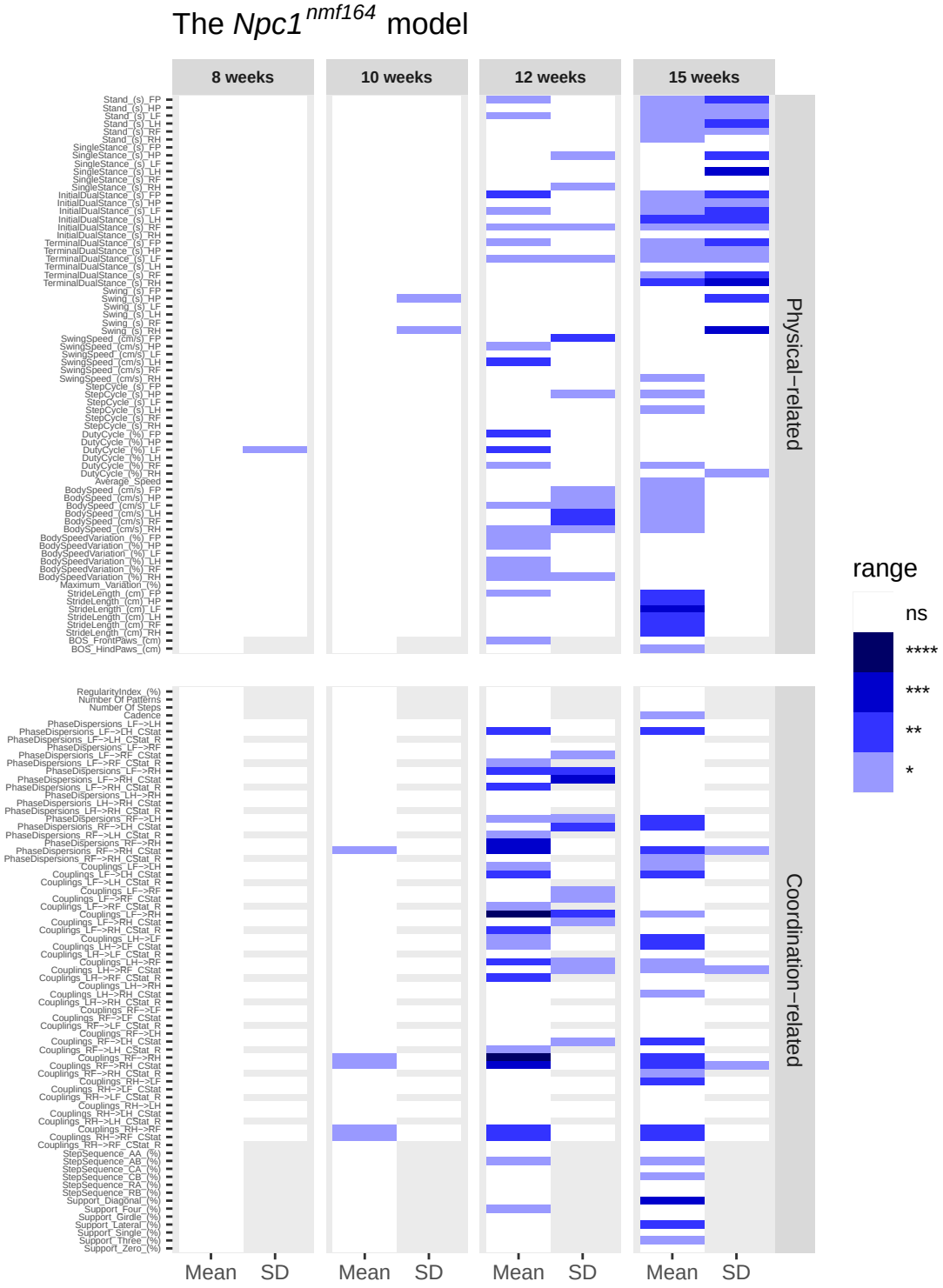


Figure 2.11: The results of unpaired t-test in the model of $Npc1^{nmf164}$.
Physical-related variables are shown in the upper figure, and the lower figure demonstrates variables related to coordination. Significance levels: ns: not significant; *=$p \leq 0.05$; **=$p \leq 0.01$; ***=$p \leq 0.001$; ****=$p \leq 0.0001$.

Npc1^{nih} model

Table 2.5 shows the number of variables which were significantly different between WT and Hom untreated groups. At 8 weeks of age, the mice were severely affected by the disease with a total number of 171 variables (97 physical-related and 74 coordination-related), which was the greatest number of variables in the observation period of the study. The number of variables gradually increased from 29 at 6 weeks of age to 171 at 8 weeks of age. The trend represents the neurodegenerative features.

Variables	Statistics	Total	weeks of age		
			6wks	7wks	8wks
Physical-related	Mean	70	22 (31.4%)	3 (4.3%)	53 (75.7%)
	SD	68	2 (2.9%)	6 (8.8%)	44 (64.7%)
	total	138	24 (17.4%)	9 (6.5%)	97 (70.3%)
Coordination-related	Mean	71	3 (4.2%)	27 (38%)	43 (60.6%)
	SD	36	2 (5.6%)	9 (25%)	31 (86.1%)
	total	107	5 (4.7%)	34 (31.8%)	74 (69.2%)

Table 2.5: The number and percentage of variables show significant differences between WT and Hom untreated groups in *Npc1*^{nih} model

Surprisingly, the number of mean variables in physical-related groups at 6 weeks of age (22) was greater than it was at 7 weeks of age (3). In the Catwalk videos, the walking behaviours between Hom and WT mice at 6 weeks of age were similar but the speed of the Hom mice was slightly slower than it of WT mice. From Fig. 2.10, the differences between WT and Hom at 6 weeks of age were mainly in Stance. The longer stance in the Hom group also affects the Step cycle at 6 weeks of age. However, the cause of the phenomenon is unclear. A possible explanation may be the delay in motor development/myelination in Hom mice, but this requires further investigation, which includes data before 6 weeks of age, to confirm. At 8 weeks of age, more than half of the variables in physical-related and coordination-related variables were observed significantly different between Hom and WT mice. This is the first statistical evidence to show the onset of gait phenotypes in *Npc1*^{nih} mice at 8 weeks of age.

Npc1^{nmf164} model

Table 2.6 shows the number of variables affected in the *Npc1^{nmf164}* model. Before 12 weeks of age, the number of variables showing significantly different in physical-related and coordination-related was less than or equal to 7. After 12 weeks of age (inclusive), the physical and coordination symptoms became severe since the number of variables at 12 and 15 weeks of age were greater than before 12 weeks of age.

Variables	Statistics	Total	weeks of age			
			8wks	10wks	12wks	15wks
Physical-related	Mean	70	0 (0%)	0 (0%)	21 (30%)	35 (50%)
	SD	68	1 (1.5%)	2 (2.9%)	13 (19.1%)	20 (29.4%)
	total	138	1 (0.7%)	2 (1.4%)	34 (24.6%)	55 (39.9%)
Coordination-related	Mean	71	0 (0%)	5 (7%)	24 (33.8%)	26 (36.6%)
	SD	36	0 (0%)	0 (0%)	12 (33.3%)	3 (8.3%)
	total	107	0 (0%)	5 (4.7%)	36 (33.6%)	29 (27.1%)

Table 2.6: The number and percentage of variables show significant differences between WT and Hom untreated groups in *Npc1^{mnf164}* model

The number of variables affected increased from 12 to 15 weeks of age, except the number of SD coordination-related variables, which decreased by 9 from 12 to 15 weeks of age. The onset of gait changes in NPC in this model is from 12 weeks of age and the number of variables affected was less than in the *Npc1^{nih}* model. The total number of variables that changed was 84 in the *Npc1^{nmf164}* model at 15 weeks of age and 171 variables in the *Npc1^{nih}* mouse at 8 weeks of age.

2.3.3 The results of Evidence Based Variable Analysis (EBVA)

Selected Physical-related variables

The Evidence Based Variable Analysis (EBVA) analysed 138 physical-related variables and its resulting p values are summarised in heat maps (see Fig. 2.12 (*Npc1^{nih}*) and Fig. 2.13 (*Npc1^{nmf164}*)). The method determines whether a variable is affected by NPC during the study. The variables with p values less than or

equal to 0.05 were considered relevant variables in the model. The number of relevant physical-related variables is summarized in Table 2.7. The *Npc1*^{nih} model had more variables affected by NPC than the *Npc1*^{nmf164} model with 50 and 41 variables respectively. Interestingly, *Npc1*^{nih} mice had more variables affecting the front paws and more SD variables were affected in the hind paws. On the other hand, the number of mean and SD variables between the front and hind paws in *Npc1*^{nmf164} were more equivalent.

Variables	Statistics	Total	*Npc1*^{nih}	*Npc1*^{nmf164}
Physical-related	Mean	70	33 (47.1%)	21 (30%)
	SD	68	17 (25%)	20 (29.4%)
	total	138	50 (36.2%)	41 (29.7%)

Table 2.7: The number and percentage of physical-related variables selected by EBVA in both models

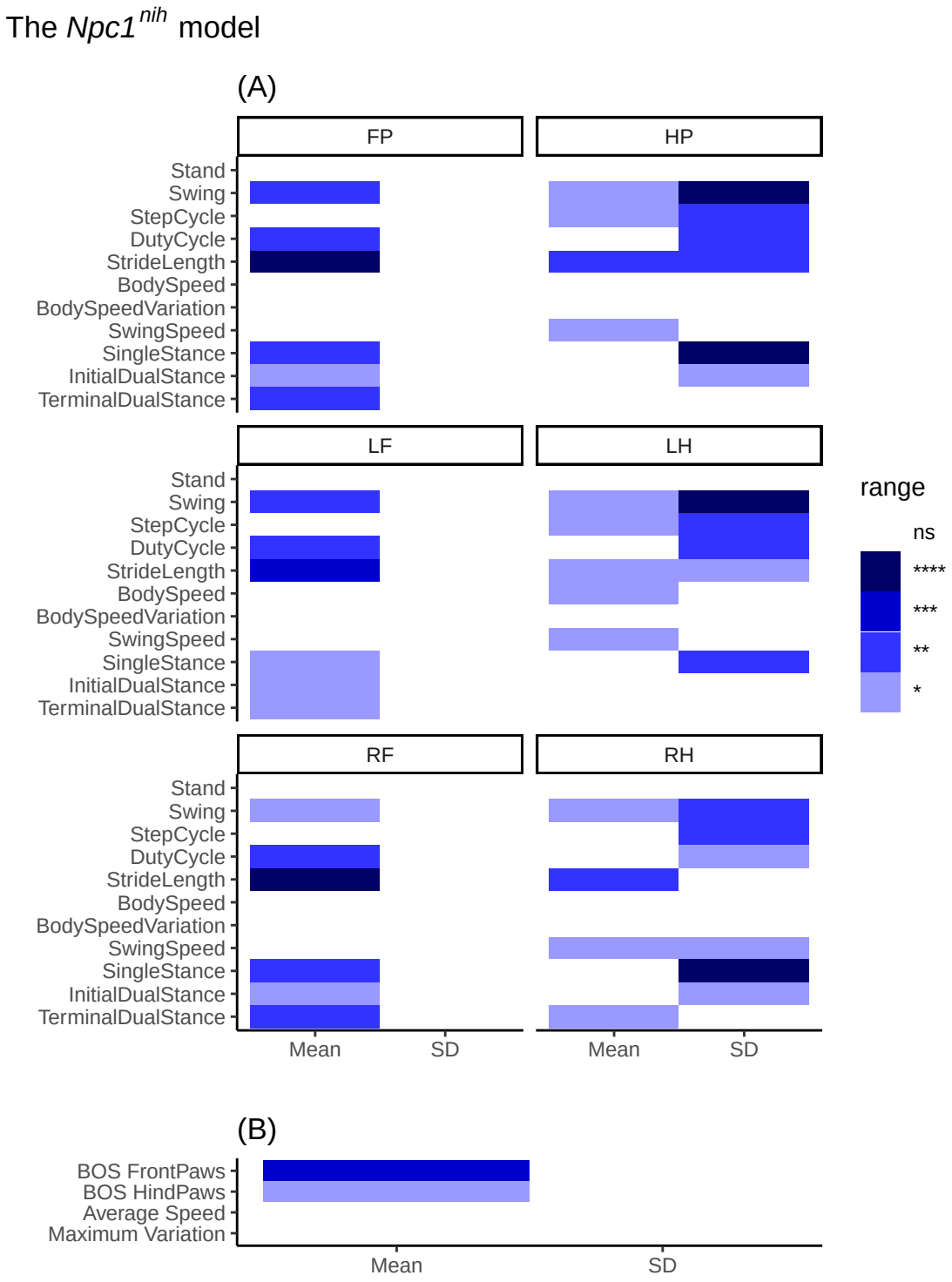


Figure 2.12: The relevant physical-related variables were found to be modified in the *Npc1*^{nih} model in (A) paw-wise and (B) non-paw-wise variables.
FP: front paws; HP: hind paws; LF: left front paw; LH: left hind paw; RF: right front paw; RH: right hind paw. The colours represent different significance levels.
Significance levels: ns: not significant; *=$p \leq 0.05$; **=$p \leq 0.01$; ***=$p \leq 0.001$; ****=$p \leq 0.0001$.

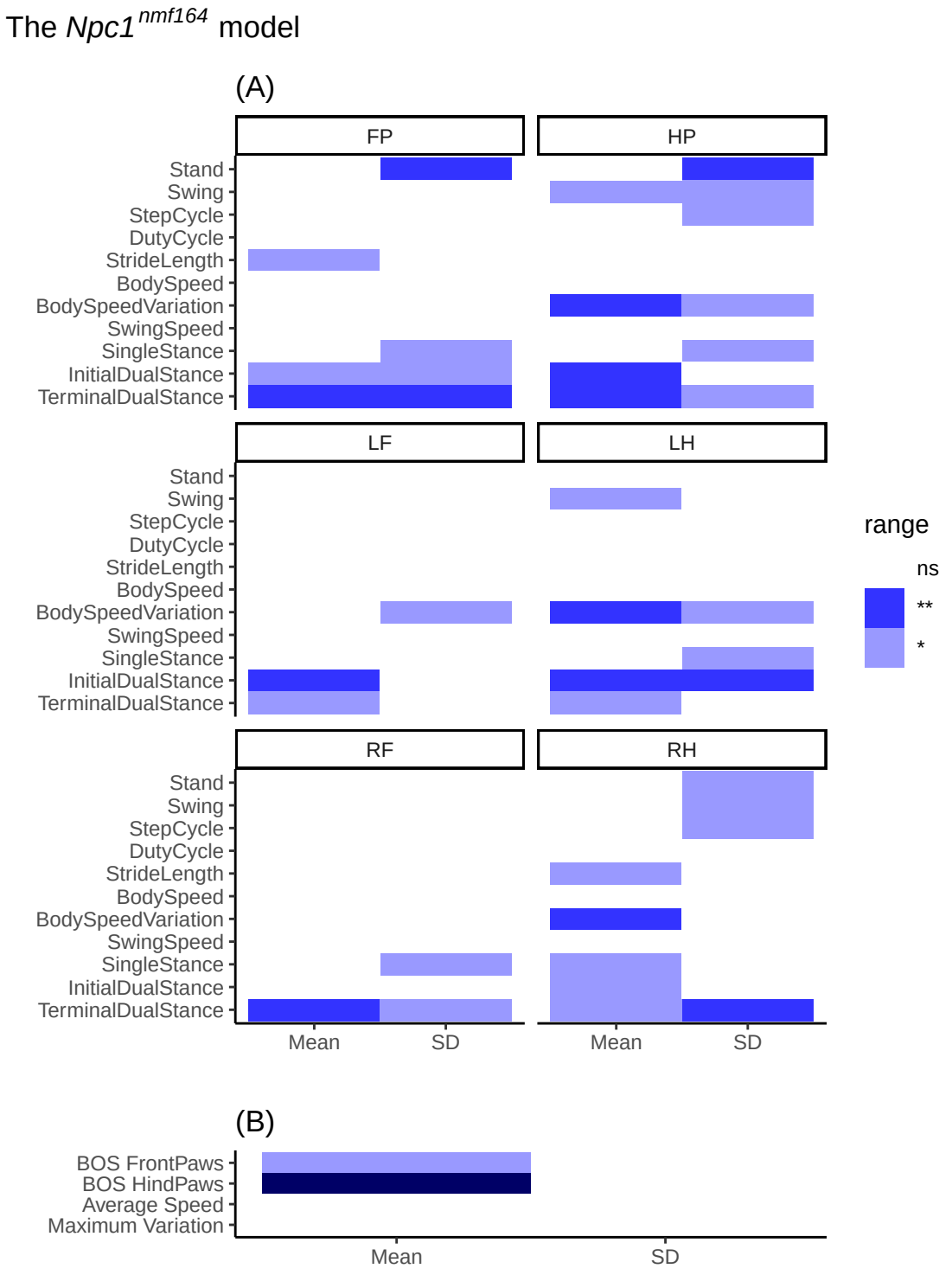


Figure 2.13: The relevant physical-related variables were found to be modified in the *Npc1*^{nmf164} model in (A) paw-wise and (B) non-paw-wise variables.
FP: front paws; HP: hind paws; LF: left front paw; LH: left hind paw; RF: right front paw; RH: right hind paw. The colours represent different significance levels.
Significance levels: ns: not significant; *=$p \leq 0.05$; **=$p \leq 0.01$; ***=$p \leq 0.001$; ****=$p \leq 0.0001$.

Table 2.8 summarises the representative variables in the FP (front paws) and the HP (hind paws) between the two models. The p value results were from EBVA and the upward arrow indicates the value in the variable is greater in disease models than in the wild type mice and vice versa. *Npc1^{nih}* mice spent less time in the FP swing and more time in the HP swing. This contributed to the longer step cycle in the HP and the longer duty cycle in the FP in *Npc1^{nih}*. *Npc1^{nih}* mice had short stride lengths in both FP and HP. In the *Npc1^{nmf164}* model, there were only two mean variables showing significance, longer swing in the HP and short stride length in the FP. Interestingly, there were no variables showing variation differences in the FP but most of the variables had large variations in the HP in the *Npc1^{nih}* model. The *Npc1^{nmf164}* mice had a large variation in stand, swing and step cycle in the HP and stand in the FP.

	mean				SD			
	Npc1^{nih}		*Npc1^{nmf164}*		*Npc1^{nih}*		*Npc1^{nmf164}*	
Variables	FP	HP	FP	HP	FP	HP	FP	HP
Stand[1]	ns	ns	ns	ns	ns	ns	↑ **	↑ **
Swing[2]	↓ **	↑ *	ns	↑ *	ns	↑ ****	ns	↑ *
StepCycle[3]	ns	↑ *	ns	ns	ns	↑ **	ns	↑ *
DutyCycle[4]	↑ **	ns	ns	ns	ns	↑ **	ns	ns
StrideLength[5]	↓ ****	↓ **	↓ *	ns	ns	↑ **	ns	ns

Table 2.8: The EBVA results of physical-related variables between models. newline ↑ means the variable has a greater value in the disease model than in the wild type model and vice versa. Significance levels: ns: not significant; *=$p \leq 0.05$; **=$p \leq 0.01$; ***=$p \leq 0.001$; ****=$p \leq 0.0001$.

Definition

[1] Duration of paw contact with the glass plate

[2] Duration of paw not contact with the glass plate

[3] Sum of Stand and Swing

[4] The percentage of Stand in a StepCycle

[5] The distance between successive placements of the same paw

Selected Coordination-related variables

There are three subgroups in coordination-related variables, including Support, Step sequence and Inter-paw interaction. The resulting variables in Inter-paw interaction were first summarized from 90 variables to 24 inter-paw labels. The details were mentioned in section 2.2.2. Fig. 2.14 and Fig. 2.15 show the heat maps of p values after the variable summarization of the Inter-paw interaction group.

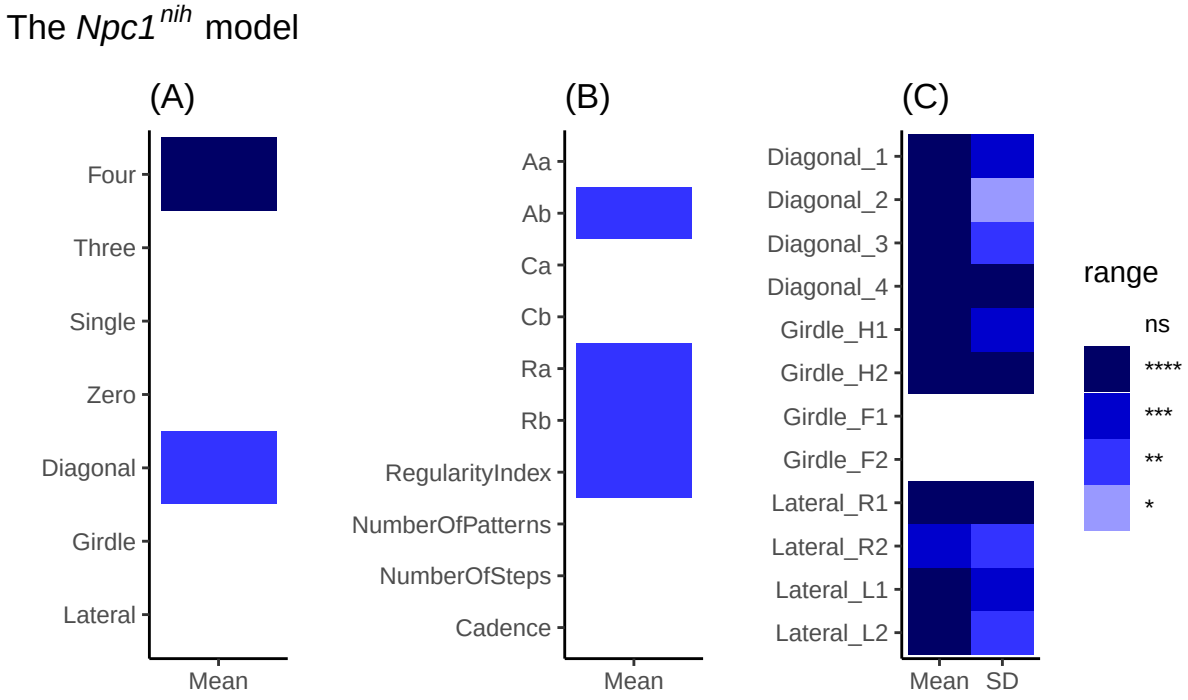


Figure 2.14: The relevant coordination-related variables were found to be modified in the *Npc1*^{nih} model.
(A) Support: a percentage of the duration of listing paw combination contacting the ground.
(B) Step Sequence: 6 pre-defined footfall patterns (Aa, Ab, Ca, Cb, Ra, Rb); Regularity Index: a percentage of the number of steps in 6 pre-defined patterns in total steps; Number of patterns; Number of steps; Cadence: number of steps in a second.
(C) Phase Dispersions/ Couplings in different inter-paw combinations.
Significance levels: ns: not significant; *=$p \leq 0.05$; **=$p \leq 0.01$; ***=$p \leq 0.001$; ****=$p \leq 0.0001$.

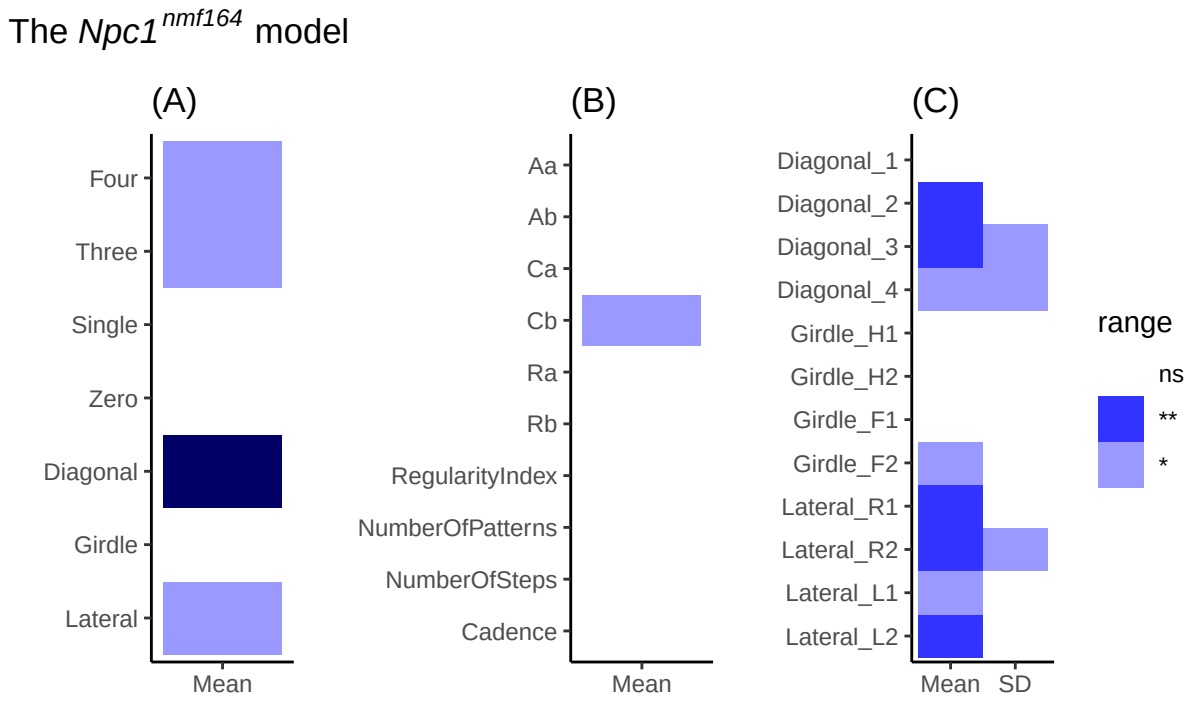


Figure 2.15: The relevant coordination-related variables were found to be modified in the *Npc1*^{nmf164} model.
(A) Support: a percentage of the duration of listing paw combination contacting the ground.
(B) Step Sequence: 6 pre-defined footfall patterns (Aa, Ab, Ca, Cb, Ra, Rb); Regularity Index: a percentage of the number of steps in 6 pre-defined patterns in total steps; Number of patterns; Number of steps; Cadence: number of steps in a second.
(C) Phase Dispersions/ Couplings in different inter-paw combinations.
Significance levels: ns: not significant; *=$p \leq 0.05$; **=$p \leq 0.01$; ***=$p \leq 0.001$; ****=$p \leq 0.0001$.

The summary of the number of relevant variables in both models was in Table 2.9. *Npc1*^{nih} had more severe coordination symptoms as the total number of relevant variables was greater than it in *Npc1*^{nmf164}. Especially, only one step sequence (Cb) was affected in the *Npc1*^{nmf164} model compared to 4 affected in step sequence (Ab, Ra, and Rb) variables in *Npc1*^{nih} mice. In the inter-paw interactions, *Npc1*^{nmf164} had better performance than the *Npc1*^{nih} mice as the variables affected were less in *Npc1*^{nmf164} and they were mainly in mean variables.

Variables	Statistics	Total	*Npc1*^{nih}	*Npc1*^{nmf164}
Coordination-related	Mean	29	16 (55.2%)	13 (44.8%)
	SD	12	10 (83.3%)	3 (25%)
	total	41	26 (63.4%)	16 (39%)

Table 2.9: The number and percentage of coordination-related variables selected by EBVA in both models.

Table 2.10 shows the EBVA results with arrows indicating whether the value is greater (upward arrow) in the disease models than in wild type mice or not (downward arrow). *Npc1*^{nih} and *Npc1*^{nmf164} mice spent less time touching the floor in diagonal paws. *Npc1*^{nih} mice had more time standing on four paws, while *Npc1*^{nmf164} Elevated the time in lateral, four and three paws on the floor. In the *Npc1*^{nih} model, mice walked less in normal step sequences (decreased Regularity Index) with decreed Ab sequence and increased Ra and Rb sequences. *Npc1*^{nmf164} only had decreased Cb sequence. The inter-paw interaction describes the status of the interaction, which means the value of variables cannot be interpreted as more or less interaction. The results can only represent whether the inter-paw interaction is normal or abnormal. *Npc1*^{nih} mice had three altered inter-paw interactions, diagonal, lateral and girdle, while *Npc1*^{nmf164} had severely affected diagonal and lateral interactions with p values less than 0.01. The *Npc1*^{nih} model had large variations in all variables, except Girdle F2. *Npc1*^{nmf164} also had large variations but only in Diagonal 3, Diagonal 4 and Lateral R2.

		mean		SD	
	Variables	*Npc1*^{nih}	*Npc1*^{nmf164}	*Npc1*^{nih}	*Npc1*^{nmf164}
Support[1]	Diagonal	↓ **	↓ ****		
	Lateral	ns	↑ *		
	Four	↑ ****	↑ *		
	Three	ns	↑ *		
Step sequence[2]	Ab	↓ **	ns		
	Cb	ns	↓ *		
	Ra	↑ **	ns		
	Rb	↑ **	ns		
	RegularityIndex	↓ **	ns		
Inter-paw interaction[3]	Diagonal 1	****	ns	↑ ***	ns
	Diagonal 2	****	**	↑ *	ns
	Diagonal 3	****	**	↑ **	↑ *
	Diagonal 4	****	*	↑ ****	↑ *
	Lateral L1	****	*	↑ ***	ns
	Lateral L2	****	**	↑ **	ns
	Lateral R1	****	**	↑ ****	ns
	Lateral R2	***	**	↑ **	↑ *
	Girdle F2	ns	*	ns	ns
	Girdle H1	****	ns	↑ ***	ns
	Girdle H2	****	ns	↑ ****	ns

Table 2.10: The EBVA results of coordination-related variables between models.
↑ means the variable has a greater value in the disease model than in the wild type model and vice versa. Significance levels: ns: not significant; *=$p \leq 0.05$; **=$p \leq 0.01$; ***=$p \leq 0.001$; ****=$p \leq 0.0001$.

Definition

[1] The duration percentage of contact with the glass plate of certain paws. For example, four paws support and diagonal paws support.

[2] The percentage of a certain pre-defined footfall pattern in a run. For example, Rb is clockwise step sequence begins from left front paw. Regularity Index is the percentage of the total number of 6 pre-defined footfall patterns in a run.

[3] The temporal relationship between placement of two paws within a StepCycle. Each interaction label is summarized from Phase Dispersions and Couplings.

2.4 Discussion

2.4.1 Neuropathology and motor behaviours

The loss of Purkinje cells in the cerebellum is one of the hallmarks of NPC, and neurodegenerative symptoms are potentially the main causes of gait abnormalities in the NPC mouse models. The apparent loss of Purkinje cells can be seen in Zebrin II-negative cells in lobules I to V of the cerebellum by the age of 7 weeks in *Npc1*^{nih} mice and spreads to Zebrin II-positive and negative cells in lobes I to IX at the age of 9 weeks [125]. Coordination-related symptoms are evident by 7 weeks of age, and both coordination-related and physical-related symptoms become severe by the age of 8 weeks. This might indicate that Zebrin II-negative cells in lobules I to V affect the coordination of the mouse, while Zebrin II-positive cells affect physical strength. The increased survival of Purkinje cells in miglustat treated *Npc1*^{nih} mice and the improvement in motor function also support the importance of Purkinje cells and motor function in *Npc1*^{nih} mice [126]. Additionally, the loss of Purkinje cell in *Npc1*^{nmf164} at 9 weeks of age is similar to *Npc1*^{nih} at 6 weeks of age [61] and there are no obvious motor symptoms in *Npc1*^{nmf164} mice before 8 weeks of age. Therefore, the interruption of signals between the climbing fibres and the mossy fibre-granule cells in the cerebellar circuit could be a potential cause of behavioral impairments [127]. Further experiments using detailed Catwalk results are required to determine the specific neuronal circuit responsible for hind or front limb control.

2.4.2 The Evidence Based Gait Analysis Method (EBGAM)

NPC is a progressive neurodegenerative disease, with ataxia as a major clinical sign due to cerebellar degeneration. The Catwalk system is widely used for rodent gait analysis [128]. It can generate data on a total of 495 variables to describe the gait features of a mouse. The Catwalk system is one of several automated systems available commercially to measure gait variables from murine models. However, to date researchers have reported only a limited number of variables typically selected based on a hypothesis, as there is no standardized process to

analyse the results in an unbiased evidence based way [114]. This hypothesis-driven selection of variables currently in the literature neglects the potential negative impacts on variables and the SD of variables, which is an indicator of variation in a variable. Furthermore, current methods do not filter out noise in the data set. In this thesis, the development of EBGAM provides a number of innovations when analysing gait data from the Catwalk system.

Almost half of all runs are wrongly classified by the Catwalk system before manual verification is performed [129]. This means the system fails to detect the noise in data sets and misleading results can therefore arise. In this thesis, EBGAM has been evaluated as an analytical approach to overcome the major limitations of gait analysis. EBGAM involves 5 sequential steps, namely data collection, data cleaning, data preparation, data analysis and data presentation. The quality of the data is guaranteed by applying EBGAM. The cleaning process in EBGAM is the step required to achieve high quality and quantity of data that can be further analysed. The gait analysis is limited to walking behaviours and non-walking behaviours were removed by data segmentation and the paw signals were optimized. This step is essential when analysing the $Npc1^{nih}$ model. The weight of $Npc1^{nih}$ mice from 8 weeks of age becomes light and it results in weak paw signals in the Catwalk system. The variables generated from the Catwalk system are fundamentally based on the values of paw signals. Therefore, the quality of paw signals is crucial to enhancing the quality and quantity of data sets from the Catwalk system. The usage of gait data from $Npc1^{nih}$ mice after 8 weeks of age can therefore be improved by using EBGAM.

2.4.3 The characterization of NPC models by Evidence Based Variable Analysis

Evidence Based Variable Analysis (EBVA) is an important and novel method within EBGAM. It is included in the data analysis step of EBGAM (see section 2.2.2). The EBVA can provide statistical evidence in identifying relevant variables for the first time. The human judgment in selecting variables can be minimized. The EBVA

can identify the relevant variables altered in an animal disease model. The relevant variables are affected by disease progression and EBVA can identify them using the mixed effects ANOVA model. The model is able to distinguish the different trends between normal healthy ageing and disease progression over well-defined time points. The collection of relevant variables provides a unique signature of a specific animal model. For instance, there is a relatively small number of NPC murine models with distinctly different phenotypes [44]. The *Npc1*^{nih} model is characterized by rapid progression of NPC disease (late infantile form, living only to 12 weeks of age) while the *Npc1*^{nmf164} model has a slower rate of progression (juvenile form, living to 16 Weeks (112 days)) [44, 61]. They have similar biological presentations, such as abnormal cholesterol accumulation in various organs, glial activation, and Purkinje cell loss. However, these presentations progress at a slower rate in the *Npc1*^{nmf164} than in the *Npc1*^{nih} model [61]. The myelination defect is less severe in the *Npc1*^{nmf164} than in the *Npc1*^{nih} [61, 130]. The slower progression in *Npc1*^{nmf164} can also be observed in behavioural performance [61]. The findings from this chapter are in agreement with these studies. The *Npc1*^{nmf164} mice have moderate disease progression in terms of gait analysis. With the power of EBVA, we can provide more insights from the Catwalk system supported by sound statistical evidence.

We found that the symptoms of gait became apparent from 12 weeks of age in *Npc1*^{nmf164} mice, while *Npc1*^{nih} mice had physical symptoms as early as 6 weeks of age and coordination defect symptoms can be seen at 7 weeks of age. The number of SD variables affected was less in the *Npc1*^{nmf164} than in the *Npc1*^{nih} model through the time points observed (Table 2.6 and Table 2.5). The SD of variables indicates the variation of corresponding features in the animal's gait. In other words, *Npc1*^{nmf164} mice had better control of movement than *Npc1*^{nih} mice. EBVA further revealed the characteristics of both models.

Npc1^{nih} mice had more severe physical signs than *Npc1*^{nmf164} mice. *Npc1*^{nih} mice had longer swing duration in the front paws, and shorter swing duration in the hind paws and the distance travelled by each step (front paws and hind paws) was reduced. The *Npc1*^{nmf164} mice only observed an adverse impact on the HP swing

duration and the FP stride length. In terms of SD variables, NPC only affected *Npc1*^{nih} mice's hind paws. *Npc1*^{nmf164} mice had increased variation in the FP and HP stand, which were unaffected in the *Npc1*^{nih} model.

Both models had different presentations in coordination-related variables, especially in step sequences. *Npc1*^{nmf164} mice only had reduced Cb[1] sequences, while there were more step sequences affected in the *Npc1*^{nih} model. Moreover, *Npc1*^{nih} mice had more variation (SD) of inter-paw interactions than *Npc1*^{nmf164}.

These disease presentation differences might be the result of the different genetic backgrounds of the two mouse models (i.e. the influences of modifying genes)[131]. *Npc1*^{nih} mice are on a BALB/c background with the null allele representing the more severe infantile NPC1 patients, whereas the *Npc1*^{nmf164} model is on a C57BL/6J background with the *nmf164* allele being a point mutation resulting a change in the cysteine-rich luminal loop of the NPC1 protein. The cysteine-rich luminal loop defect in NPC1 protein is a common human mutation [61]. However, the extent to which the differences observed here can be segregated by genetic background as opposed to the level of functional *Npc1* requires further research, ideally replication of EBGAM in two mouse models with the same *NPC1* status and with the only independent variable being genetic background.

The results of variable selection provide more evidence to distinguish between these two models, at the functional level. The different ages of disease onset are clearly detected by EBGAM and can be seen in the overview of the results.

In summary, EBGAM is a novel method to analyse gait data from the Catwalk system. It reveals similarities and unique differences between the two models of NPC. Having established the EBGAM method and validated it in two NPC mouse models, the next question I wanted to answer was whether EBGAM is sensitive enough to identify the differential effects of disease-modifying therapies. This important question is investigated in Chapter 3.

[1]Cb step sequence: LF-RF-LH-RH

3

Catwalk data analysis of *Npc1*$^{-/-}$ mice treated with miglustat, the HSP70 inducing drug (arimoclomol) or a combination of both

Contents

3.1 Introduction 52
3.2 Materials and Methods 53
3.2.1 Animal model 53
3.2.2 Treatments 53
3.2.3 The Evidence Based Gait Analysis Method 54
3.2.4 Data presentation 55
3.2.5 Statistical analysis environment 55
3.2.6 The definition of variables and statistics 55
3.3 Results 55
3.3.1 The summary of the data set 55
3.3.2 The results of Evidence Based Variable Analysis 57
3.3.3 Treatments results 61
3.3.4 The summary of treatments 72
3.3.5 Improvement Scores 75
3.4 Discussion 78
3.4.1 The results of EBVA 78
3.4.2 The effects of treatments 79

3.1 Introduction

One of the challenges of using mouse models of lysosomal storage diseases, such as NPC, is that we lack sensitive methods to monitor functional changes in treated mice to better understand the differential effects of drugs that target different steps in the pathogenic cascade. Furthermore, a greater degree of analytical sensitivity is essential for determining the effects of combination therapies. As described in Chapter 2, Evidence Based Gait Analysis Method (EBGAM) is a promising method for analysing gait data in the Catwalk system. It generates objective and reliable results with minimal data noise. In this chapter, the focus is on a combination study in NPC null mice ($Npc1^{nih}$) treated with miglustat and arimoclomol. We only looked at the effects of treatments on gait performance using the Catwalk system with EBGAM. Miglustat is currently the only treatment approved for NPC in most countries, except in the USA [74]. It can reduce the levels of glycosphingolipids (GSLs) by irreversibly inhibiting the enzyme glucosylceramide synthase [132]. Miglustat can improve motor function and prolong survival in NPC animal models [72] and in clinical studies [133–135]. The other small molecule is the heat shock protein 70 (HSP70) inducer, arimoclomol. It can amplify a stress response by increasing the levels of the heat shock protein 70 (HSP70) [136]. Indeed, when recombinant HSP70 was administered to the $Npc1^{nih}$ mouse model functional benefits were observed, particularly through improvements in myelin structure and function [136]. Arimoclomol was evaluated in a clinical trial and was shown to improve the 5-domain NPCCSS (NPC Clinical Severity Scale) [137]. The 5-domain assessment includes Ambulation (walking), Swallow, Cognition, Speech and Fine Motor skills [137]. In this study, their differential and combined effects were studied in depth using gait analysis as an indicator of cerebellar dysfunction and differential response to therapy.

Apart from the EBGAM, the improvement score also is introduced in this chapter to summarize the results. The score is defined as a significant improvement

in either the mean or SD of a variable. Instead of showing the resulting p value of treatment in a figure, the improvement score can summarize the result from multiple treatment studies in one figure. By doing this, the results can be more easily compared and interpreted.

All in all, the usefulness, and the power of differentiating therapeutic effects on a combination study will be demonstrated by the Catwalk system with EBGAM. The results of EMGAM can provide statistical evidence for therapies in further pre-clinical or clinical experiments.

3.2 Materials and Methods

3.2.1 Animal model

Npc1^{nih}

See section 1.5.1

3.2.2 Treatments

This study was conducted by Dr Maysa Falah in the Platt Laboratory, Department of Pharmacology, University of Oxford. There were three treatment arms in the study, namely miglustat (Mig, section 1.6.1), arimoclomol (Arim, section 1.6.2) and combination (Comb) therapy (miglustat and arimoclomol). The dose of arimoclomol in drinking water was $30mg/Kg/day$. The dose of miglustat in the powdered diet was $600mg/Kg/day$. The treatments started at 3 weeks of age at weaning.

The rationale for the selected dose levels was based on previous studies showing an increased rate of survival in animals receiving arimoclomol $30mg/kg/day$ in drinking water [136] or miglustat 600 mg/kg/d in food [121, 126] when animals were treated from 3 weeks of age. The sample size was also based on previous studies of the *Npc1^{nih}* mouse model in our laboratory and power calculations and known effect sizes from pilot studies. Only females were included to allow group housing of mice. No sex differences have been observed in response to either of these treatments in multiple studies in this mouse model.

3.2.3 The Evidence Based Gait Analysis Method

The detail of the standard process is in section 2.2.2. From this chapter to Chapter 4, the variables selected by EBVA were analysed by one-way ANOVA with Tukey HSD at each time point in the data analysis step in EBGAM, which will be mentioned in the following sections.

Data analysis

Multiple one-way ANOVA with post hoc analysis One-way ANOVA compares Hom untreated and treated groups at a specific time point. This is included in the data analysis step in the procedure of EBGAM. The trend of the effectiveness of treatments can be uncovered using the one-way ANOVA at multiple time points. The Tukey honest significant difference test (Tukey HSD) is followed and adjusts the p value in group comparisons. The resulting p value indicates the comparison of Hom untreated with either miglustat (Mig) or arimoclomol (Arim) or combination (Comb) treated mice. Additionally, the directional sign will add to the resulting p value to determine whether the significant change of a variable is an improvement (positive) or a deterioration (negative), which will be mentioned in the following section.

The directional sign of a change in a variable The directional sign is to determine whether a significant difference between the untreated and treated group is improvement or deterioration in a variable. The definition of a positive sign (improvement) is that the sign of the value difference between the untreated and treated group is the same as the sign of the value difference between the untreated and WT group. In another word, the treatment can alter the value of a variable in $Npc1^{nih}$ mice close to the value in the WT group.

3.2.4 Data presentation

The improvement score

Apart from presenting the resulting p value as heat maps, the improvement score summarizes the statistics (mean and SD) of a variable and reduces the number of heat maps in comparing the results between groups. The definition of an improvement score is a significant improvement in either the mean or SD of a variable. Therefore, the highest score is 2 from improvements in both the mean (one score) and SD (one score) of a variable. The improvement is defined as a positively significant change of a variable (the significance level is defined as p value≤ 0.05). On the other hand, the negatively significant change is a minus score.

3.2.5 Statistical analysis environment

See section 2.2.2

3.2.6 The definition of variables and statistics

See Appendix A.1

3.3 Results

3.3.1 The summary of the data set

This study involved two control groups (untreated WT and untreated Homs) and three treatment arms, miglustat (Mig), arimoclomol (Arim) and the combination (Comb) of Mig and Arim. There were 6 mice in each control group (WT and Hom), 8 mice for Mig and Comb and 7 mice for the Arim group. The summary of the data set after the data cleaning process is shown in Table 3.1. The gait of mice was measured at 6, 8 and 10 weeks of age. The AD means absent data in the trial column. The absent data was frequently caused by mice reluctant to walk or immobile mice.

The AD were removed from the data set in the following data analysis. The number of trials included is shown in Table 3.2. Gait measurement of individual mice in the Catwalk system generated a trial.

ID	Group	Age	Trial	Age	Trial	Age	Trial
869.4f	WT	6	Trial0015	8	Trial0034	10	Trial0055
869.4h	WT	6	Trial0016	8	Trial0035	10	Trial0056
875.5e	WT	6	Trial0018	8	Trial0037	10	Trial0058
901.1g	WT	6	Trial0022	8	Trial0040	10	Trial0053
901.1j	WT	6	Trial0023	8	Trial0041	10	Trial0063
902.2f	WT	6	Trial0017	8	Trial0036	10	Trial0057
861.5d	Hom	6	Trial0021	8	Trial0042	10	Trial0052
899.1e	Hom	6	AD	8	Trial0038	10	AD
899.1g	Hom	6	AD	8	Trial0039	10	AD
917.3d	Hom	6	Trial0046	8	Trial0067	10	Trial0079
929.2d	Hom	6	Trial0047	8	Trial0068	10	Trial0078
941.1g	Hom	6	Trial0072	8	AD	10	AD
864.4d	Mig	6	Trial0030	8	Trial0049	10	Trial0071
865.4e	Mig	6	Trial0009	8	Trial0024	10	Trial0043
877.2j	Mig	6	Trial0010	8	Trial0025	10	Trial0044
877.4h	Mig	6	Trial0079	8	AD	10	Trial0099
910.2g	Mig	6	Trial0074	8	AD	10	AD
910.5d	Mig	6	Trial0036	8	Trial0058	10	Trial0073
917.3g	Mig	6	Trial0045	8	Trial0066	10	Trial0077
923.4c	Mig	6	Trial0043	8	Trial0064	10	Trial0080
885.3d	Arim	6	Trial0032	8	Trial0051	10	AD
904.5d	Arim	6	Trial0035	8	Trial0053	10	Trial0071
909.1c	Arim	6	Trial0014	8	Trial0029	10	AD
910.1f	Arim	6	Trial0013	8	Trial0028	10	AD
910.5c	Arim	6	Trial0037	8	Trial0057	10	AD
917.1d	Arim	6	Trial0033	8	AD	10	AD
934.2d	Arim	6	Trial0059	8	Trial0075	10	AD
864.4g	Comb	6	Trial0031	8	Trial0050	10	Trial0072
877.2f	Comb	6	Trial0011	8	Trial0026	10	Trial0045
885.5a	Comb	6	Trial0093	8	AD	10	AD
885.5f	Comb	6	Trial0094	8	AD	10	AD
909.1b	Comb	6	Trial0012	8	Trial0027	10	Trial0046
911.3h	Comb	6	AD	8	Trial0007	10	Trial0016
920.2e	Comb	6	Trial0008	8	Trial0010	10	AD
930.1e	Comb	6	Trial0009	8	Trial0011	10	Trial0034

Table 3.1: The data summary of the arimoclomol study.
WT: wild-type untreated mice; Hom: *Npc1^{nih}* untreated mice; Mig: miglustat treated mice; Arim: arimoclomol treated mice; Comb: miglustat and arimoclomol treated mice. AD: absent data.

		No. trials		
Groups	No. mice	6wks	8wks	10wks
WT	6	6	6	6
Hom	6	4	5	3
Mig	8	8	6	7
Arim	7	7	6	1
Comb	8	7	6	5

Table 3.2: The number of trials between groups.
WT: wild-type untreated mice; Hom: *Npc1^{nih}* untreated mice; Mig: miglustat treated mice; Arim: arimoclomol treated mice; Comb: miglustat and arimoclomol treated mice.

3.3.2 The results of Evidence Based Variable Analysis

Selected Physical-related variables

A total of 79 variables were associated with physical features in the *Npc1*^{nih} model in this study that manifested between 6 to 10 weeks of age. There are 49 mean and 30 SD of variables summarized in Table 3.3. Over half of physical-related variables (57.2%) were shown to be affected in this model between 6 to 10 weeks of age with 70 per cent of mean variables and 44 per cent of SD variables. Fig 3.1 shows the p value results of EBVA of physical-related variables and displays the results in two manners, a paw-wise manner (FP: front paws; HP: hind paws; LF: left front; LH: left hind; RF: right front; RH: right hind) and a non-paw-wise manner.

Variables	Statistics	Total	Hom
Physical-related	Mean	70	49 (70%)
	SD	68	30 (44.1%)
	total	**138**	**79 (57.2%)**

Table 3.3: The number of relevant physical-related variables selected by EBVA.

In Fig 3.1, the variables in the front and hind paws were affected in a similar manner. The mean of Duty Cycle was only present in the FP and the SD of the Initial Dual Stance was only observed in the HF. The number of SD with a significance level of $p \leq 0.001$ in the hind paws is more than those in the front paws, especially in Swing, Step Cycle and Terminal Dual Stance. The significance levels in the mean of variables were similar in both FP and HP while the level of significance in SD variables was prominent in the HP.

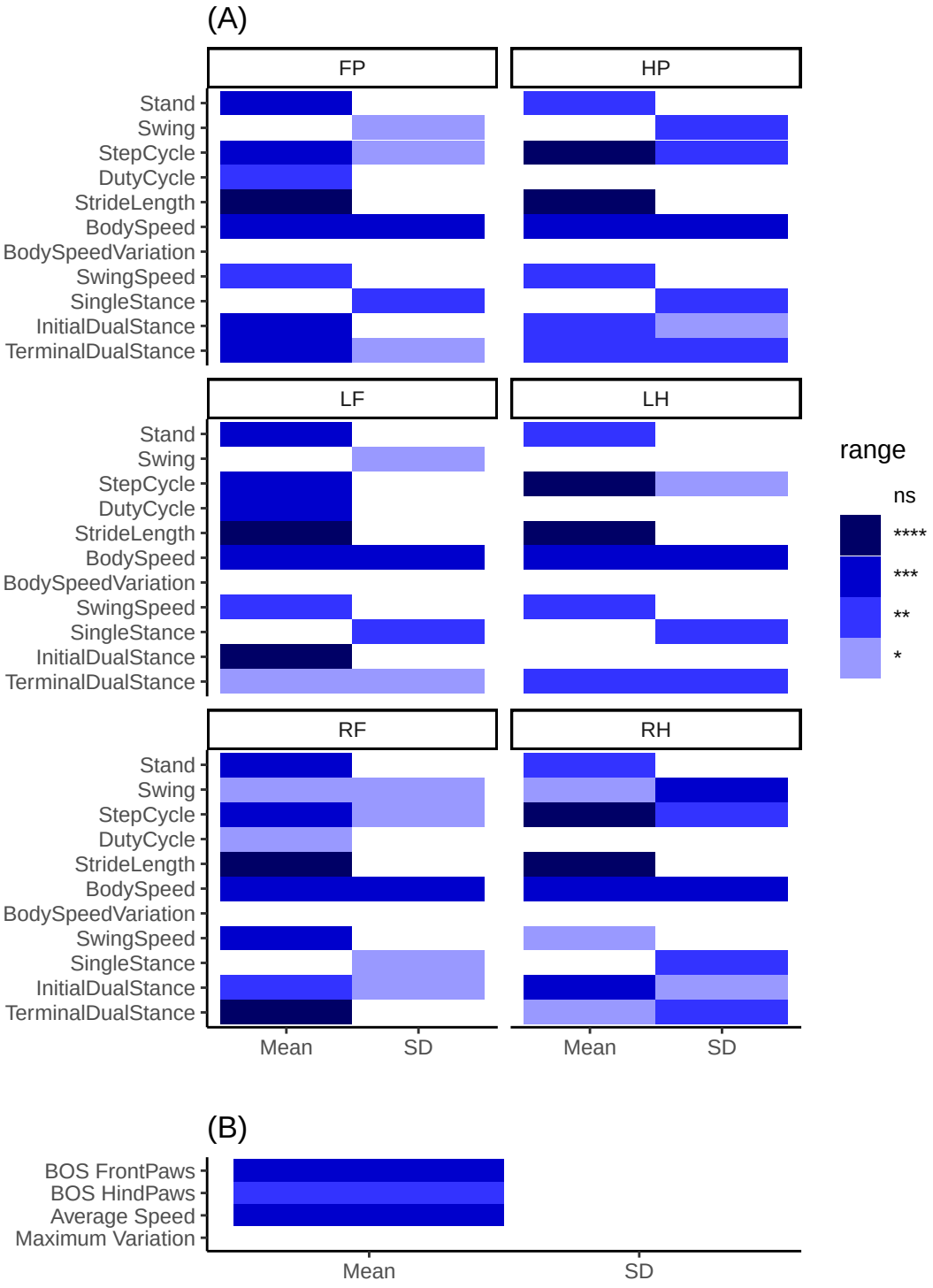


Figure 3.1: The relevant physical-related variables were found to be modified in the *Npc1*^{nih} model in (A) paw-wise and (B) non-paw-wise variables in the arimoclomol study. FP: front paws; HP: hind paws; LF: left front paw; LH: left hind paw; RF: right front paw; RH: right hind paw. The colours represent different significant levels.
Significance levels: ns: not significant; *=$p \leq 0.05$; **=$p \leq 0.01$; ***=$p \leq 0.001$; ****=$p \leq 0.0001$.

Selected Coordination-related variables

There was a total of 52 variables selected in the coordination-related group, which was just below 50% of the total (107) in Table 3.4. In order to better interpret the circular statistics (CStat) in the results of Phase Dispersion and Couplings, these variables were summarized into 12 interlimb labels with mean and SD (see section 2.2.2). After summarization, there were 30 out of 41 variables that were relevant to this study, over two-thirds of the total (73.2%) in Table 3.5.

Variables	Statistics	Total	Hom
Coordination-related	mean	35	14 (40%)
	SD	18	11 (61.1%)
	CStat mean	18	6 (33.3%)
	CStat SD	18	7 (38.9%)
	CStat R	18	14 (77.8%)
	total	107	52 (48.6%)

Table 3.4: The number of relevant coordination-related variables selected by EBVA before summarization. CStat: circular statistics

Variables	Statistics	Total	Hom
Coordination-related	Mean	29	22 (75.9%)
	SD	12	8 (66.7%)
	total	**41**	**30 (73.2%)**

Table 3.5: The number of relevant coordination-related variables selected by EBVA after summarization.

The p values are shown in Fig 3.2. Fig 3.2 A displays the Support variables, the time duration of touching the floor with all four paws, diagonal paws and girdle paws (front paws or hind paws) were observed to significantly change with diseases progression. In Fig 3.2 B, the step sequences of walking were affected in Ab, Ca, Ra and Rb sequences (the 6 predefined step sequences were explained in Appendix A.1). In addition, the Regularity Index, Number of Patterns and Cadence of *Npc1*$^{-/-}$ mice were also shown to be affected (see Appendix A.1). The mean of

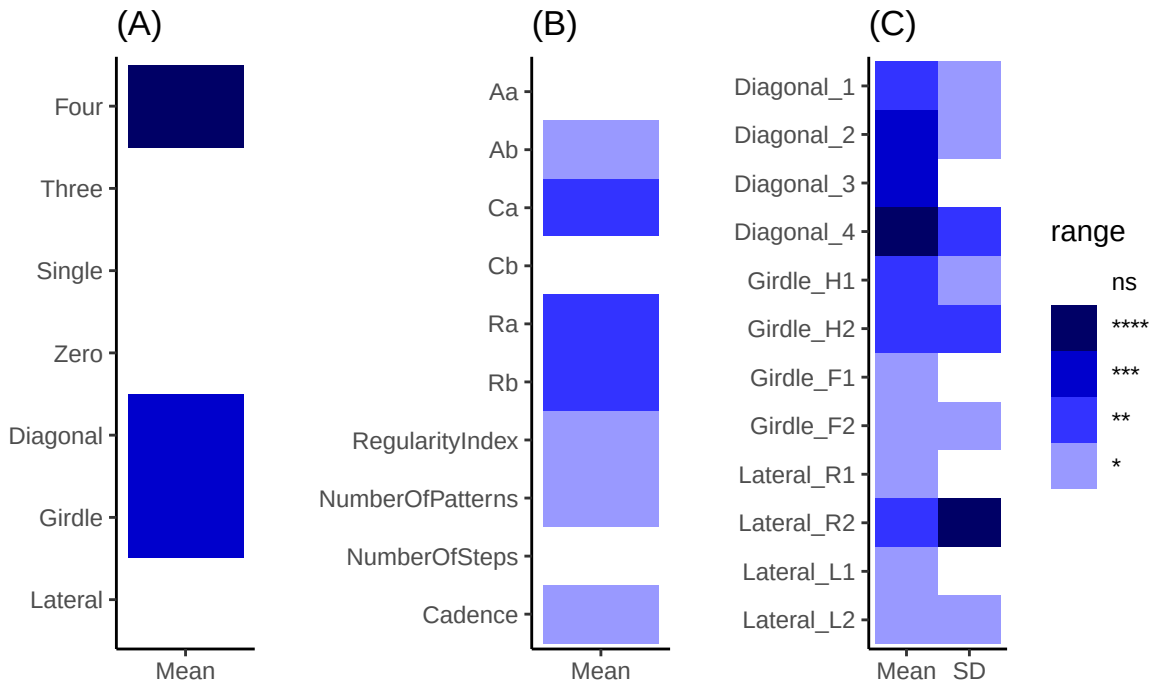


Figure 3.2: The relevant coordination-related variables were found to be modified in the *Npc1*^{nih} model in the arimoclomol study.
(A) Support: a percentage of the duration of listing paw combination contacting the ground.
(B) Step Sequence: 6 pre-defined footfall patterns (Aa, Ab, Ca, Cb, Ra, Rb); Regularity Index: a percentage of the number of steps in 6 pre-defined patterns in total steps; Number of patterns; Number of steps; Cadence: number of steps in a second.
(C) Phase Dispersions/ Couplings in different inter-paw combinations.
Significance levels : ns: not significant; *=$p \leq 0.05$; **=$p \leq 0.01$; ***=$p \leq 0.001$; ****=$p \leq 0.0001$.

inter-paw interaction variables were all altered in Fig 3.2 C, especially in diagonal paw interaction with a high significance level (p value ≤ 0.01).

3.3.3 Treatments results

Physical-related variables

Following the results from EBVA, there were 79 physical-related variables considered relevant to this study with 49 mean and 30 SD variables in Table 3.3. The one-way ANOVA and Tukey HSD only focused on these variables at 6, 8 and 10 weeks of age. In order to determine whether there was an improvement or a deterioration of a significant change in a variable from group comparison, the p values were multiplied by the directional sign (see section 3.2.3). Table 3.6 summarizes the number of variables showing either positive (improvement) or negative (deterioration) effects between the treated groups. The number of improved variables in the Comb and Mig groups gradually increased and there was no negative effect observed from these two groups during the treatment period. The number of variables with improvement in the Mig group was greater than in the Comb group. However, there was only deterioration of variables in the Arim group at 10 weeks of age without any positive effects.

		Improvement			Deterioration		
Groups	Statistics	6weeks	8weeks	10weeks	6weeks	8weeks	10weeks
Mig	mean (49)	1 (2%)	28 (57.1%)	38 (77.6%)	0 (0%)	0 (0%)	0 (0%)
Arim		0 (0%)	0 (0%)	0 (0%)	0 (0%)	0 (0%)	7 (14.3%)
Comb		0 (0%)	19 (38.8%)	21 (42.9%)	0 (0%)	0 (0%)	0 (0%)
Mig	SD (30)	0 (0%)	4 (13.3%)	14 (46.7%)	0 (0%)	0 (0%)	0 (0%)
Arim		0 (0%)	0 (0%)	0 (0%)	0 (0%)	0 (0%)	8 (26.7%)
Comb		0 (0%)	2 (6.7%)	7 (23.3%)	0 (0%)	0 (0%)	0 (0%)

Table 3.6: The summary of the number and percentage of variables showing either improvement or deterioration effects between treated groups in physical-related variables. Mig: miglustat; Arim:arimoclomol; Comb: miglustat and arimoclomol.

The resulting p values from Tukey HSD are presented in the following four heat maps (Fig. 3.3, Fig. 3.4, Fig 3.5 and Fig. 3.6). The first three heat maps (Fig. 3.3 , Fig. 3.4 and Fig 3.5) display variables in a paw-wise manner.

The last heat map (Fig. 3.6) includes variables in a non-paw-wise manner. The significance levels were defined as $p \leq 0.05$(*), ≤ 0.001 (**), ≤ 0.001(***) and ≤ 0.0001(*****). The colours (blue and red) indicate improvement (positive) and deterioration (negative) of a variable respectively.

Miglustat Fig 3.3 shows the results of Tukey HSD, comparing the Hom untreated and the Mig treated group. The grey cells in the heat map in Fig. 3.3 indicate irrelevant variables identified by the EBVA. There was no significant difference in these variables at 6 weeks of age. The treatment benefits of Mig were apparent from 8 weeks of age. The effects of Mig were mainly in the mean of physical-related variables. The number and significance levels of improved variables increased from 8 to 10 weeks of age. Body Speed (the distance the mouse's body travelled during the swing time of a specific paw), Stride Length and Step Cycle were improved from 8 weeks of age in all four paws. Mig had more positive effects on the front paws as the number and significance levels of improved variables were greater than those in the hind paws. In terms of SD variables, Mig was more effective in the hind paws since the number of SD improved variables was greater than that in the front paws at 8 and 10 weeks of age.

Arimoclomol Fig. 3.4 shows the results of Tukey HSD, comparing Hom untreated and Arim treated *Npc1*^{nih} mice. Before 8 weeks of age, Arim had no significant effect on the paw variables. However, the hind paws were negatively affected by Arim at 10 weeks of age. The deterioration of the hind paws can be seen in variables associated with stances, such as Stance, Terminal Dual Stance and Step Cycle. Additionally, the variation (SD) of these variables in the Arim group became greater than those in the untreated group at 10 weeks of age.

Combination Fig. 3.5 shows the group comparison results from Tukey HSD between the Hom untreated and the Comb (miglustat and arimoclomol) treated groups. The profile of results is similar to the profile of Mig treatment at the onset of the treatment effect, beginning from 8 weeks of age. The number and significance

levels of improved variables in the FP and HP decreased from 8 to 10 weeks of age. The front paw had more beneficial effects by Comb than in the hind paws since the number of improved variables in the front paws was greater than it in the hind paws. The improvements in Step Cycle and Stride Length occurred in different paws and time points, while these improvements were observed in all four paws from 8 to 10 weeks of age in the Mig group (Fig. 3.3). Body Speed was one of the improved variables in the Mig treated mice, but there was no improvement in any paws in the Comb Group. The deteriorations in stance related variables in the Arim group at 10 weeks of age were counteracted by miglustat in the combination.

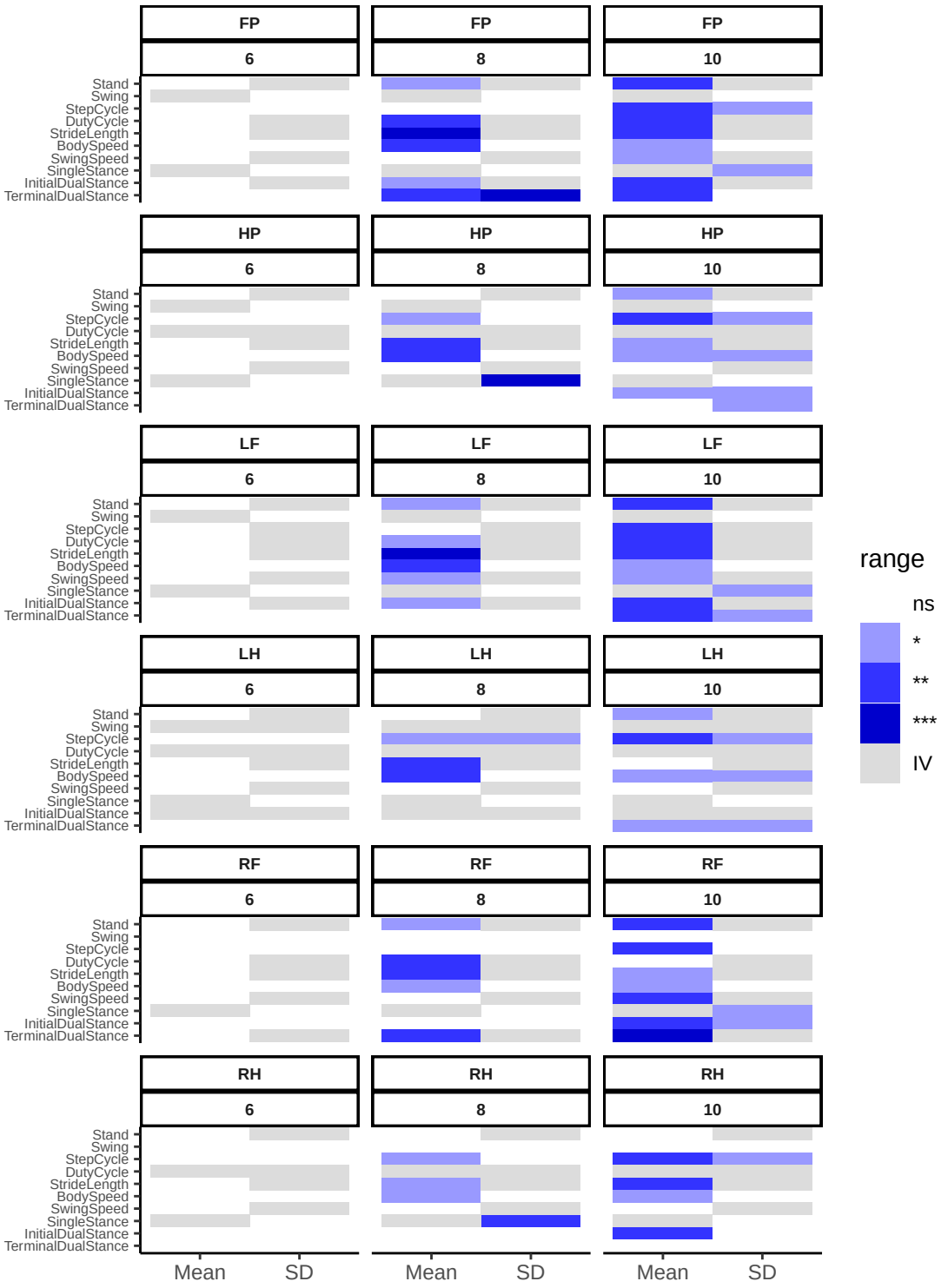


Figure 3.3: Heatmap of the results from one-way ANOVA and post hoc analysis in paw-wise variables in *Npc1*^{nih} with miglustat therapy. FP: front paws; HP: hind paws; LF: left front paw; LH: left hind paw; RF: right front paw; RH: right hind paw. The colours represent different significant levels. The grey colour indicates irrelevant variables (IV).
IV: irrelevant variables; Significance levels: ns: not significant; *=$p \leq 0.05$; **=$p \leq 0.01$; ***=$p \leq 0.001$; ****=$p \leq 0.0001$.

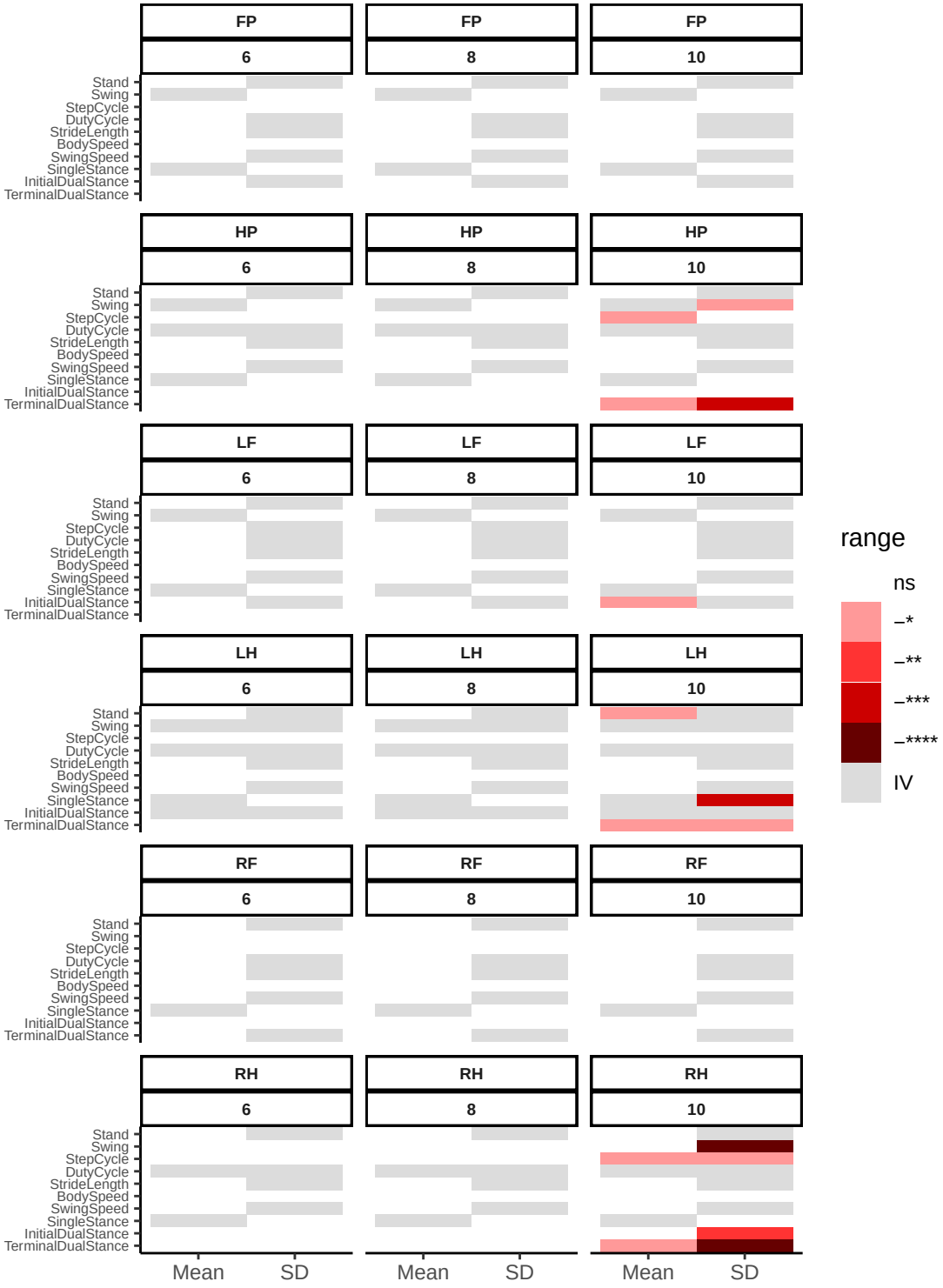


Figure 3.4: Heatmap of the results from one-way ANOVA and post hoc analysis in paw-wise variables in *Npc1^{nih}* with arimoclomol therapy. FP: front paws; HP: hind paws; LF: left front paw; LH: left hind paw; RF: right front paw; RH: right hind paw. The colours represent different significant levels. The grey colour indicates irrelevant variables (IV).
IV: irrelevant variables; Significance levels: ns: not significant; *=$p \leq 0.05$; **=$p \leq 0.01$; ***=$p \leq 0.001$; ****=$p \leq 0.0001$.

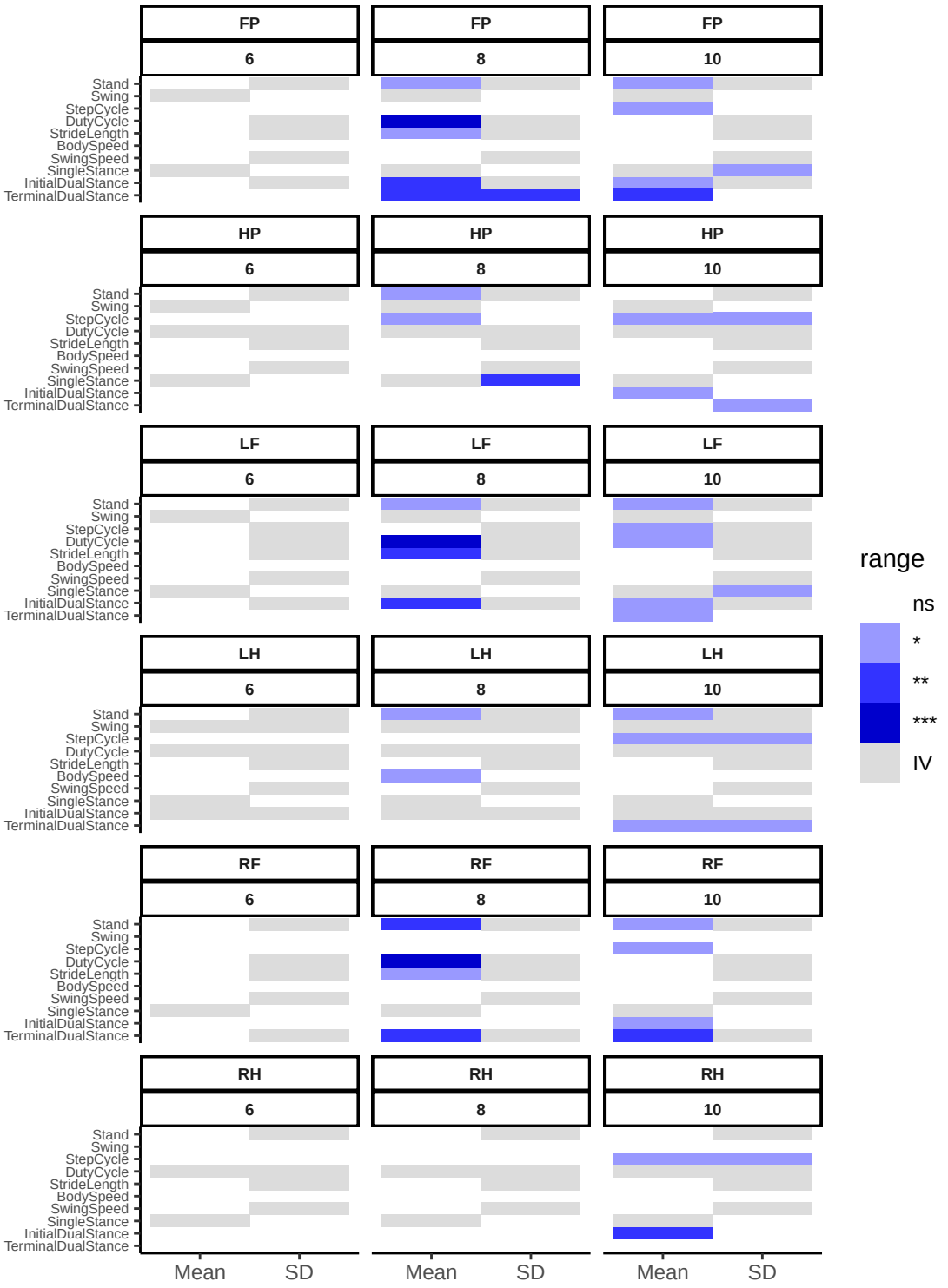


Figure 3.5: Heatmap of the results from one-way ANOVA and post hoc analysis in paw-wise variables in *Npc1*^{nih} with combination therapy. FP: front paws; HP: hind paws; LF: left front paw; LH: left hind paw; RF: right front paw; RH: right hind paw. The colours represent different significant levels. The grey colour indicates irrelevant variables (IV).
IV: irrelevant variables; Significance levels: ns: not significant; *=$p \leq 0.05$; **=$p \leq 0.01$; ***=$p \leq 0.001$; ****=$p \leq 0.0001$.

Non-paw-wise variables Fig 3.6 shows three variables (Average Speed, Base of Support (BOS) hind paws and Base of Support front paws) in the three treatment groups at 6, 8 and 10 weeks of age. Mice treated with Arim did not show any improvement in these three variables during the time frame studied. In the Comb group, the average speed was improved only at 8 weeks of age, while the speed associated variables in paw, Body Speed, did not show improvements. The front paws' BOS (base of support) was improved from 8 to 10 weeks of age in both Comb and Mig groups. The improvement in the hind paws' BOS was only seen at 6 weeks of age in the Mig group.

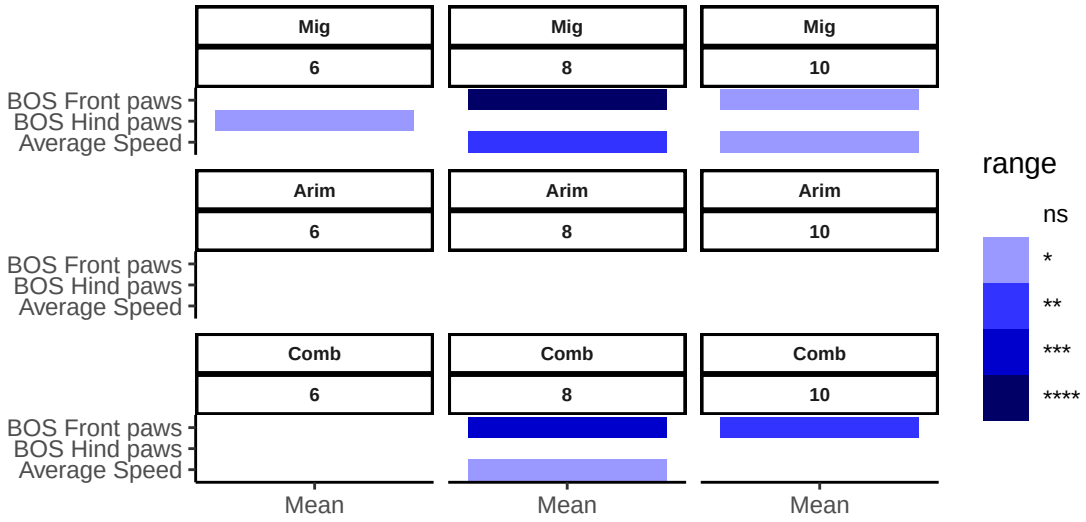


Figure 3.6: Heatmap of the results from one-way ANOVA and post hoc analysis in non-paw-wise variables in $Npc1^{nih}$.
The columns from left to right present time points from 6 to 10 weeks of age. The rows from top to bottom are group comparisons with Hom untreated group from miglustat, arimoclomol and combination. The colours represent different significant levels.
Significance levels: ns: not significant; *=$p \leq 0.05$; **=$p \leq 0.01$; ***=$p \leq 0.001$; ****=$p \leq 0.0001$.

Coordination-related variables

Table 3.7 and Table 3.8 show the number and percentage of variables which were impacted by the treatments. There are five statistics, including circular statistics in Table 3.7. After variable summarization in Table 3.8, the Mig and Comb groups had their best effects on coordination-related mean variables at 8 weeks of age with 31.8% and 18.2% variables improved respectively, while there is no SD variables improvement observed. In the Arim group, there were 9.1% mean variables improved at 6 weeks of age and 10 weeks of age, but there were also negative effects seen at 10 weeks of age in mean and SD variables with 22.7% and 25% variables deteriorated respectively.

		Improvement			Deterioration		
Groups	Statistics	6weeks	8weeks	10weeks	6weeks	8weeks	10weeks
Mig	mean (14)	4 (28.6%)	6 (42.9%)	4 (28.6%)	0 (0%)	0 (0%)	0 (0%)
Arim		2 (14.3%)	0 (0%)	2 (14.3%)	0 (0%)	0 (0%)	4 (28.6%)
Comb		4 (28.6%)	5 (35.7%)	2 (14.3%)	0 (0%)	0 (0%)	0 (0%)
Mig	SD (11)	0 (0%)	0 (0%)	0 (0%)	0 (0%)	0 (0%)	0 (0%)
Arim		0 (0%)	0 (0%)	0 (0%)	0 (0%)	0 (0%)	2 (18.2%)
Comb		0 (0%)	0 (0%)	0 (0%)	0 (0%)	0 (0%)	0 (0%)
Mig	CStat mean (6)	0 (0%)	6 (100%)	0 (0%)	0 (0%)	0 (0%)	0 (0%)
Arim		0 (0%)	0 (0%)	0 (0%)	0 (0%)	0 (0%)	0 (0%)
Comb		0 (0%)	3 (50%)	0 (0%)	0 (0%)	0 (0%)	0 (0%)
Mig	CStat SD (7)	0 (0%)	0 (0%)	0 (0%)	0 (0%)	0 (0%)	0 (0%)
Arim		0 (0%)	0 (0%)	0 (0%)	0 (0%)	0 (0%)	0 (0%)
Comb		0 (0%)	0 (0%)	0 (0%)	0 (0%)	0 (0%)	0 (0%)
Mig	CStat R (14)	0 (0%)	0 (0%)	0 (0%)	0 (0%)	0 (0%)	0 (0%)
Arim		0 (0%)	0 (0%)	0 (0%)	0 (0%)	0 (0%)	1 (7.1%)
Comb		0 (0%)	0 (0%)	0 (0%)	0 (0%)	0 (0%)	0 (0%)

Table 3.7: The summary of the number and percentage of variables showing either improvement or deterioration effects between treated groups in coordination-related variables before summarization.
Mig: miglustat; Arim: arimoclomol; Comb: miglustat and arimoclomol.

Groups	Statistics	Improvement			Deterioration		
		6weeks	8weeks	10weeks	6weeks	8weeks	10weeks
Mig	mean (22)	4 (18.2%)	7 (31.8%)	4 (18.2%)	0 (0%)	0 (0%)	0 (0%)
Arim		2 (9.1%)	0 (0%)	2 (9.1%)	0 (0%)	0 (0%)	5 (22.7%)
Comb		4 (18.2%)	5 (22.7%)	2 (9.1%)	0 (0%)	0 (0%)	0 (0%)
Mig	SD (8)	0 (0%)	0 (0%)	0 (0%)	0 (0%)	0 (0%)	0 (0%)
Arim		0 (0%)	0 (0%)	0 (0%)	0 (0%)	0 (0%)	2 (25%)
Comb		0 (0%)	0 (0%)	0 (0%)	0 (0%)	0 (0%)	0 (0%)

Table 3.8: The summary of the number and percentage of variables showing either improvement or deterioration effects between treated groups in coordination-related variables after summarization.
Mig: miglustat; Arim: arimoclomol; Comb: miglustat and arimoclomol.

Fig. 3.7 shows the detail of p value from group comparison results in three coordination-related subgroups (Support, Step Sequence and Inter-paw interaction). These variables were selected by the EBVA. Support variables (Fig.3.7 A) describe the percentage duration of stances in paw combinations, namely four paws, diagonal paws, and girdle[1] paws. The Support improvements in girdle[1] paws were only observed at 6 weeks of age in all three treatment groups. The support in diagonal paws was improved at 8 weeks of age in the Comb and Mig groups. Four paws support variables were positively affected by the Comb and Mig groups between 8 and 10 weeks of age. At 10 weeks of age, there were negative impacts on four paws and girdle[1] paw support in the Arim treated mice.

In terms of step sequence variables (Fig.3.7 B) the Regularity Index[2] was not improved in all treated groups from 6 to 10 weeks of age, but improvements were observed in individual step sequences. Rb[3] was improved at 6 and 10 weeks of age in all groups, while Ra[4] was only positively affected by the Comb and Mig groups at 6 weeks of age. A deterioration of Rb[3] was observed in the Arim group at 10

[1]Girdle paws: front paws or hind paws
[2]Regularity Index: the number of normal step sequence patterns relative to the total number of paw placements.
[3]Rb step sequence: LF-RF-RH-LH
[4]Ra step sequence: RF-LF-LH-RH

weeks of age. Comb and Mig also had positive effects on Ca[5] at 6 to 8 weeks of age. The improvement in Cadence[6] was only seen in the Mig group at 10 weeks of age.

In the Inter-paw relationships variables in Fig. 3.7 C, the improvements were seen only in diagonal paws interaction at 8 weeks of age in the Comb and Mig groups and at 10 weeks of age in the Mig group. The Arim group had negative effects on diagonal, girdle[1] and lateral paws interaction at 10 weeks of age.

[5]Ca step sequence: RF-LF-RH-LH
[6]Cadence: steps per second

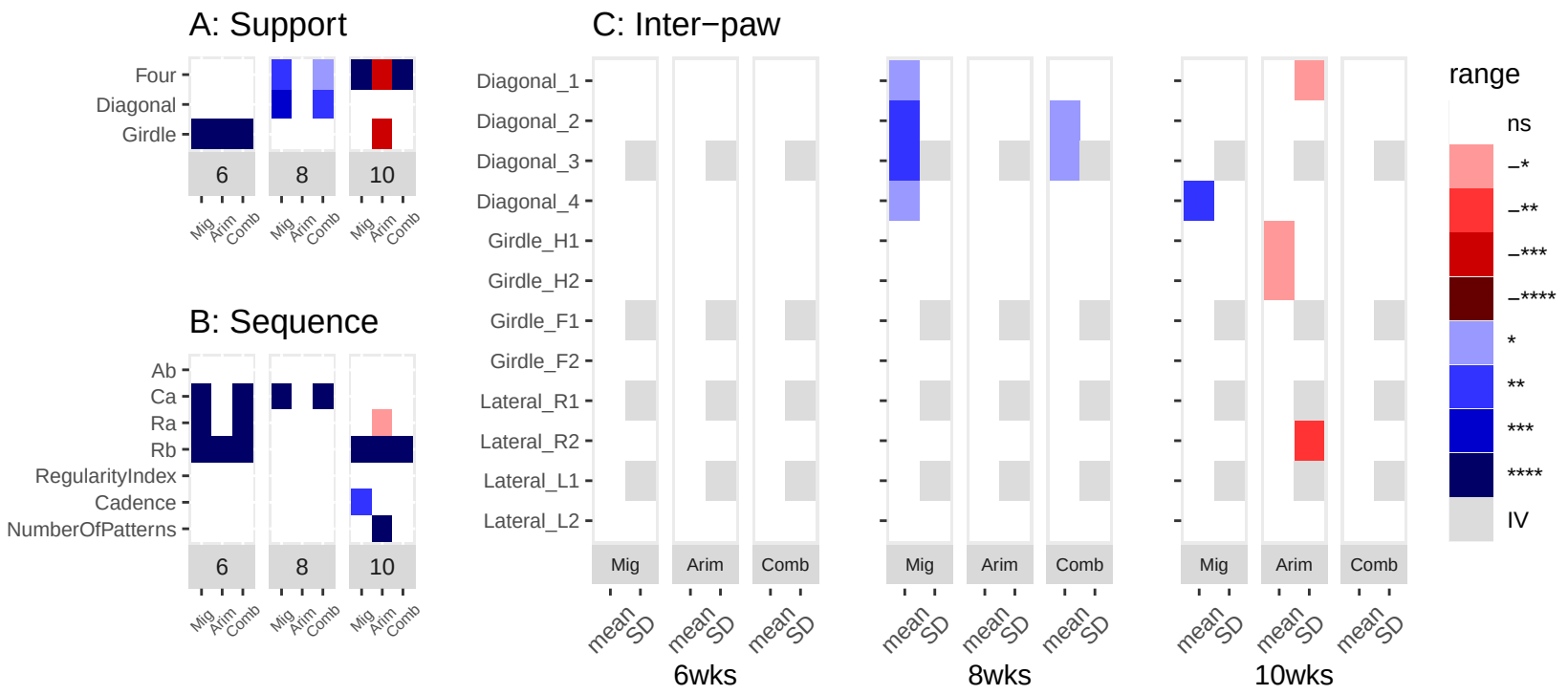


Figure 3.7: Heatmap of the results from one-way ANOVA and post hoc analysis in Coordination-related variables.
(A) Support: a percentage of the duration of listing paw combination contacting the ground.
(B) Step Sequence: 6 pre-defined footfall patterns (Aa, Ab, Ca, Cb, Ra, Rb); Regularity Index: a percentage of the number of steps in 6 pre-defined patterns in total steps; Number of patterns; Number of steps; Cadence: number of steps in a second.
(C) Phase Dispersions/ Couplings in different inter-paw combinations.
The colours represent different significance levels. Blue indicates improvement and red indicates deterioration. The grey colour indicates irrelevant variables.
IV: irrelevant variables; Significance levels: ns: not significant; *=$p \leq 0.05$; **=$p \leq 0.01$; ***=$p \leq 0.001$; ****=$p \leq 0.0001$.

3.3.4 The summary of treatments

Table 3.9 and Table 3.10 summarize the effectiveness of treatments at the age of maximum benefit. Table 3.9 shows the effects of treatments on physical-related variables at 10 weeks of age. Miglustat was the most beneficial treatment among the three treatments. Arimoclomol did not improve any variables but caused a deterioration in the mean of Step Cycle in HP and SD of Swing in the HP.

Table 3.10 demonstrates the results in coordination-related variables at 8 weeks of age, as Table 3.8 and Fig. 3.7 indicate the maximum effectiveness in coordination-related variables was at 8 weeks of age. Miglustat and combination treatments had similar benefits on these variables in Table 3.10. The improvements from these two groups can be seen in diagonal and four paws support, Ca[7] sequence and diagonal inter-paw relationship. However, arimoclomol did not show any benefits.

[7]Ca step sequence: RF-LF-RH-LH

	mean						SD					
	Mig		Arim		Comb		Mig		Arim		Comb	
Variables	FP	HP	FP	HP	FP	HP	FP	HP	FP	HP	FP	HP
Stand[1]	↑**	↑*	ns	ns	↑*	ns	-	-	-	-	-	-
Swing[2]	-	-	-	-	-	-	ns	ns	ns	↓*	ns	ns
StepCycle[3]	↑**	↑**	ns	↓*	↑*	↑*	↑*	↑*	ns	ns	ns	↑*
DutyCycle[4]	↑**	-	ns	-	ns	-	-	-	-	-	-	-
StrideLength[5]	↑**	↑*	ns	ns	ns	ns	-	-	-	-	-	-

Table 3.9: The summary results of physical-related variables between therapies.
Mig: miglustat; Arim: arimoclomol; Com: combination; ↑ means the variable has greater value in disease model than in wild type model and vice versa. Significance levels : ns: not significant; *$\leq$ 0.05; **$\leq$ 0.01; ***$\leq$ 0.001; **** $\leq$ 0.0001.

Definition
[1] Duration of paw contact with the glass plate
[2] Duration of paw not contact with the glass plate
[3] Sum of Stand and Swing
[4] The percentage of Stand in a StepCycle
[5] The distance between successive placements of the same paw

		mean			SD		
	Variables	Mig	Arim	Comb	Mig	Arim	Comb
Support[1]	Diagonal	↑***	ns	↑**	-	-	-
	Girdle	ns	ns	ns	-	-	-
	Four	↑**	ns	↑*	-	-	-
Step Sequence[2]	Ab	ns	ns	ns	-	-	-
	Ca	↑****	ns	↑****	-	-	-
	Ra	ns	ns	ns	-	-	-
	Rb	ns	ns	ns	-	-	-
	RegularityIndex[4]	ns	ns	ns	-	-	-
	Cadence[5]	ns	ns	ns	-	-	-
	NumberOfPatterns	ns	ns	ns	-	-	-
Inter-paw interaction[3]	Diagonal 1	↑*	ns	ns	ns	ns	ns
	Diagonal 2	↑**	ns	↑*	ns	ns	ns
	Diagonal 3	↑**	ns	↑*	-	-	-
	Diagonal 4	↑*	ns	ns	ns	ns	ns
	Lateral L1	ns	ns	ns	-	-	-
	Lateral L2	ns	ns	ns	ns	ns	ns
	Lateral R1	ns	ns	ns	-	-	-
	Lateral R2	ns	ns	ns	ns	ns	ns
	Girdle F1	ns	ns	ns	-	-	-
	Girdle F2	ns	ns	ns	ns	ns	ns
	Girdle H1	ns	ns	ns	ns	ns	ns
	Girdle H2	ns	ns	ns	ns	ns	ns

Table 3.10: The summary results of coordination-related variables between therapies. Mig: miglustat; Arim: arimoclomol; Com: combination; ↑ means the variable has greater value in disease model than in wild type model and vice versa. Significance levels : ns: not significant; ↑≤ 0.05; ↑↑≤ 0.01; ***≤ 0.001; **** ≤ 0.0001.

Definition
[1] The duration percentage of contact with the glass plate of certain paws. For example, four paws support and diagonal paws support.
[2] The percentage of a certain pre-defined footfall pattern in a run. For example, Rb is clockwise step sequence begins from left front paw.
[3] The temporal relationship between placement of two paws within a StepCycle. Each interaction label is summarized from Phase Dispersions and Couplings.
[4] The percentage of the total number of 6 pre-defined footfall patterns in a run.
[5] The number of step in a second.

3.3.5 Improvement Scores

The aim of the improvement score is to summarize the mean and SD of variables into a single score. The definition of the improvement score is a positively significant change in either the mean or SD of a variable. A negative significant change is represented by a minus score. The significance level was defined as a p value ≤ 0.05. Fig. 3.8 and Fig. 3.9 show the summarized results. There were four figures (Fig. 3.3, Fig. 3.4, Fig. 3.5 and Fig. 3.6) presenting the results of physical-related variables and there was only one figure with improvement score in Fig. 3.8. In Fig. 3.8 and Fig. 3.9, the dark blue with 2 scores implies the treatment can improve the mean and SD of a variable. There were more variables with dark blue in the Mig group, which suggests miglustat monotherapy was the most beneficial treatment in gait among all treatments.

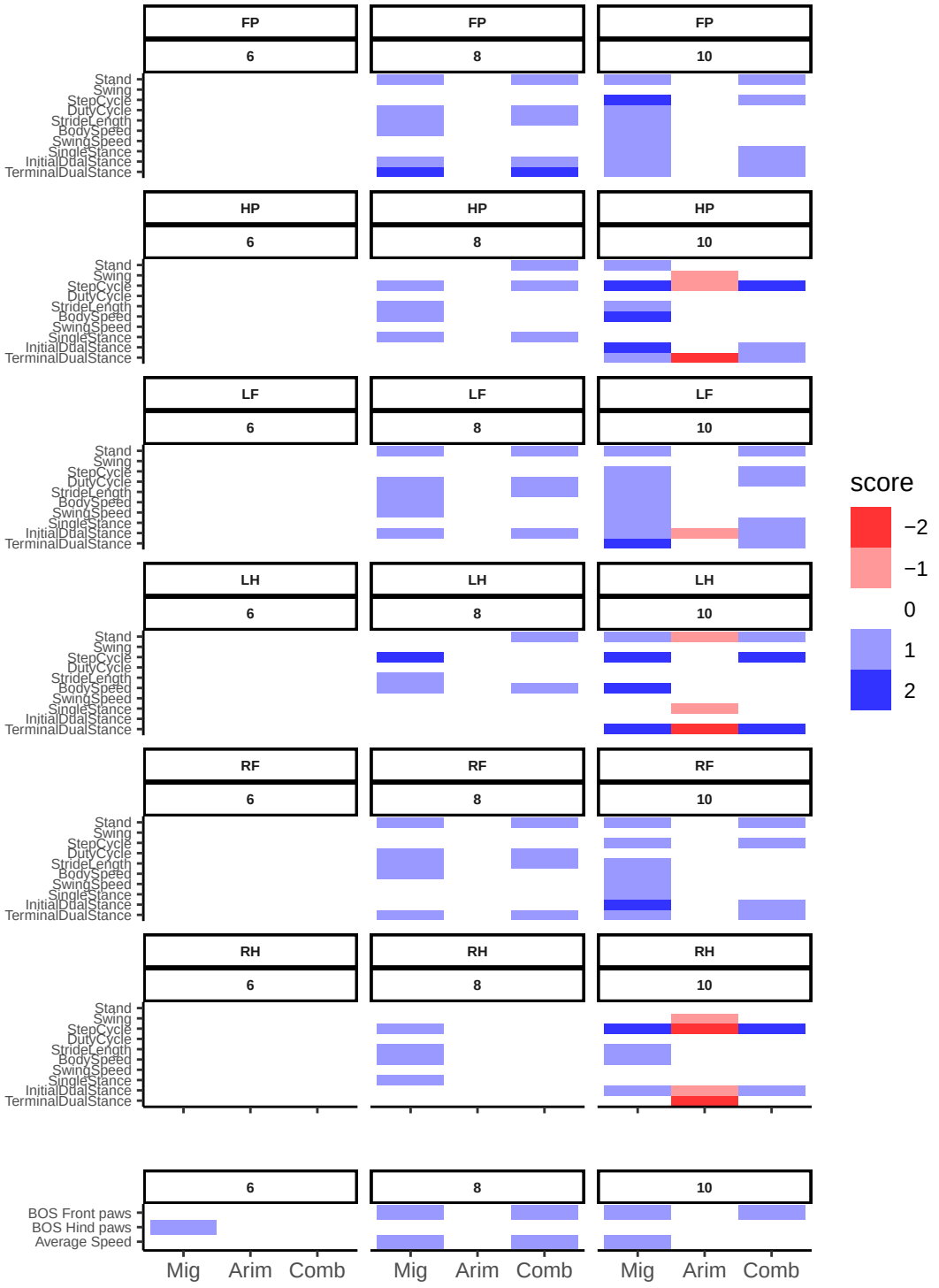


Figure 3.8: The behavioural scores of physical-related variables.
FP: front paws; HP: hind paws; LF: left front paw; LH: left hind paw; RF: right front paw; RH: right hind paw. The colours represent different behavioural scores. The score is defined as a significant (p value ≤ 0.05) change either on the mean or SD of a variable. A positive score indicates improvement, and a negative score indicates deterioration.

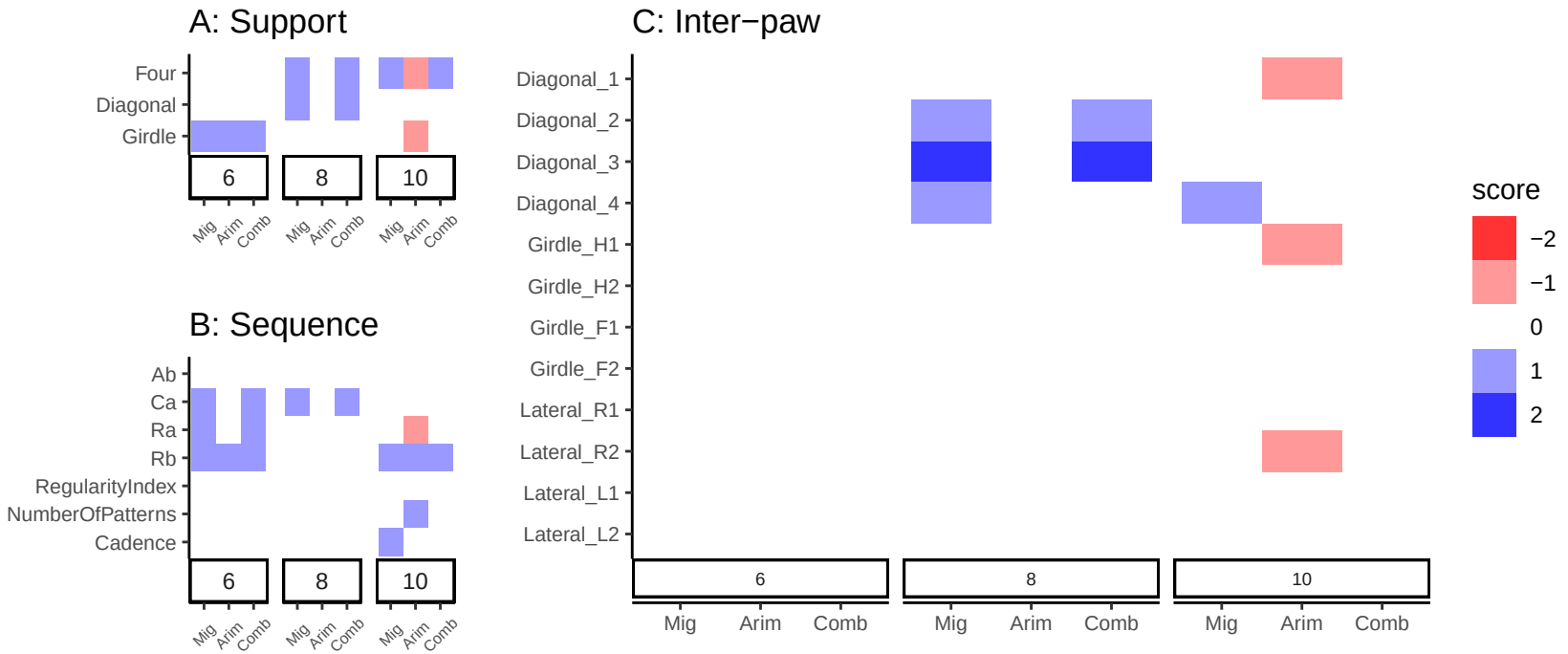


Figure 3.9: The behavioural scores of coordination-related variables.
(A) Support: a percentage of the duration of listing paw combination contacting the ground.
(B) Step Sequence: 6 pre-defined footfall patterns (Aa, Ab, Ca, Cb, Ra, Rb); Regularity Index: a percentage of the number of steps in 6 pre-defined patterns in total steps; Number of patterns; Number of steps; Cadence: number of steps in a second.
(C) Phase Dispersions/ Couplings in different inter-paw combinations. The score is defined as a significant (p valueleq0.05) change either on the mean or SD of a variable. The positive score indicates improvement and a negative score indicates deterioration.

3.4 Discussion

3.4.1 The results of EBVA

This chapter builds upon the Evidence Based Gait Analysis Method (EBGAM) in Chapter 2 and demonstrate the power of EBGAM to detect the differential effects of combination therapy. The gait data from the Catwalk system of the arimoclomol combination study was processed using this procedure for the first time. The *Npc1*^{nih} mouse model has been analysed twice so far by the procedure of EBGAM. First, the last chapter compares two independent mouse models of NPC and the second time was in this chapter, but the relevant variable profiles of the *Npc1*^{nih} model between these two studies are slightly different. The total number of variables selected in the Chapter 2 mouse cohort was 120 with 50 in physical-related and 70 in coordination-related, while in this chapter the number increased to 131 with 79 in physical-related and 52 in coordination-related.

The differences between the two studies can be explained by the different time points studied. In Chapter 2, the mice were evaluated at 6, 7 and 8 weeks of age, while the arimoclomol combination study in this chapter included 6, 8 and 10 weeks of age. Because the symptoms of the *Npc1*^{nih} mouse model are progressive [121], the inclusion of the 10-week time point will identify variables unaffected at earlier time points. Therefore, we expect the number of variables affected by NPC to be greater in a study including late age mice compared to a study with early age points analysed.

From the number of physical-related variables, there were 50 variables presented in the Chapter 2 study and 79 variables in this combination therapy study chapter. In Fig. 3.1 and Fig. 3.2, not only is the number of variables greater in this study, the significance level is also higher (more variables with p value≤ 0.01). Especially, the Stand and Body Speed of four paws were more significantly affected at the late age of the *Npc1*^{nih} mouse model. In terms of coordination-related variables, paradoxically the number of variables in the late age study (52 variables) is less than is in the early age study (70 variables). Surprisingly, the number of coordination-related variables affected did not increase when the disease progressed. Particularly, the number of

variables in the inter-paw subgroup was greater in the early age study than in the late age study. However, the number of variables after summarization (see section 2.2.2) was 26 in the early age study and 30 in the late-age study. This means there were more circular statistics in inter-paw variables identified in the early age study, but fewer inter-paw interactions were affected. Although the number of variables in the inter-paw subgroup was less in the late-age study, the number of inter-paw interactions affected was greater in the late-age study. Therefore, the coordination of *Npc1*^{nih} mice deteriorates with disease progression. The relevant variable profiles of the *Npc1*^{nih} model are also discussed in the following chapter.

3.4.2 The effects of treatments

Miglustat

Miglustat (Mig) is the only approved treatment for NPC and has been shown to improve mobility in *Npc1* null mice [138] and extend patient life span by one decade [74]. Only a few variables have been reported while evaluating its therapeutic effects in mice, such as speed. This only exploits parts of the Catwalk data and other relevant variables are neglected. Here, all variables from the Catwalk system were evaluated systematically by the EBGAM procedure. In this chapter, the profiles of Mig treatment on gait analysis are shown for the first time in detail, including establishing the treatment effects on specific paw-related variables.

The improvements of Mig began at 8 weeks of age when the gait symptoms became obvious and its effects extended to 10 weeks of age in Fig. 3.3. Physical-related variables (Body Speed, Stand and Stride Length in all four paws) were improved in the Mig groups at 8 and 10 weeks of age. Interestingly, Mig was more effective in the front paw variables as the number of improved variables in the front paws was greater than in the hind paws. In general, mice treated with Mig could walk faster (Average Speed) with narrower BOS in the front paws consistent with improved cerebellar function. Compared to the improvements in physical-related variables, the improvements in coordination-related variables were more modest. Between 8 to 10 weeks of age, Support in four paws, step sequences

(Rb and Ca) and diagonal inter-paw interaction were improved and the maximum effectiveness was at 8 weeks of age since the number of improved variables was the largest at 8 weeks of age in Table 3.8.

Overall, the onset of Mig mediated benefits was seen at 8 weeks of age and its effects extended to 10 weeks of age. Mig was more effective on physical-related variables, especially in the front paws and the improvements are more significant at 10 weeks of age. On the other hand, the best coordination improvements are at 8 weeks of age, especially in diagonal inter-paw relationships.

Arimoclomol and Combination Therapy with Miglustat

Arimoclomol elevates the level of heat shock protein 70 (HSP70), which improves the motor function of the *Npc1* $^{-/-}$ mouse model by increasing myelin quality. Catwalk data can therefore be used to evaluate the arimoclomol effects on motor function in mice. Fig. 3.4 shows the results of physical-related variables in arimoclomol monotherapy. Before 10 weeks of age, mice treated with Arim were not significantly different from Hom untreated mice. At 10 weeks of age, Arim had negative impacts on the Swing in the hind paws. Fig. 3.7 displays variables associated with coordination in the Arim group. Arim can improve Support in girdle paws and Rb step sequence at 6 weeks of age, but inter-paw interaction in diagonal, lateral and girdle was negatively affected at 10 weeks of age.

The treatment combining Arim and Mig eliminated the variable deterioration seen at 10 weeks of age in Arim monotherapy. However, the effects of Mig were reduced in the Comb group as the number of improved variables in Comb was less than in the Mig monotherapy group during the treatment period in Table 3.6 and Table 3.8. The reduction of physical-related effects in the Comb group can be seen in Average Speed, Body Speed, Stand and Stride Length which were all improved in the Mig group. On the other hand, the improvements in coordination variables were similar between Comb and Mig groups. The time point of the effects of Comb treatment was the same as Mig therapy, starting from 8 weeks of age and continuing to 10 weeks of age. However, the effects of Comb were less than Mig monotherapy.

Overall, Comb therapy can remove all negative impacts from Arim monotherapy but at the expense of some of the benefits of Mig monotherapy. Although the effects of Comb are similar to Mig monotherapy, the strength of effects from Mig monotherapy is reduced in the Comb group. This study, therefore, provides evidence that the new method of analysing gait developed in Chapter 2 can discriminate between two drug treatments given as monotherapies and detect further complex changes attributable to combination therapy.

4

Catwalk data analysis of Acetyl-DL-leucine (Tanganil) study

Contents

4.1 Introduction 82
4.2 Materials and Methods 84
4.2.1 Animal Model 84
4.2.2 Treatments 84
4.2.3 The Evidence Based Gait Analysis Method 84
4.3 Results 85
4.3.1 The summary of data set 85
4.3.2 The results of Evidence Based Variable Analysis 85
4.3.3 Comparison of data from wild type and *Npc1*^{nih} cohorts 89
4.3.4 Treatments results 95
4.4 Discussion 100
4.4.1 The results of EBVA across chapters 100
4.4.2 The limitation of the Catwalk system 101

4.1 Introduction

In this chapter, I tested the feasibility and potential of the Catwalk system using EBGAM by analysing two proven treatments for NPC that have different mechanisms of action. It also allowed me to test the reproducibility of EBVA in

identifying relevant variables in *Npc1^{nih}* mouse model in two independent mouse cohort studies. For this purpose, I have analysed a new data set from the *Npc1^{nih}* mouse with and without treatments including miglustat, a substrate reduction therapy drug that is standard of care for NPC patients [139] and acetyl leucine analogues that improve ataxia and are neuroprotective in NPC [140, 141] and one of which, Acetyl-L-leucine (ALL) is currently in Phase 3 clinical trials in NPC patients (ClinicalTrials.gov NCT05163288) with the aim of reducing symptoms of ataxia.

There were three variants of acetyl leucine evaluated in this chapter, Acetyl-DL-leucine (ADLL), Acetyl-D-leucine (ADL) and Acetyl-L-leucine (ALL). ADLL has been a treatment for acute vertigo since 1957 [95]. Although its mechanism of action remains unclear, the potential mechanism for its neuroprotection is enhancing cerebellar function by activation of cerebral glucose metabolism in the cerebellum [98]. Clinical studies have reported gait improvement in patients with cerebellar ataxia [140, 141] including patients with NPC [96]. ADLL is therefore viewed as a potentially safe symptomatic treatment for NPC. Based on previous studies [98], ALL is believed to be the active enantiomer in the racemic mixture of ADLL in terms of its neuroprotective properties and was also found to improve motor function in a vestibular lesion study in a rat model [99].

From the previous chapter, we observed that the benefits of Mig can be detected by the Catwalk system. Based on the evidence from publications, we expected that the neuroprotection of ALL also can be reflected in gait improvements in the Catwalk analysis using EBGAM but likely to a lesser extent than miglustat. For example, Kaya et al. [98] showed only a small number of gait variables improved with ALL and ADLL treatment. In this chapter, I was able to evaluate whether this small number of variables was a true reflection of the treated phenotype or was an underestimation using a more powerful variable selection method (EBGAM). If the results can detect the therapeutic effects in gait using EBGAM from therapies with different mechanisms of action, the Catwalk data using EBGAM can be applied to other studies with confidence and may help inform the development of an optimal combination therapy regimen for treating NPC patients. Therefore, answering

these questions and probing the strengths and limitations of EBGAM Catwalk analysis will have broader implications on how different treatment strategies can be assessed in this widely used animal model and directly impact the potential for proposing and validating novel treatments that may later inform a clinical evidence-based combination therapy.

4.2 Materials and Methods

4.2.1 Animal Model

Npc1^{nih} model

See section 1.5.1.

4.2.2 Treatments

The mouse treatment studies were conducted by Dr Ecem Kaya in the Platt Laboratory, Department of Pharmacology, University of Oxford. This study uses an independent data set distinct from the study published in 2021 [98]. There were four treatment arms to this study namely miglustat (Mig), Acetyl-DL-leucine (ADLL), Acetyl-L-leucine (ALL) and Acetyl-D-leucine (ADL). Miglustat (see section 1.6.1 was used at a dose of $600mg/Kg/day$ as dry admix in a powdered diet (miglustat was provided by Actelion). Acetyl-DL-leucine (Tanganil^{TM}, see section 1.6.3) and its enantiomers (Tanganil, Molekula #73891210, ALL: Sigma Aldrich #441511, ADL: Sigma #A0876) were administered as dry admix in powdered mouse diet (PicoLab Rodent Diet 20/5053, LabDiet) at a dose of $0.1g/kg/day$. The four treatments commenced at 3 weeks of age and had behavioural assessments in the Catwalk system at 8 weeks of age. The control groups were untreated wild type and *Npc1*$^{-/-}$ mice.

4.2.3 The Evidence Based Gait Analysis Method

See section 2.2.2.

4.3 Results

4.3.1 The summary of data set

There were 6 groups of mice analysed in this study. The size of each group ranged from 5 to 10 mice. Gait measurement of individual mice in the Catwalk system generated a trial, including at least one run per mouse per time point (minimum=1, maximum=6, and mean=3.5) in the Catwalk system. The number of valid trials (excluding absent data) is summarised in Table 4.1. Any absent data were caused by reluctance to walk or light body weight. The control groups had gait performance collected at 6, 7 and 8 weeks of age, however, gait was only measured at 8 weeks of age in the treated groups.

	No. trials		
Group	6wks	7wks	8wks
WT	6	6	6
Hom	5	4	5
Mig	-	-	10
ADLL	-	-	7
ADL	-	-	5
ALL	-	-	8

Table 4.1: The number of trials between groups.
WT: wild-type; Hom: *Npc1* mutant; Mig: miglustat; ADLL: acetyl-DL-leucine; ADL: acetyl-D-leucine; ALL: acetyl-L-leucine

4.3.2 The results of Evidence Based Variable Analysis

Selected Physical-related variables

This study included the Catwalk data at 6, 7 and 8 weeks of age in untreated wild type and *Npc1*$^{-/-}$ groups. These data were therefore analysed by EBVA to determine the variables relevant to this mouse model. A total of 51 physical-related variables (37% of total physical-related variables) were found to be modified in the *Npc1*^{nih} model that manifested between 6 to 8 weeks of age. There were 37 (52.9%) mean and 14 (20.6%) SD of variables found to be modified in the *Npc1*^{nih} model and are summarised in Table 4.2.

Variables	Statistics	Total	Hom
Physical-related	Mean	70	37 (52.9%)
	SD	68	14 (20.6%)
	total	**138**	**51 (37%)**

Table 4.2: The number and percentage of relevant physical-related variables selected by EBVA.

The results of EBVA for each variable are summarized as a heatmap (see Fig. 4.1). Fig. 4.1 A and Fig. 4.1 B are presented as paw-wise and non-paw-wise variables respectively. In terms of the number of variables, there were minimal differences observed between the variables relating to the front and hind paws, however, there were some front and hind paw specific variables identified. For example, the variables of Stand and DutyCycle were only affected in the front paws and Swing, StepCycle and SwingSpeed in the hind paws. StrideLength and BodySpeed were affected in both the front and hind paws.

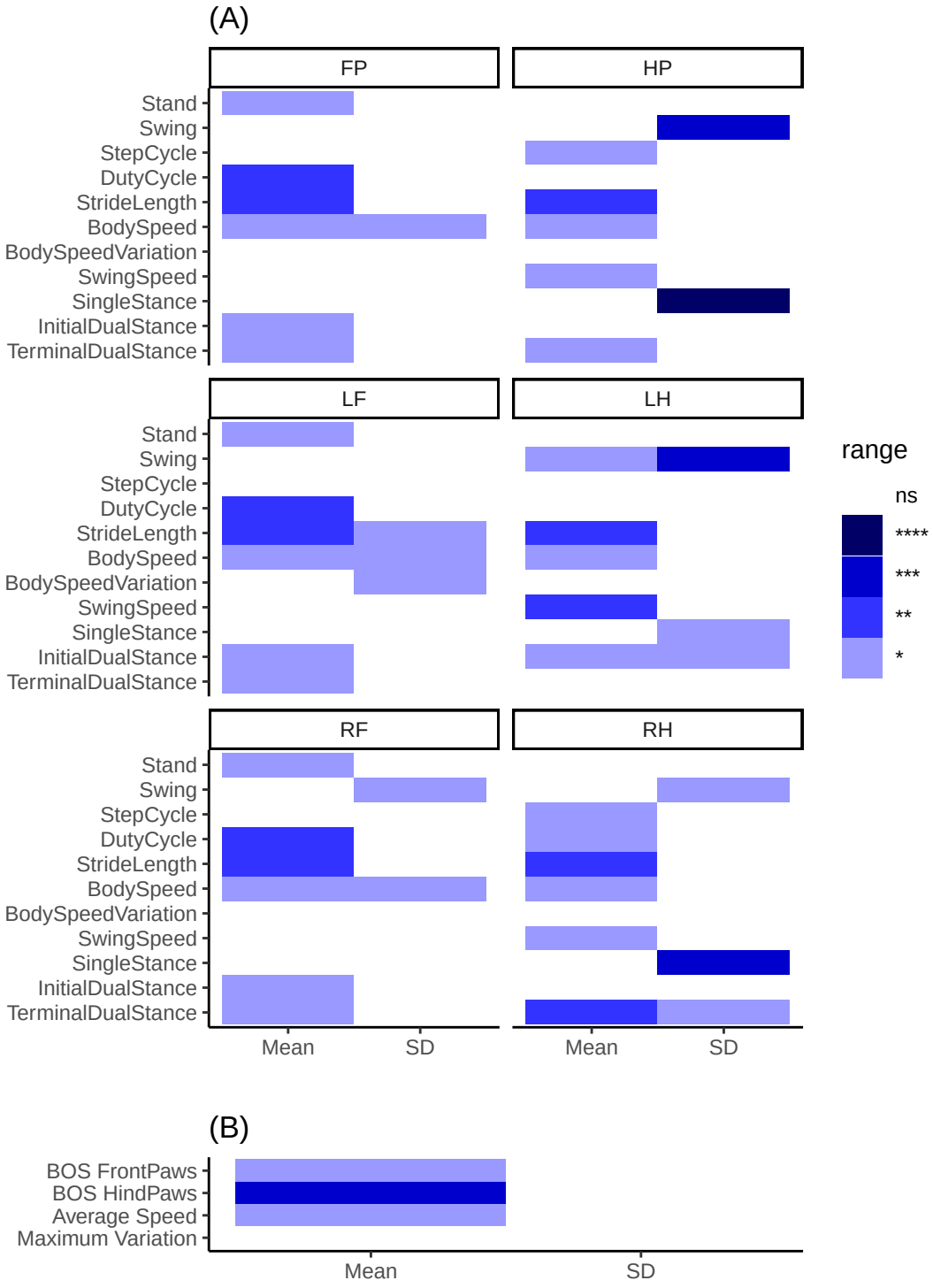


Figure 4.1: The relevant physical-related variables were found to be modified in the *Npc1^{nih}* model in (A) paw-wise and (B) non-paw-wise variables.
FP: front paws; HP: hind paws; LF: left front paw; LH: left hind paw; RF: right front paw; RH: right hind paw. The colours represent different significance levels.
Significance levels: ns: not significant; *=$p \leq 0.05$; **=$p \leq 0.01$; ***=$p \leq 0.001$; ****=$p \leq 0.0001$.

Selected Coordination-related variables

There were 55 coordination-related variables identified that are relevant in this study cohort. This was just above half of the total coordination-related variables (51.4%). The variables are summarized in Table. 4.3. There were more than half of the circular statistic (CStat) variables (CStat mean, SD and R), which were found to affected by disease progression.

Variables	Statistics	Total	Hom
Coordination-related	mean	35	12 (34.3%)
	SD	18	10 (55.6%)
	CStat mean	18	12 (66.7%)
	CStat SD	18	9 (50%)
	CStat R	18	12 (66.7%)
	total	**107**	**55 (51.4%)**

Table 4.3: The number of relevant coordination-related variables selected by EBVA before summarization.
CStat: circular statistics.

The CStat variables were further summarised into 12 interlimb labels with mean and SD (see section 2.2.2) for better interpretation. There were 21 results variables with 14 mean and 7 SD that were relevant to the study and the percentage of mean and SD were about half of the total (see Table 4.4).

Variables	Statistics	Total	Hom
Coordination-related	Mean	29	14 (48.3%)
	SD	12	7 (58.3%)
	total	**41**	**21 (51.2%)**

Table 4.4: The number of relevant coordination-related variables selected by EBVA after coordination-related variable summarization.

The results of EBVA in terms of individual coordination-related variables are summarized in Fig. 4.2. The Support variables (the time spent in contact with the floor) that changed with disease progression are summarized in Fig. 4.2 A. In Fig.

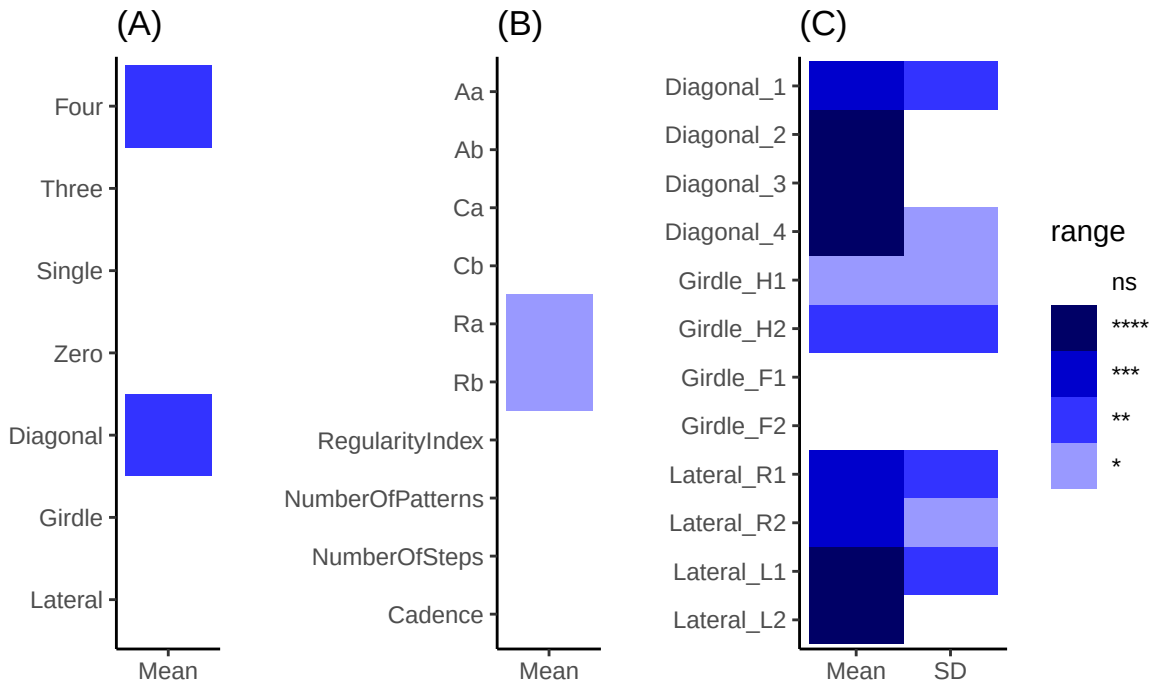


Figure 4.2: The relevant coordination-related variables were found to be modified in the *Npc1*^{nih} model.
(A) Support: a percentage of the duration of listing paw combination contacting the ground.
(B) Step Sequence: 6 pre-defined footfall patterns (Aa, Ab, Ca, Cb, Ra, Rb); Regularity Index: a percentage of the number of steps in 6 pre-defined patterns in total steps; Number of patterns; Number of steps; Cadence: number of steps in a second.
(C) Phase Dispersions/ Couplings in different inter-paw combinations.
Significance levels: ns: not significant; *=$p \leq 0.05$; **=$p \leq 0.01$; ***=$p \leq 0.001$; ****=$p \leq 0.0001$.

4.2 B, the Ra and Rb step sequences (see Appendix A.1) were considered as relevant variables. In the interlimb relationship in diagonal, girdle in hind paws and lateral (see Appendix A.1) were observed to significantly change with disease progression.

4.3.3 Comparison of data from wild type and *Npc1*^{nih} cohorts

As EBVA was also performed on another independent cohort in Chapter 2, I began by comparing how closely matched the variables selected were between the *Npc1*^{nih} from the two independent data sets as a measure of how robust this variable

selection method is. There are a total of 245 variables (107 physical-related and 138 coordination-related variables) measured by the Catwalk system which are required to determine whether they are relevant to the study using EBVA. The *Npc1*^{nih} mouse model, which is widely used in NPC study [44], was utilized in Chapters 2, 3 and 4 and Catwalk was measured at two different sets of time points. In Chapters 2 and 4, the time points of gait determination were at 6, 7 and 8 weeks of age, while in Chapter 3, gait was measured at 6, 8 and 10 weeks of age. The results of EBVA in Chapter 3 were not included in the following variables comparisons as the study in Chapter 3 had different time points measured compared with the other two cohorts both consistently evaluated the mice from 6 to 8 weeks of age. Therefore, comparing the studies in Chapter 2 and 4 can not only determine the extent of the robustness of EBVA but also identify the most consistent relevant variables in *Npc1*^{nih} mouse model during 6 to 8 weeks of age. Table 4.5 shows the number of trials included at the different time points between Chapters 2 and 4. One Catwalk trial corresponded to a particular mouse, thus, the number of trials is equivalent to the number of mice evaluated. The number of trials/mice in Chapter 2 was about two-fold higher than that of Chapter 4.

		No. trials		
Chapter	Group	6wks	7wks	8wks
ch2	Hom	11	7	9
	WT	12	12	12
ch4	Hom	5	4	5
	WT	6	6	6

Table 4.5: The number of trials and time points between Chapters 2 and 4.
WT: wild-type; Hom: *Npc1* mutant; ch2: Chapter 2; ch4: Chapter 4.

The Venn diagram in Fig. 4.3 shows the overlapped variables between Chapter 2 and 4 data sets. Fig. 4.3 A gives an overview of overlapping variables in both chapters. Other subfigures demonstrate overlapping variables in physical,

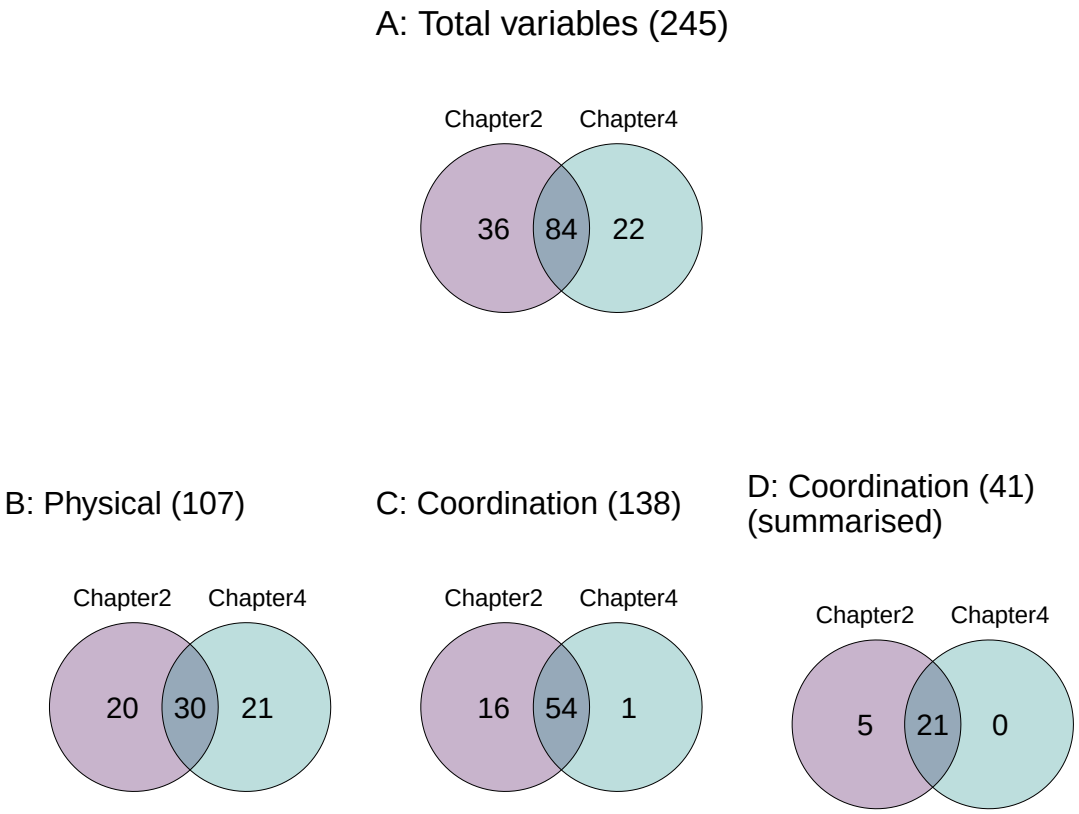


Figure 4.3: Venn diagram of relevant variables between Chapter 2 and 4.
(A) Total variables: 245 variables including physical-related and coordination-related variables; (B) Physical: 138 physical-related variables; (C) Coordination: 107 coordination-related variables; (D) Coordination-related (summarised): 41 summarised coordination-related variables.

coordination and summarized coordination-related matters. The numbers in parenthesis are the number of variables in the preceding label.

The number and percentage of relevant variables identified are summarised in Table 4.6. The percentages in the table indicate the proportion of the number of overlapping variables in the particular chapter from the other. Given each study has a different number of relevant variables, the overlapping part of these variables, therefore, come out with different percentages of the whole. In terms of physical-related variables, the number of relevant variables discussed in chapters 2 and 4 was similar (around 50 variables) and about 60 per cent of variables in each

chapter overlapped. The number of coordination-related variables was 70 and 50 in Chapters 2 and 4 respectively and the percentages of overlapped variables were from 77% in Chapter 2 to 98% in Chapter 4. After adjusting for repetition, the number of coordination variables reduced from 138 to 41 variables (see section 2.2.2). Thus, the coordination summarization row in Table 4.6 is more ideal for interpretation. Looking at this row, the percentages of overlapping variables exceeded 80%.

		Npc1^{nih}	
	Overlapping	ch2	ch4
Physical	30	50 (60%)	51 (59%)
Coordination	54	70 (77%)	55 (98%)
Physical + Coordination	84	120 (70%)	106 (79%)
Coordination summarisation	21	26 (81%)	21 (100%)

Table 4.6: The number of relevant variables and the percentage of overlapping variables in *Npc1^{nih}* mouse model selected by EBVA between Chapter 2 and Chapter 4. Overlapping: the number of overlapping relevant variables between Chapter 2 and 4. Physical: the number of relevant physical-related variables and the percentage of overlapping variables; Coordination: the number of relevant coordination-related variables and the percentage of overlapping variables; Coordination summarisation: the number of relevant coordination-related variables after summarisation and the percentage of overlapping variables; ch2: Chapter 2; ch4: Chapter 4.

The results of variables selection between two independent cohort studies had a noticeable percentage of overlapping variables. This is evidence that EBVA is a robust method for selecting relevant variables in the same mouse model within the same time frame, despite different mouse numbers being evaluated in the two studies.

Looking at Fig. 4.4, one noticeable overlapping physical-related variable, which is present in all four paws, is StrideLength. Additionally, the BOS (base of support) in the front and hind paws is altered between studies. That means *Npc1^{nih}* mice commonly develop travelled distance defects regardless of the cohort/group size tested.

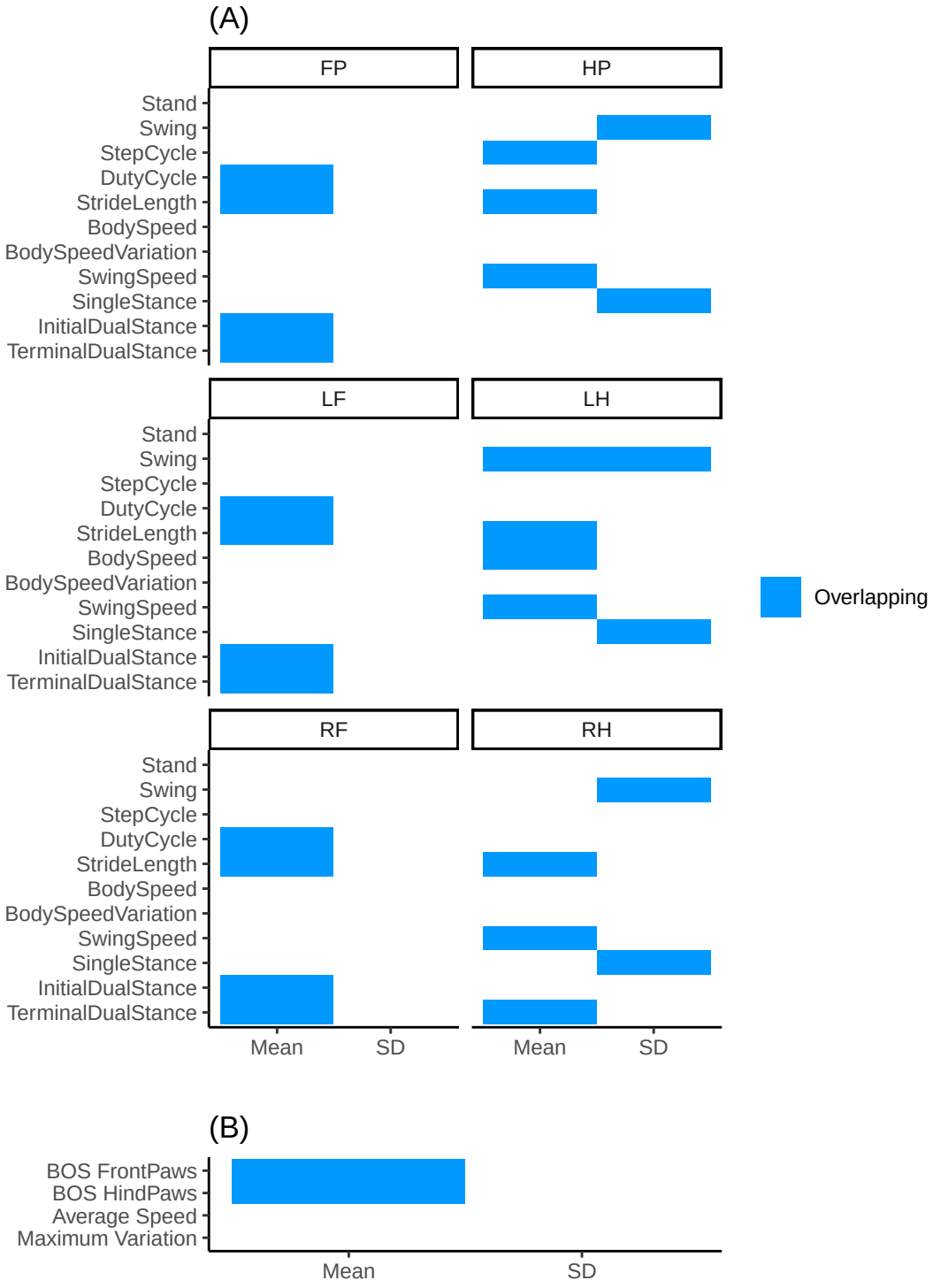


Figure 4.4: The overlapping physical-related variables in (A) paw-wise and (B) non-paw-wise variables in the model of $Npc1^{nih}$.
FP: front paws; HP: hind paws; LF: left front paw; LH: left hind paw; RF: right front paw; RH: right hind paw. The colours represent different significance levels.

In the next heat map in Fig. 4.5, defects in gait are observed across the majority of the inter-paw coordination-related variables, in particular diagonal, girdle in hind and lateral, meaning that *Npc1*^{nih} mice also had difficulties with coordination between paws.

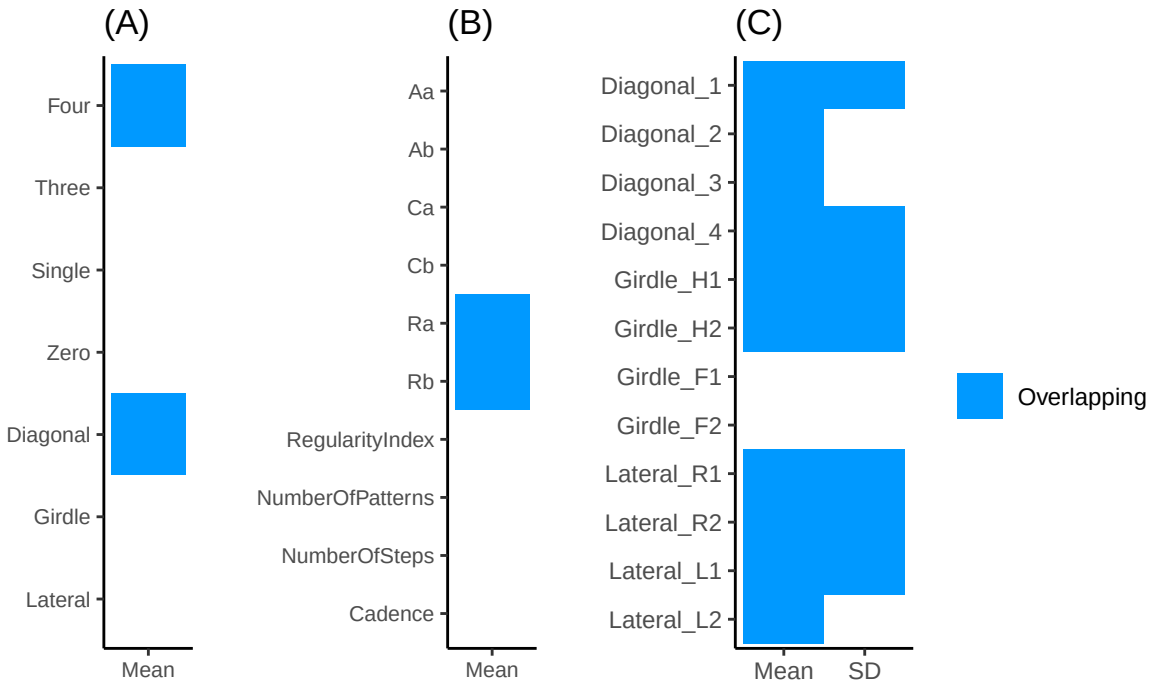


Figure 4.5: The overlapping Coordination-related variables in the model of *Npc1*^{nih}.
(A) Support: a percentage of the duration of listing paw combination contacting the ground.
(B) Step Sequence: 6 pre-defined footfall patterns (Aa, Ab, Ca, Cb, Ra, Rb); Regularity Index: a percentage of the number of steps in 6 pre-defined patterns in total steps; Number of patterns; Number of steps; Cadence: number of steps in a second.
(C) Phase Dispersions/ Couplings in different inter-paw combinations.

Table 4.7 ranks the top 10 overlapping variables according to the p-value of EBVA. Apart from the travelled distance defects in four paws (see Fig 4.4), there is also a variation of Swing and SingleStance observed in hind paws. The diagonal inter-paw interactions are the most apparent impacted features.

	Physical-related				Coordination-related		
Rank	Variables	Statistics	Paws	p value	Variables	Statistics	p value
1	SingleStance[1]	SD	HP	****	Diagonal 2	Mean	****
2	SingleStance[1]	SD	RH	****	Diagonal 3	Mean	****
3	Swing	SD	LH	****	Diagonal 4	Mean	****
4	Swing	SD	HP	****	Lateral L1	Mean	****
5	StrideLength	Mean	FP	****	Lateral L2	Mean	****
6	StrideLength	Mean	RF	****	Lateral R1	Mean	****
7	StrideLength	Mean	LF	***	Girdle H2	Mean	****
8	BOS FrontPaws	Mean		***	Lateral R1	SD	****
9	BOS HindPaws	Mean		***	Four[2]	Mean	****
10	Swing	SD	RH	**	Girdle H2	SD	****

Table 4.7: The top 10 overlapped variables in *Npc1^{nih}* mouse model across chapters. FP: front paws; HP: hind paws; LF: left front paw; LH: left hind paw; RF: right front paw; RH: right hind paw. Significance levels: **=$p \leq 0.01$; ***=$p \leq 0.001$; ****=$p \leq 0.0001$

Definition

[1] The duration of contact for a single paw.

[2] The duration percentage of contact with the glass plate in four paws.

4.3.4 Treatments results

Having further validated the phenotypes observed in the two untreated cohorts I then evaluated the miglustat and acetyl-leucine treated NPC mice. Gait performance was captured by the Catwalk system at 8 weeks of age in the treated groups. The effects of treatments were only evaluated in the relevant variables, which were identified by EBVA in this chapter. There were 106 variables identified in total. One-way ANOVA with Tukey HSD post hoc analysis was used to evaluate the treatment benefits. The heat maps of p values are from the results of Tukey HSD analysis, comparing one treated and untreated groups, and are presented in the following sections, separated into physical and coordination variables. The significant levels are defined as p value $\leq 0.05(*), \leq 0.01(**), \leq 0.001(***), \leq 0.0001(*****)$

Physical-related variables

Table 4.8 shows the number and percentage of physical-related variables altered by treatments between the four treatment groups at 8 weeks of age. There was no treatment that caused a deterioration of gait variables relative to untreated *Npc1* null mice. Mig improved 81.1% of mean relevant variables and 14.3% of SD variables, while there was only one mean variable (BOS hind paws) improved by the acetyl L-leucine derivative (ALL).

		8weeks	
Groups	Statistics	Improvement	Deterioration
Mig	mean (37)	30 (81.1%)	0 (0%)
ADLL		0 (0%)	0 (0%)
ADL		0 (0%)	0 (0%)
ALL		1 (2.7%)	0 (0%)
Mig	SD (14)	2 (14.3%)	0 (0%)
ADLL		0 (0%)	0 (0%)
ADL		0 (0%)	0 (0%)
ALL		0 (0%)	0 (0%)

Table 4.8: Summary of the number and percentage of physical-related variables shown improvement and deterioration effects relative to*Npc1* null mice at 8 weeks of age.
Mig: miglustat; ADLL: acetyl-DL-leucine; ADL: acetyl-D-leucine; ALL: acetyl-L-leucin

The details of improved variables are shown in Fig. 4.6. Mig improved most of the mean variables in both the front and hind paws, including Stand and StepCycle in the front paws and Swing and StepCycle in the hind paws. ALL improved BOS in the hind paws.

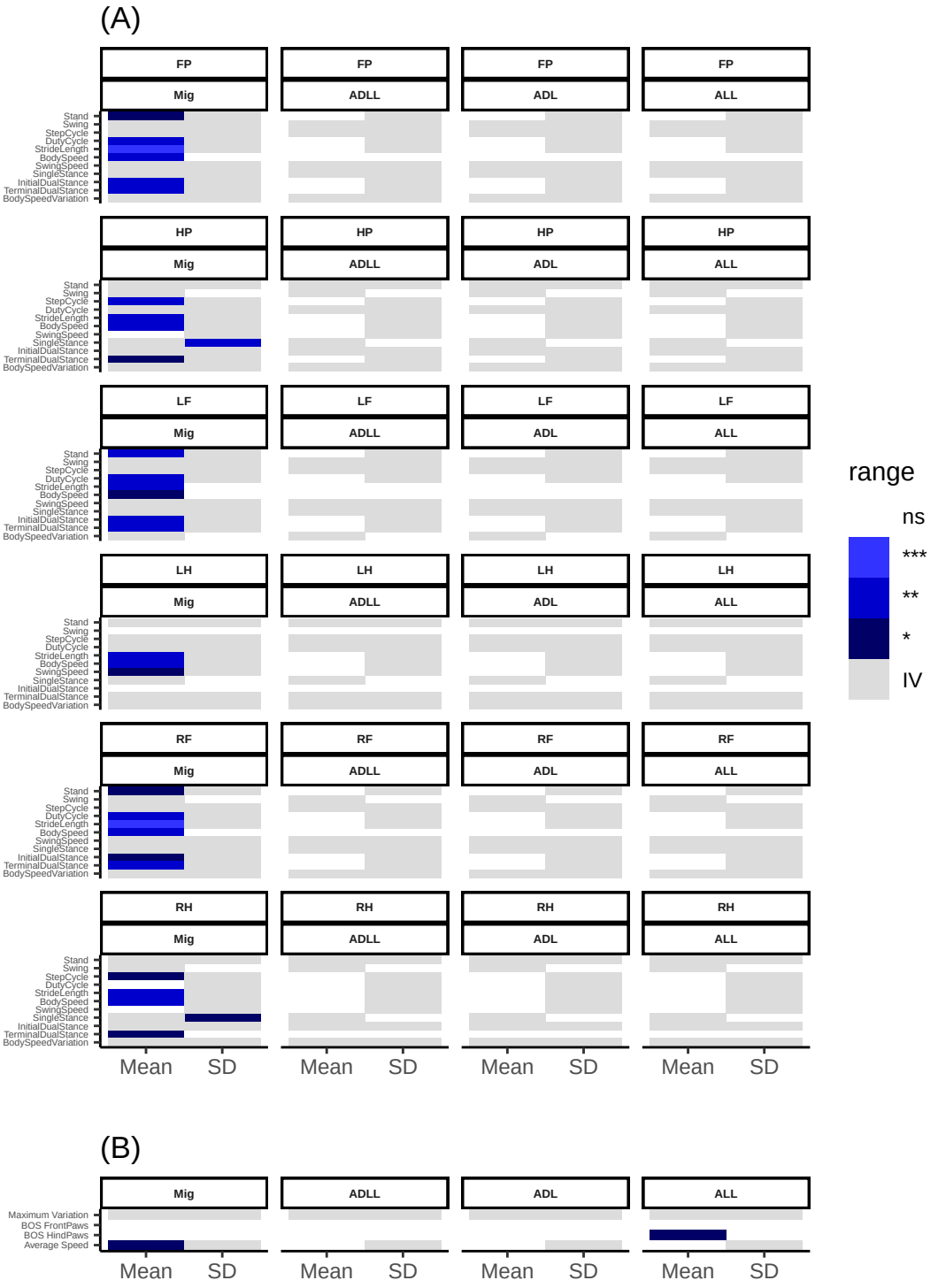


Figure 4.6: Heatmap of the results from one-way ANOVA and post hoc analysis in (A) paws-wise and (B) non-paw-wise variables (B) variable.
Mig: miglustat; ADLL: acetyl-DL-leucine; ADL: acetyl-D-leucine; ALL: acetyl-L-leucin; FP: front paws; HP: hind paws; LF: left front paw; LH: left hind paw; RF: right front paw; RH: right hind paw. The colours represent different significant levels. The grey colour indicates irrelevant variables (IV).
IV: irrelevant variables; Significance levels: ns: not significant; *=$p \leq 0.05$; **=$p \leq 0.01$; ***=$p \leq 0.001$; ****=$p \leq 0.0001$.

Coordination-related variables

Table 4.9 shows the number and percentage of altered variables after variable summarization (see section2.2.2). There was no deterioration observed in treated groups relative to untreated *Npc1* null mice. Mice treated with Mig had improvements in 9 mean and 7 SD variables. There was one mean and one SD variable (diagonal interlimb relationship variables) improved by ADLL treatment.

		8weeks	
Groups	Statistics	Improvement	Deterioration
Mig	mean (14)	9 (64.3%)	0 (0%)
ADLL		1 (7.1%)	0 (0%)
ADL		0 (0%)	0 (0%)
ALL		0 (0%)	0 (0%)
Mig	SD (7)	7 (100%)	0 (0%)
ADLL		1 (14.3%)	0 (0%)
ADL		0 (0%)	0 (0%)
ALL		0 (0%)	0 (0%)

Table 4.9: Summary of the number and percentage of coordination-related variables shown either improvement or deterioration effects relative to*Npc1* null mice at 8 weeks of age after variable summarization.
Mig: miglustat; ADLL: acetyl-DL-leucine; ADL: acetyl-D-leucine; ALL: acetyl-L-leucin.

From Fig. 4.7, we can see that Mig improved most variables relating to Support and interlimb relationship but had no effects on Step Sequences (Ra and Rb). ADLL was the only effective treatment improving coordination-related variables among the acetyl leucine derivatives tested but improved only one diagonal interlimb variable (in mean and SD).

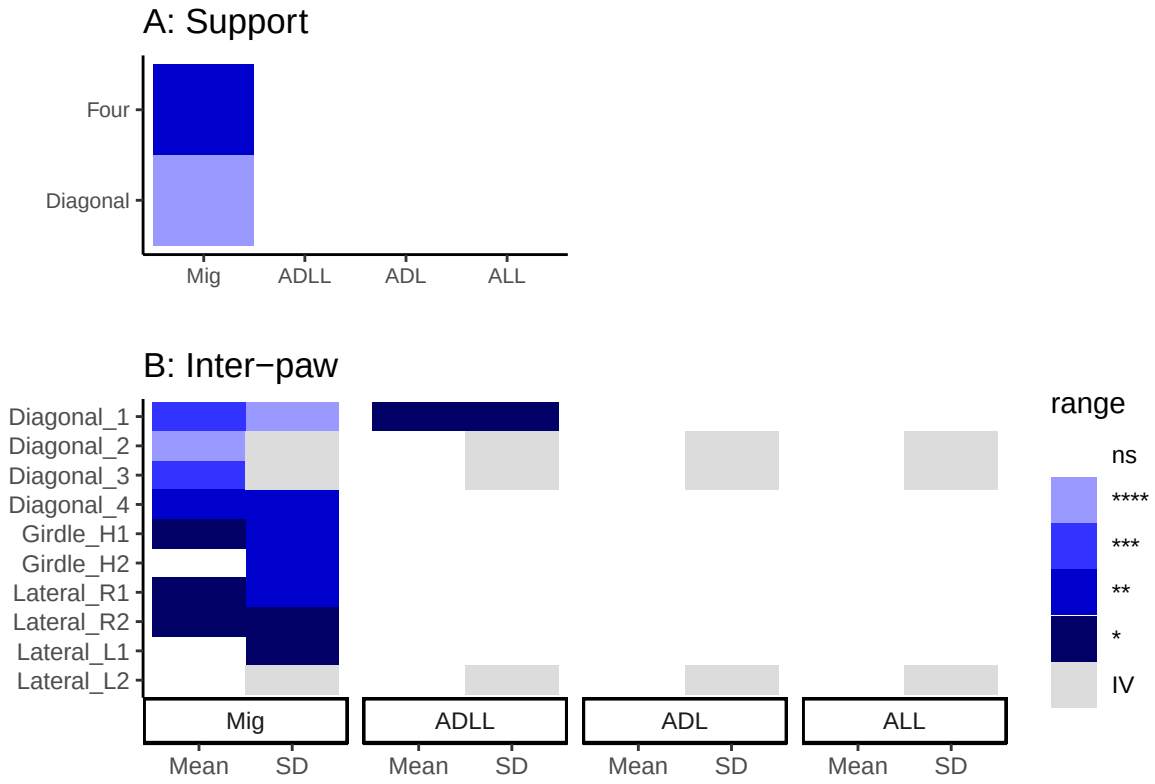


Figure 4.7: Heatmap of the results from one-way ANOVA and post hoc analysis in Coordination-related variables.
(A) Support: a percentage of the duration of listing paw combination contacting the ground.
(B) Phase Dispersions/ Couplings in different inter-paw combinations.
Mig: miglustat; ADLL: acetyl-DL-leucine; ADL: acetyl-D-leucine; ALL: acetyl-L-leucin.
The colours represent different significance levels. Blue indicates improvement.
Significance levels: ns: not significant; *=$p \leq 0.05$; **=$p \leq 0.01$; ***=$p \leq 0.001$; ****=$p \leq 0.0001$.

4.4 Discussion

4.4.1 The results of EBVA across chapters

Evidence Based Variable Analysis (EBVA) is used to determine whether variables are relevant to the *Npc1*^{nih} mouse model across time points. In this thesis, I have evaluated multiple independent cohort data sets and because Chapter 2 and 4 included evaluations at the same time points, I took advantage of this to compare the consistency of variable selection across cohorts. Looking solely at Chapters 2 and 4, approximately 60% of physical-related and 80% of coordination-related variables were common to both studies (termed overlapping variables) (see Table 4.6). The two studies had different sample sizes. The sample size in Chapter 2 was greater than in Chapter 4 and consequently, the number of relevant variables identified was also greater (120) than in Chapter 4 (101). This is because with the greater number of mice present in the sample in Chapter 2, there is more variability. Thus, there is only around 60% of physical-related variables overlapping. However, the percentage of overlapping coordination-related variables is around 80%. It is less likely for coordination-related features to be impacted by the variation in sample size. This shows that EBVA is an effective method for selecting relevant variables in the *Npc1*^{nih} model. This adds to the confidence in identifying suitable variables in the treatment analysis using EBGAM. Among the overlapping variables, the distance of paws travelled per step and the width of paws are commonly identified features in *Npc1*^{nih} mice. Moreover, defects were observed in the diagonal, girdle in hind and lateral coordination variables. These variables are commonly identified across cohorts and should be closely monitored prior to using EBVA. This means that in other studies with limited time points (e.g., a study that only includes data at 8 weeks of age), the results of overlapping variables from this chapter can be used as a proxy to compare the treatment effects without using EBVA.

4.4.2 The limitation of the Catwalk system

The Catwalk system and EBGAM have shown their potential to differentiate therapeutic effects in the combination study in Chapter 3. In order to validate the method further, two proven treatments, which have different mechanisms of action, were included in this data set. Mig treatment (current clinical standard of care) improved most physical-related and coordination-related variables (see chapter 3) in keeping with its ability to delay disease progression in animal models [72] and NPC patients [142]. However, ADLL and ALL have been shown to improve ataxia rapidly symptomatically in both an NPC clinical trial [100] and in mouse model studies [98]. In addition, ALL is also neuroprotective slowing disease progression [98]. The results of the Catwalk data using EBGAM in this chapter show few improvements specifically in gait in the ADLL and ALL groups. ADL therapy, which is the enantiomer that is not metabolised [143], did not show any effects in gait analysis from the Catwalk data. However, the minor detected improvements in diagonal paw coordination (ADLL group) and BOS hind paws (ALL group) in the Catwalk do not seem consistent with their neuroprotective benefits suggesting they do not protect the neuronal circuits responsible for these drugs' neuroprotective effects. However, there were noticeable improvements in ataxia in ALL treated mice observed from viewing the Catwalk videos. The problem is the Catwalk system fails to quantify these features as it does not measure deviations from walking in a straight line, so it cannot quantify ataxia, the main clinical sign that ALL improves. Dr Ecem Kaya was able to manually measure this to show the significant improvements in ataxia between ADLL, ADL and ALL groups by analysing walking path coordinates on printouts from the Catwalk videos [98]. Therefore, I believe that gait analysis using the Catwalk system is insufficient to evaluate the full efficacy of the treatments specifically relating to ataxia. There are several reasons for this assumption. Firstly, the system does not capture dynamic body movement. The Catwalk generates its data depending on the paw signals. There are no variables to detect body movements in relation to the axis of movement/travel in the Catwalk system. Secondly, the quality of results heavily relies on the quality of paw signals. The quality of the paw

signal dramatically decreases as *Npc1*$^{-/-}$ mice become symptomatic due to weight loss. Thus, there was more absent data in the Catwalk system at the symptomatic stages than at the pre-symptomatic stages. If a treatment is not able to increase or maintain the body weight in *Npc1*$^{-/-}$ mice, the quality of the paw signal would not be improved and subsequently affect the quality of the data captured. Thus, gait should be carefully assessed by the Catwalk system in different mouse models and with different treatment strategies.

To sum up, the results of EBVA in the same time frame studies (Chapters 2 and 4) were similar with 60% and 80% of overlapping physical-related and coordination-related variables respectively. The top 10 overlapping variables are essential to measure when evaluating gait performance in the *Npc1*^{nih} mouse model. The quality of the Catwalk data was optimised by using EBGAM, but the Catwalk system did not quantify the observed improvements in ataxia from ALL treated mice evident in the Catwalk videos. This demonstrates the limitations of the Catwalk system as it cannot evaluate dynamic movement, such as path changes due to ataxia. To overcome these limitations, we, therefore, developed a walking path analysis using deep learning techniques to solve this major limitation of the Catwalk system and these studies are the basis for Chapter 5.

5

Walking path analysis

Contents

5.1 Introduction 103
5.2 Materials and Methods 105
5.2.1 Animal model 105
5.2.2 Treatments 105
5.2.3 Walking path analysis (WPA) 105
5.3 Results 119
5.3.1 Summary of the data set 119
5.3.2 The reference points of a mouse 120
5.3.3 The velocity 121
5.3.4 X direction variables 122
5.3.5 Y direction variables 124
5.3.6 Rotating angle variables 125
5.3.7 The summary of treatments 128
5.4 Discussion 129

5.1 Introduction

Cerebellar ataxia is one of the main features of NPC and gait analysis is used to evaluate this feature in NPC animal models. In Chapter 4, the Catwalk system was unable to detect the rapid improvements in ataxia of acetyl leucine analogues in *Npc1*^{nih} as very few gait variables were altered in response to this drug [98]. Catwalk

measures coordination and motor features in relation to all four paws but what it lacks is the capability to measure deviations from a straight line, which is the main feature of ataxia. This chapter, therefore, aimed to develop a method to overcome the limitations of the Catwalk system and quantify the body coordination of this mouse model. In the publication from Dr Ecem Kaya [98], she managed to measure ataxia by manually analysing the walking paths of the *Npc1*^{nih} mice using printouts from heat maps generated by the Catwalk system. The deviations between the centre of the body and a straight line trajectory were manually measured over a run. This walking path analysis was scientifically very useful for determining treatment effects but was very labour-intensive and time-consuming. This chapter, therefore, aimed to improve the method developed by Dr Ecem Kaya [98] and refine it by employing a machine learning algorithm, DeepLabCut (DLC). DLC was developed for animal behavioural studies [144] and was trained by the Catwalk videos from our studies rather than using heat maps. We used DLC to track the walking path of a mouse and established a standard procedure to process the data generated from the DLC to give us a numeric output on deviations from walking in a straight line. The standard procedure we developed consisted of five steps, namely data collection, data cleaning, data preparation, data analysis and data presentation. There are 21 variables investigated in this chapter to capture ataxia. The validity of walking path analysis (WPA) was determined by evaluating two proven treatments with different mechanisms of action, miglustat (Mig) and acetyl leucine analogues (the drugs evaluated in Chapter 4), and we determined the extent to which WPA could differentiate the effects on ataxia between the three acetyl leucine analogues (ADLL, ALL and ADL, see Chapter 4).

The development and evaluation of WPA is essential to improve gait assessments and is complementary to Catwalk and EBGAM as it adds information on the path of the mice that is not analysed by Catwalk. The amalgamation of Catwalk and WPA may to a degree partially eliminate some of the limitations faced when using Catwalk EBGAM alone. For instance, when using Catwalk EBGAM on its own, body coordination of some of the lighter mice cannot be detected and

these data cannot be utilised, however, with WPA, this issue is bypassed as WPA focuses on an image-based analysis of the whole-body mouse videos, not paw prints and thereby we do not lose any data unnecessarily greatly increasing the volume of data that can be analysed.

All in all, our conclusion is that by combining these two methods we can provide a more comprehensive analysis of gait performance in mouse models and have. more sensitive read out on the differential effects of therapeutics. In this chapter, I have therefore tested this methodology for the first time and analysed and validate the utility of this approach.

5.2 Materials and Methods

5.2.1 Animal model

Npc1^{nih} model

See section 1.5.1.

5.2.2 Treatments

See section 4.2.2

5.2.3 Walking path analysis (WPA)

In walking path analysis (WPA), there are five steps based on EBGAM (Fig. 5.1), namely data collection, data cleaning, data preparation, data analysis and data presentation. This provides a standard procedure to ensure the quality and reproducibility of results. The analysis requires walking videos from the Catwalk system. Here, WPA begins with training DLC with the Catwalk videos and focused on the data generated from DLC. Each step in WPA will be explained in the following sections.

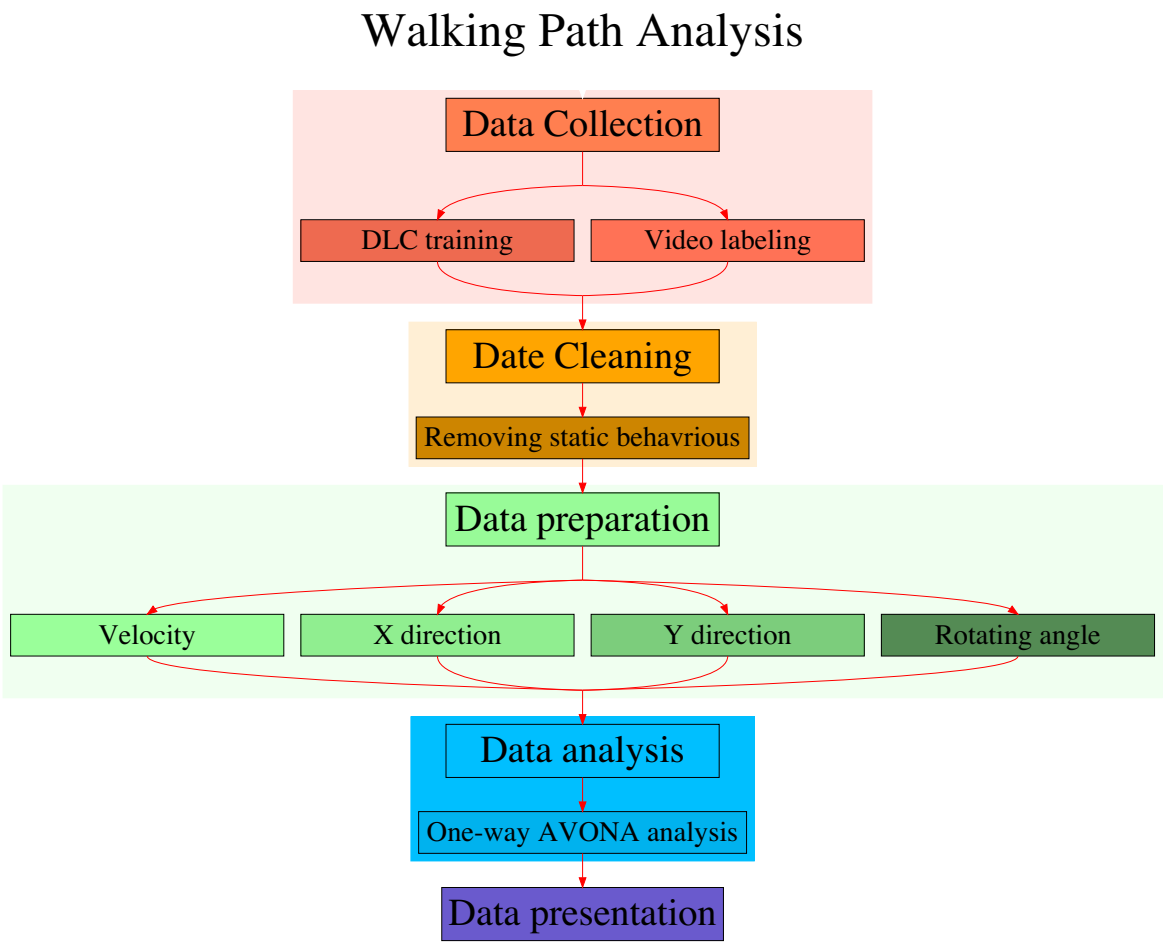


Figure 5.1: Walking Path Analysis (WPA).
There are 5 main steps, namely data collection, data cleaning, data preparation, data analysis and data presentation.

Data collection

DeepLabCut training In data collection, firstly, DLC had to be trained to be capable of labelling mice in the Catwalk videos and then the X and Y coordinates of the walking path were collected using the trained DLC. The training process followed the protocol of DLC [144]. DLC is based on deep neural networks which can achieve a high degree of accuracy with minimal training data [145]. The protocol is summarized into three steps and will be explained in depth in subsequent paragraphs (see Fig. 5.2).

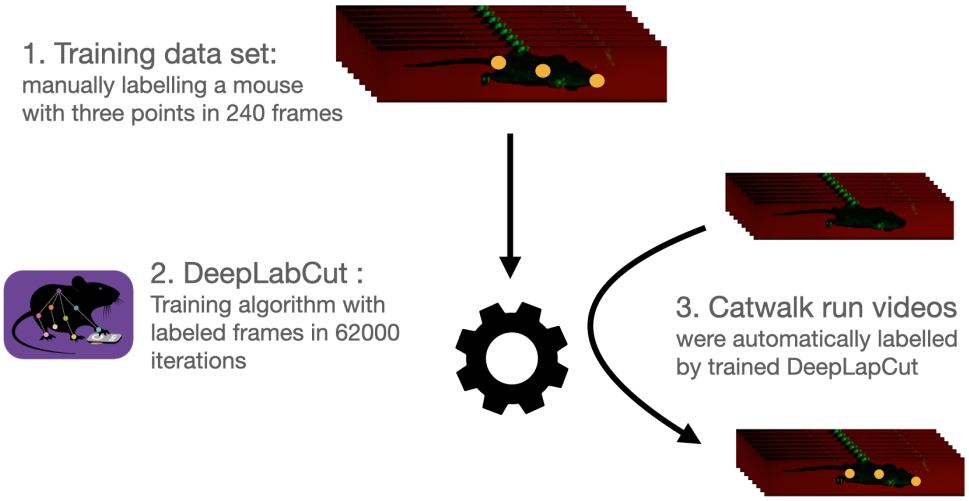


Figure 5.2: Summary of DLC training process in the protocol.
1. The training data set is prepared by manually labelling 240 frames with three reference points of a mouse, namely nose, body centre and base of the tail from Catwalk videos in *Npc1*^{nih} null mice. 2. DLC is trained by the data prepared in step one. The iteration of the training process is based on loss of function, which measures the accuracy of DLC. 3. All runs are then labelled automatically by trained DLC.

There were 240 frames manually labelled at three anatomical reference points of *Npc1*^{nih} mice, namely nose, body centre and base of the tail (Fig. 5.3) and these frames were the training data. While DLC is trained, the algorithm is able to label these three reference points in the Catwalk videos automatically.

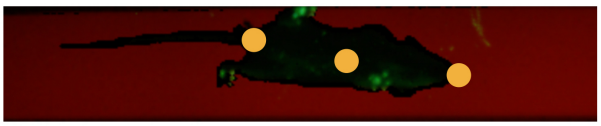


Figure 5.3: Example of anatomical labels.
There are three yellow points, namely the base of the tail, body centre and nose (from left to right)

The number of training iterations (using the *Npc1* null mice to train- be clear about this) was determined by the loss of function instructed by the protocol [144].

Fig. 5.4 shows the loss of function curve and the curve reached to its lowest plateau after 62000 iterations, where the deviation between predicted coordinates and actual coordinates was the least. In other words, the accuracy of DLC cannot be further improved by more iterations after 62000 iterations. Therefore, in this chapter, the iteration of training terminated at 62000 iterations.

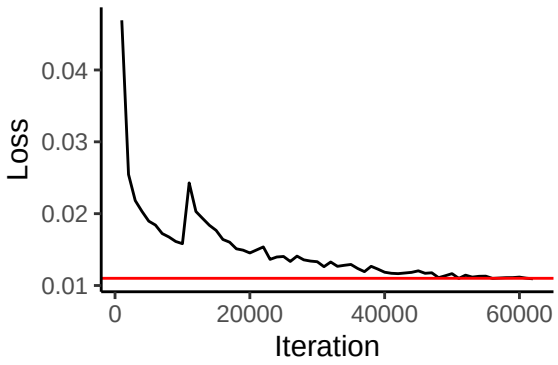


Figure 5.4: The loss function curve in DeepLabCut training.
The curve shows the accuracy of DLC improved by more iterations. The red reference line indicates the least deviation between predicted and actual coordinates.

Video labeling All walking videos from the Catwalk system were exported as avi video format. The trained DLC labelled all videos in one batch. The data generated by DLC includes X-Y coordinates at three anatomical points on a mouse and the likelihood of these coordinates. The likelihood is the indicator of the accuracy of coordinates. The results were saved as CSV files for further steps in WPA. The unit of the X-Y coordination is in pixels. DLC records X and Y coordinates in pixels of a frame and there is no exact conversion of pixels to centimetres (cms). The estimation of the conversion is $45cm/500pixel$. As this is only an estimation in relation to distance, I elected to keep the units as pixels.

Data cleaning

The possible noise in the data set generated by DLC was removed in this stage. Firstly, any coordinates with a likelihood less than 0.9 were excluded. They were the periods of the beginning and the end of videos where only the nose or base of tail of a mouse appeared. For example, at the beginning of a video, there was a nose

of a mouse in the video and the likelihood of the body centre and base of tail was low (less than 0.9). By removing data with low likelihood, only data including the whole mouse body remains in the data set. Secondly, the non-walking behaviours were identified and removed from the data set. The non-walking behaviours, such as standing still and exploring while stationary, are identified by slow forward speed (the speed in X direction). Fig. 5.5 shows a graph of the X coordinate against time of a mouse by runs. Because the mouse can be placed at either the left or right end of the Catwalk walkway, X coordinate of a mouse can begin either from 0 or around 500$pixels$. The direction of X coordinates will not affect our analysis. In Fig. 5.5, the blue circle points the stationary period of a mouse where no or little changes in X coordinate are observed while time passed. Other lines in Fig. 5.5 present a normal walking condition.

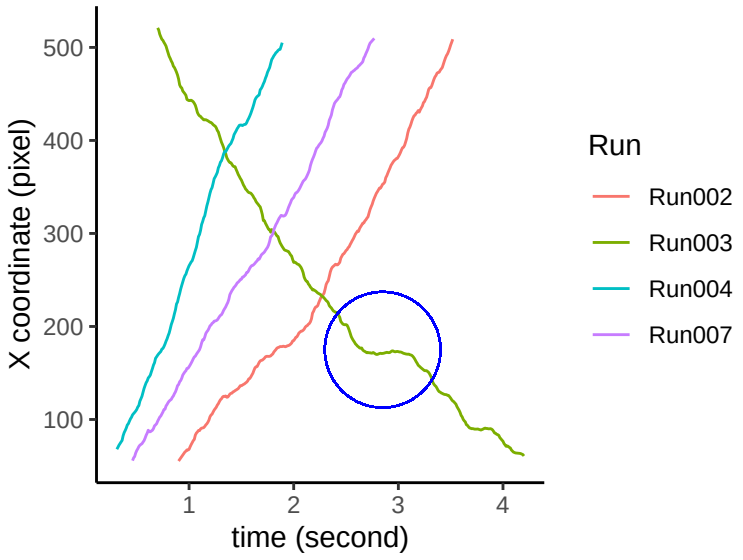


Figure 5.5: Example of non-walking behaviour in a run.
x-axis : time (second) in a run; y-axis: the X coordinate (pixel) of the centre body of a mouse in a walking way. The colours indicate the runs of a mouse. The blue circle pinpoints an obvious non-walking behaviour in a run. The detection of lines indicates the starting points of a run. The downward line (green) means the mouse began from the left end of the walkway. The direction of the line simply reflects whether the run is right to left or left to right and has no intrinsic relevance to the analysis.

The threshold of forward speed was determined by viewing the videos and was defined based on visual evidence as $100 pixels/second$ continuously in more than $0.1 second$. In Fig. 5.6, an example is shown of non-walking behaviour removal. Fig. 5.6 A, the non-walking behaviours were identified by the criteria of forward speed below $100 pixels/second$ in more than $0.1 second$ continually period. Fig. 5.6 B shows the data removed stationary period. Fig. 5.6 C shows the graph connected walking period. After this process, all data include coordinates with a high degree of accuracy as exclusively contain walking behaviour.

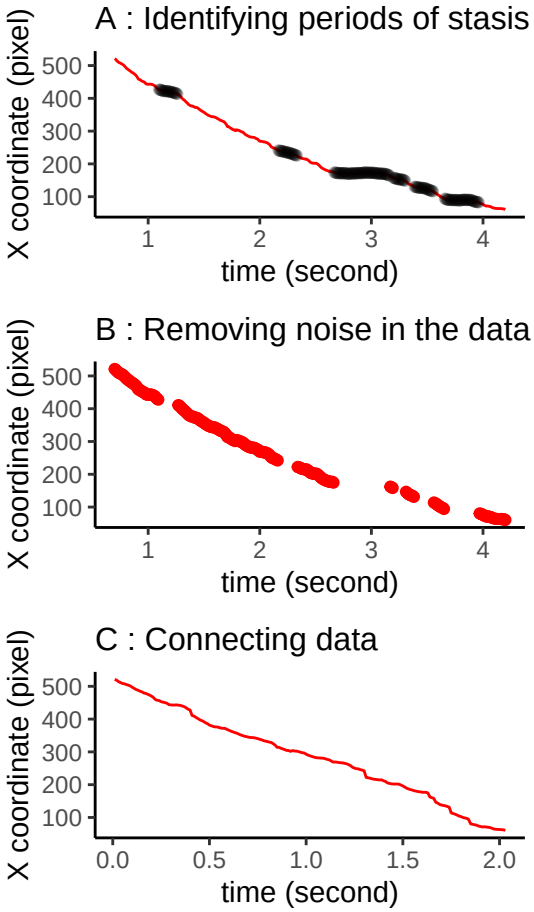


Figure 5.6: Example of removing stationary behaviours in a run.
A: identifying periods of stasis in a run by forward speed (less than 100 pixels/second) lasting more than 0.1 seconds continuously. B: removing noise in the data. C: Connecting the data. The divided walking periods are connected to a high-quality run.

Data preparation

In this step, I evaluated a small number of variables describing the dynamic movements of a mouse. They are general velocity and other variables falling into three main groups, X-direction, Y-direction, and rotating angle. All variables were calculated from coordinates generated from DLC. Fig. 5.7 shows an example of a run from a wild-type mouse in the data set. X coordinates ranged from 0 to around 500 pixels and Y coordinates were between around 35 and around 50*pixels* in Fig. 5.7 A. Fig. 5.7 B and C show graphs with Y coordinates (periodic curve) and X coordinates (straight line) against time respectively. These groups of variables will be explained in detail in the following sections. There were graphs with one mouse from either wild-type or *Npc1*$^{-/-}$ group to demonstrate the data and there were no statistical results included in the demonstrating graphs as they are for illustrative purposes at this stage.

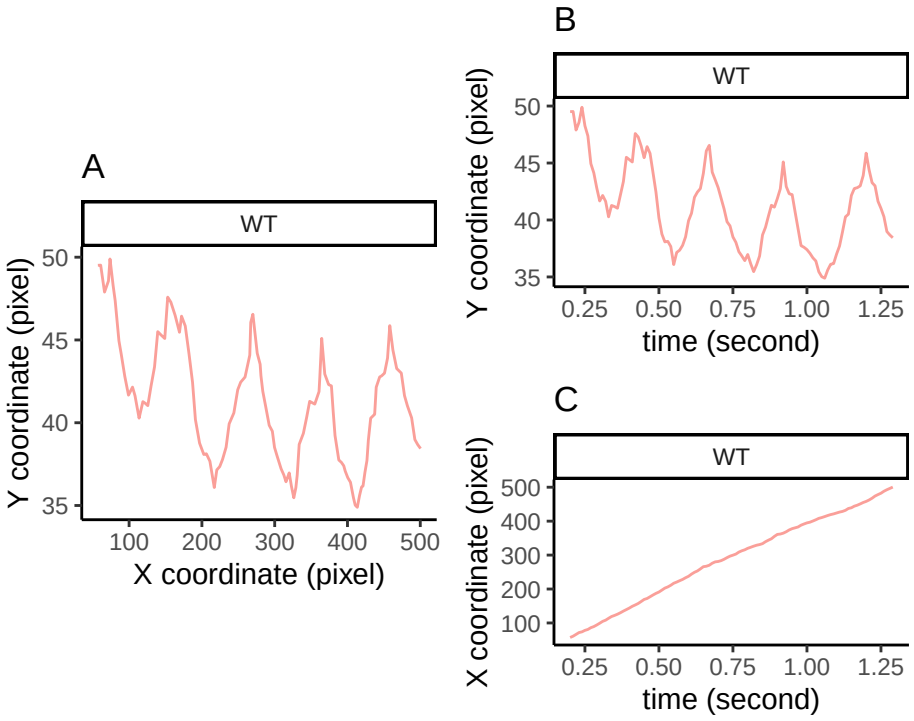


Figure 5.7: Examples of the walking path of a wild-type mouse.
A: The walking path of a mouse along the walkway in the Catwalk device. B: Y coordinate of a mouse against time. C :X coordinate of a mouse against time. WT: wild-type mouse.

The summary of variables is shown in Fig. 5.8. There are 20 variables generated in this section. In the X direction variable group, we calculated mean, SD, and CV (coefficient of variation) of forward speed. Because the graphs of Y coordinates and rotating angle against time show periodic features, we not only generated mean and SD of the Y coordinate and rotating angle but also obtained the mean and SD of their cycle and amplitude.

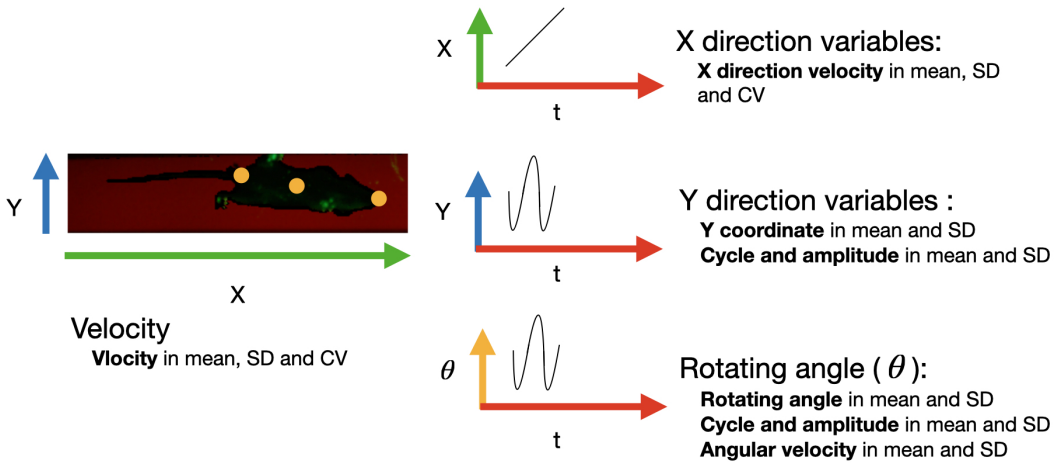


Figure 5.8: Summary of variables in walking path analysis.
Blue arrow: Y coordinate; green arrow: X-coordinate; red arrow: time; yellow arrow: rotating angle.

X direction variables In the X-coordinate against time (X-t) graph in Fig. 5.9, there are two lines from wild-type (turquoise) and *Npc1*$^{-/-}$ (Hom) mice (red). The smoothness of the line reflects the walking behaviour. If a mouse walks forward at a steady speed, the line in X-t graph is smooth, as seen in the wild-type mice (turquoise) (see Fig. 5.9). However, the line of the *Npc1*$^{-/-}$ mouse (red) in Fig. 5.9 is rough with slight fluctuations. This is an indicator of ataxia. In order to quantify the condition of the line in X-t, the slope of the line was used. The slope is defined as the travelled X distance within $0.01 second$. The time duration ($0.01 second$) was due to the sampling rate of the Catwalk camera ($100 Hz$). The slope of X-t line

reflects the forward velocity of a mouse. In Fig. 5.9, the mean of slope (forward velocity) in the wild-type mouse is greater than it is in the *Npc1*$^{-/-}$ mouse. The variation of the slope is an indicator of the smoothness of the line, the smoother the line the more regularity of movement is occurring. However, the SD of the wild-type mouse (126.10) is greater than in *Npc1*$^{-/-}$ mouse (89.73). Therefore, the coefficient of variation (CV) was also introduced to represent the variation of the slope. The CV is defined as $SD/mean * 100$ and is used to compare groups with distinct differences in mean [146]. The CV is more representative of deviation of the line in this case and so better captures the ataxic feature on NPC mice.

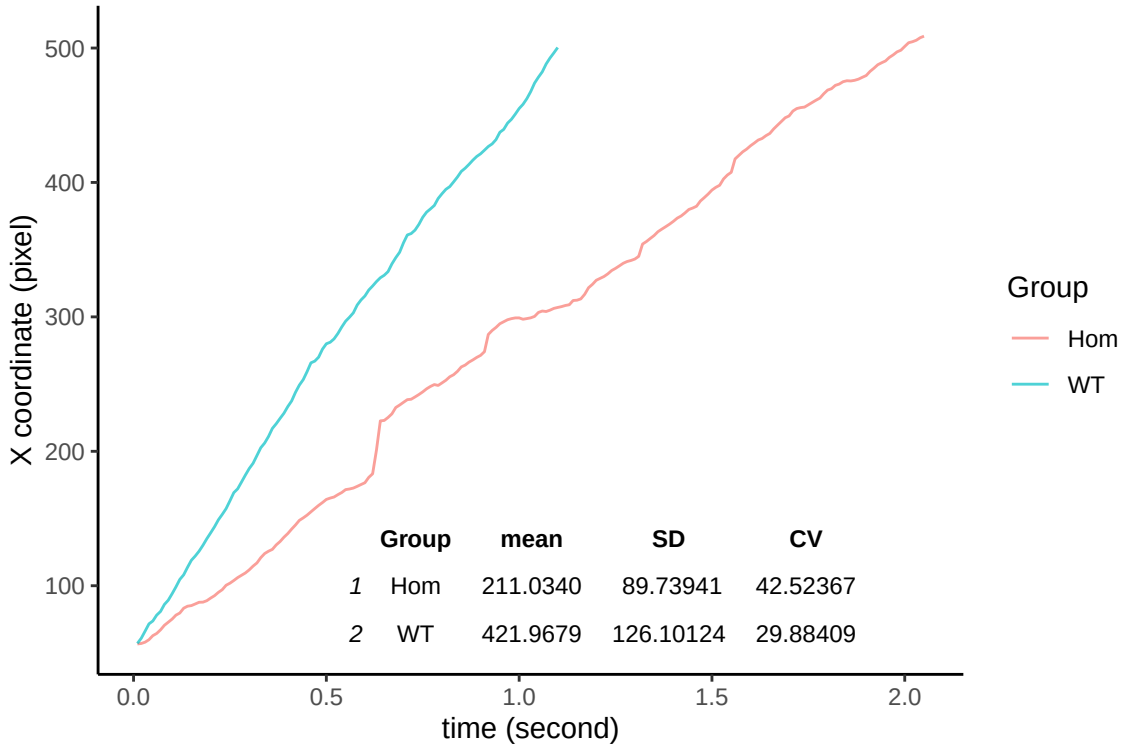


Figure 5.9: X-coordinate against time.
The colours indicate groups (blue: WT; red: Hom). The table shows 3 variables related with the X coordinate. mean the mean of slop (forward speed); SD: the standard deviation of slop; CV: the coefficient of variation of slop.

Y direction variables In the Y coordinates plotted against time (Y-t) (see Fig. 5.10), there are two lines one from the wild-type (turquoise) and one from the *Npc1*$^{-/-}$ group (red). The variables related to the Y-coordinate determine how well a mouse walks in a straight line. Although all mice walk in a sigmoidal way when walking forward, the range of the Y-coordinate is small in the wild-type group compared to *Npc1*$^{-/-}$ which shows greater lateral displacement due to their underlying cerebellar dysfunction. In the previous study [98], the deviation of the Y coordinate from a straight line was used as a marker of ataxia using manually selected points. Here, Y coordinates were generated from DLC, which is objective and recorded at a sample rate of $100Hz$. There were at least 100 points along the walkway in a run. The SD of the Y coordinate presents the deviation, and it can be seen the value was smaller in the wild-type mouse (3.72) than it was in the *Npc1*$^{-/-}$ mouse (6.12) (see Fig. 5.10). The travelling distance in the Y direction is also representative of the deviation of lateral displacement. The travelled Y distance is small when a mouse walks in an approximately straight line.

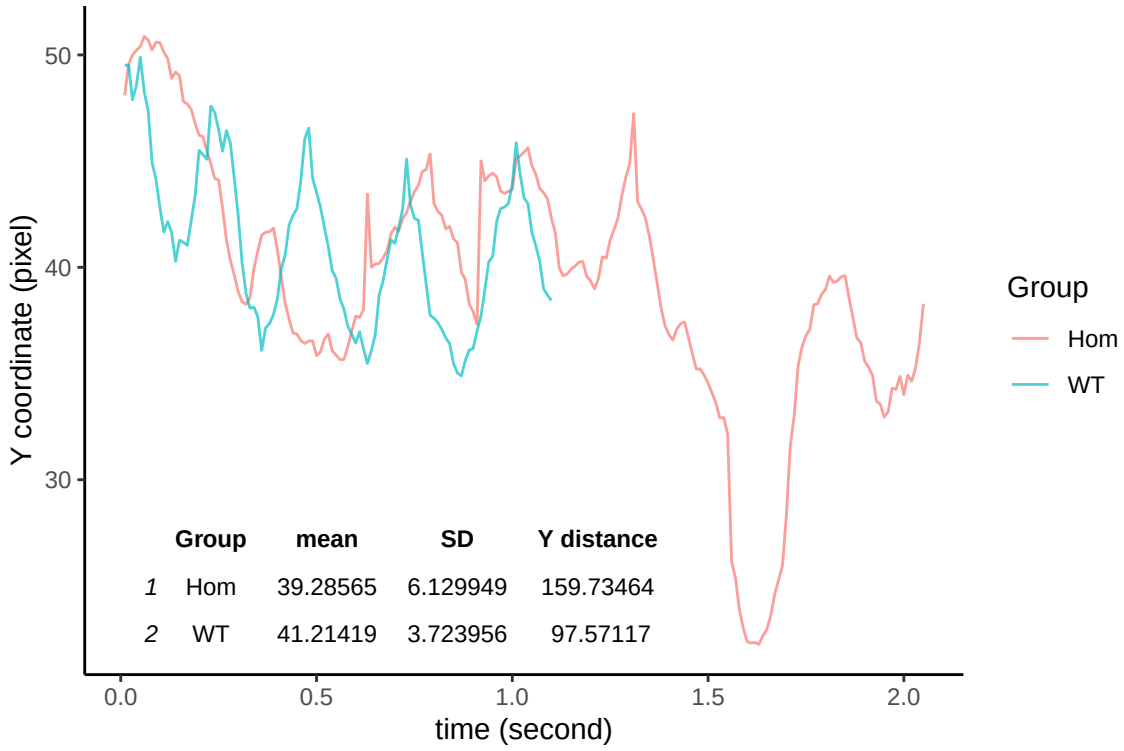


Figure 5.10: Y-coordinate against time.
The colours indicate groups (blue: WT ;red: Hom). The table shows 2 variables related to the Y coordinate. mean: the mean of Y-coordinate; SD: the standard deviation of Y-coordinate; Y distance: the mean of Y travelled distance.

Moreover, there is an obvious periodic feature in the Y-t graph (see Fig. 5.10). Therefore, we used cycle and amplitude to describe the periodic pattern. The cycle is defined as the duration between two peaks in the curve and the amplitude is the Y coordinate difference between the peak and valley of the curve (see Fig. 5.11). The example shows the wild-type mouse had smaller values in cycle (mean, SD) and amplitude (mean, SD) than in the *Npc1*$^{-/-}$ mouse (see Fig. 5.11). The table in Fig. 5.11 summarized all cycle and amplitude of exemplified runs.

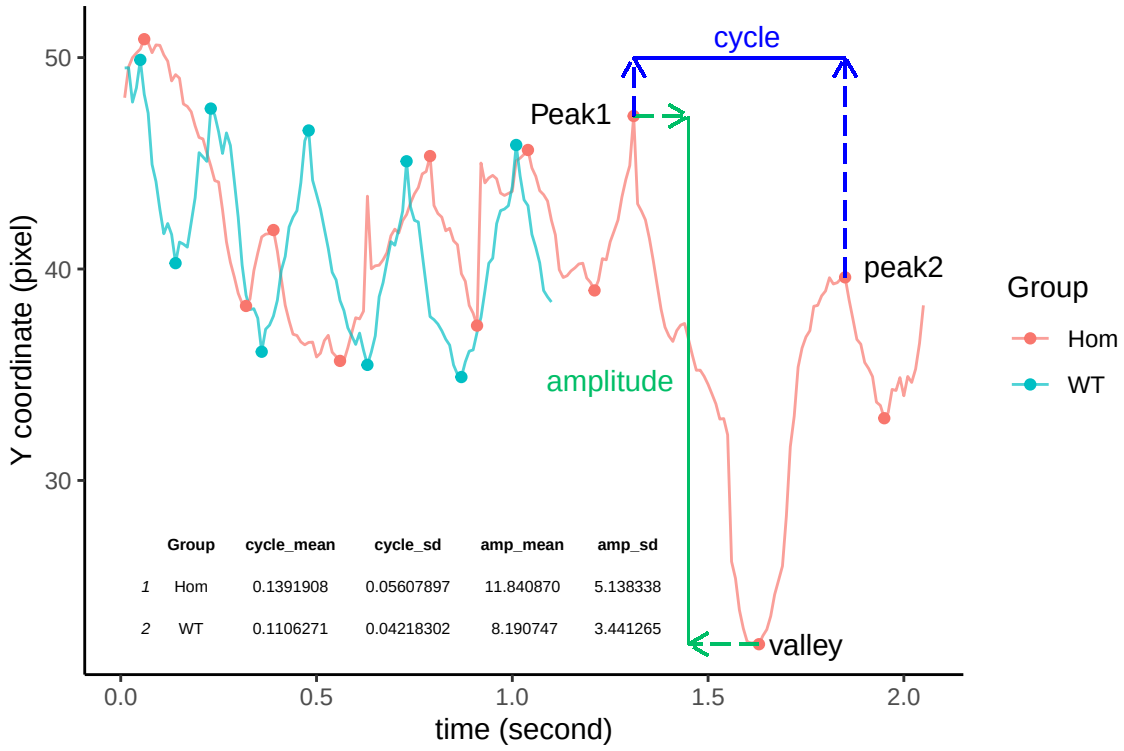


Figure 5.11: Y-coordinate against time with cycle and amplitude.
The colours indicate groups (blue: WT; red: Hom). The points along the curves are either peaks or valleys. Cycle (blue): the time between two peaks. For example, the duration between peak1 and peak2. Amplitude (green): the distance between the peak and valley. The table demonstrates cycle and amplitude (amp) variables related to the Y-t line. cycle_mean: the mean of cycle; cycle_sd: the standard deviation of cycle; amp_mean: the mean of amplitude; amp_sd: the standard deviation of amplitude.

Rotating angle variables The rotating angle ((θ)) is to determine how a mouse rotates its head while walking. From careful observation *Npc1*$^{-/-}$mice tend to turn their head at a large angle. The definition of a rotating angle is the angle between a horizon line and the line between the centre of body and the head (see Fig. 5.12).

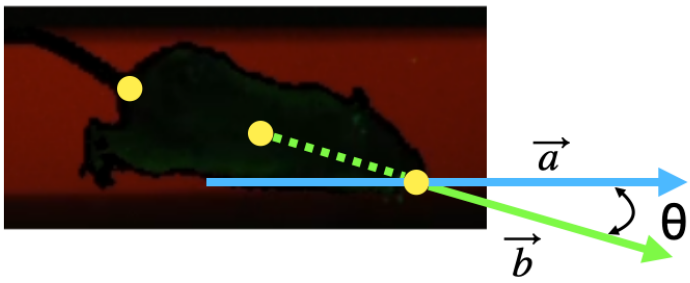


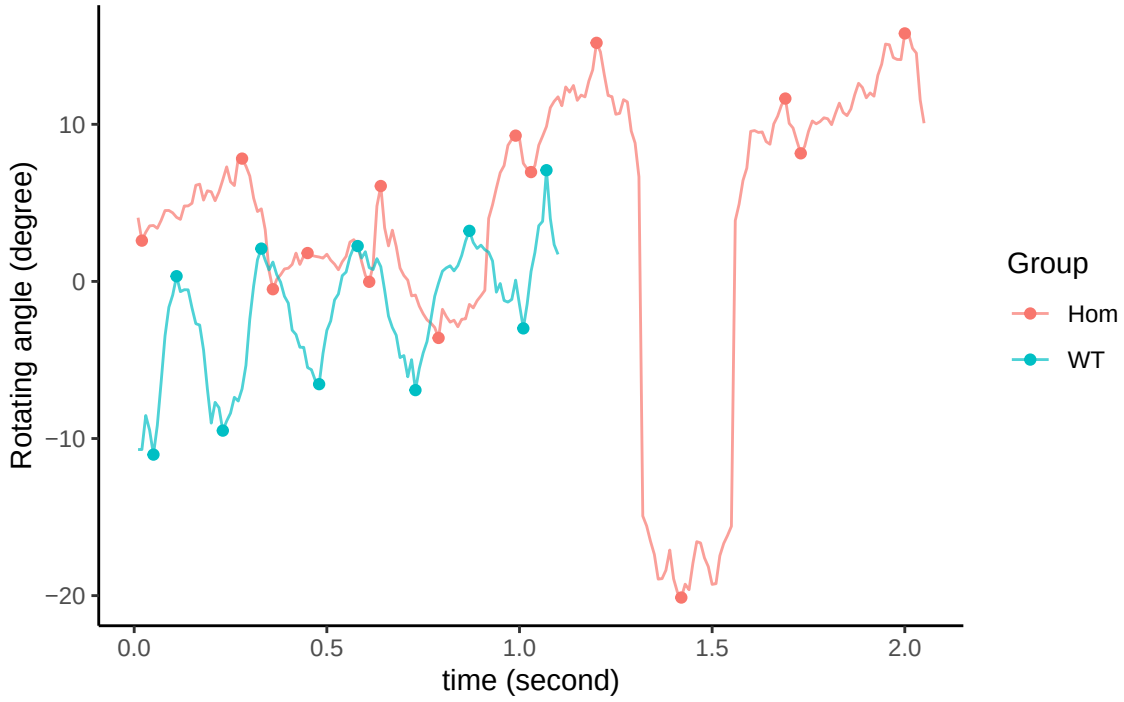
Figure 5.12: Example of rotating angle (θ).
Yellow points: base of tail, body centre and nose (from left to right); $\vec{a}$: a horizontal line in blue; $\vec{b}$: a green line between body centre and nose.

In order to obtain the rotating angle, we apply trigonometric functions in equation (5.1). $\vec{b}$ is obtained from the coordinates of the body centre and the head points of a mouse, which were labelled by DLC and $\vec{a}$ is a horizontal line. The positive θ means there is a left turn when a mouse is walking from left to right on the walkway and vice versa.

$$\vec{a} * \vec{b} = |\vec{a}| * |\vec{b}| * \cos\theta \tag{5.1}$$

$\vec{a}$ = the horizontal line.; $\vec{b}$ = the line between centre and head of a mouse.

From Fig. 5.13, there are 8 variables generated from the rotating angle. They include the mean and SD of the rotating angle and angular velocity. Because of the periodic feature in the rotating angle curve, the mean and SD of cycle and amplitude are also included (see Fig. 5.13).



	Group	angle_mean	angle_sd	angular_vel_mean	angular_vel_sd	cycle_mean	cycle_sd	amp_mean	amp_sd
1	Hom	3.475647	9.116401	0.6633098	88.79009	0.1523077	0.08936385	10.388018	10.79149
2	WT	−2.005350	3.873072	11.3946860	124.83495	0.1133333	0.03570714	9.530223	1.61342

Figure 5.13: Rotating angle against time with cycle and amplitude variables. The colours indicate groups (blue: WT; red: Hom). The points along the curves are either peaks or valleys. The table demonstrates cycle and amplitude (amp) variables related to the rotating angle-t line. cycle_mean: the mean of cycle; cycle_sd: the standard deviation of cycle; amp_mean: the mean of amplitude; amp_sd: the standard deviation of amplitude.

Data analysis

One-way ANOVA was used here to compare all groups. Dunnette's test (post hoc analysis) was followed by one-way ANOVA to obtain the group comparisons. The significance levels are defined as * = $p \leq 0.05$; ** = $p \leq 0.01$; *** = $p \leq 0.001$; **** = $p \leq 0.00001$

Data presentation

The values of 21 variables were plotted as box plots and the results of p values from Dunnett's test were also added to the plots. The p values only included the comparison between Hom untreated and other groups.

5.3 Results

5.3.1 Summary of the data set

The study was performed by Dr Ecem Kaya and is the same Catwalk Data set analysed in Chapter 4. The run videos were exported from the Catwalk system as avi files and the number of mice and runs for each group at 8 weeks of age are shown in Table 5.1. There were also 5-week treatments (from 3 to 8 weeks of age) in this study (miglustat and the acetyl leucine analogues). Each trial corresponded to an individual mouse and there were at least 3 runs in a trial.

	WT	Hom	Mig	ADLL	ADL	ALL
No. trials/mice	6	5	9	7	5	8
No. runs	14	12	29	23	22	25

Table 5.1: The number of trials/mice and runs used for each group at 8 weeks of age. WT: wild-type; Hom: *Npc1* mutant; Mig: miglustat; ADLL: acetyl-DL-leucine; ADL: acetyl-D-leucine; ALL: acetyl-L-leucine

The run videos were labelled at three points by trained DLC, as previously described. The data set generated from DLC included X and Y coordinates of the nose, body centre and base of tail of a mouse. These coordinates were transformed into different variables mentioned previously. The variables were evaluated to determine whether it is appropriate to describe ataxia features in

Npc1^{nih} mice and capture the neuroprotective benefits from the treatments of Mig and ADLL and its enantiomers.

5.3.2 The reference points of a mouse

There were three points labelled in a mouse by DLC, namely the nose, body centre and base of the tail. Apart from rotating angle variables, the variables can be generated according to the X and Y coordinates of these points. However, only the X and Y coordinates of the body centre were used in the following analysis, as the centre has the highest number of variables with p value ≤ 0.0001 between WT and Hom untreated groups among all points (see Table 5.2).

Points	*	**	***	****	ns
centre	0	1	2	7	3
nose	0	3	2	6	2
tail	3	2	1	3	4

Table 5.2: The number of significant variables between WT and Hom groups in different body points of mice.
Significance levels : ns: no significant; *=$p \leq 0.05$; **=$p \leq 0.01$; ***=$p \leq 0.001$; ****=$p \leq 0.0001$.

5.3.3 The velocity

The results of group comparison in the velocity of mean, SD and the coefficient of variation (CV) are displayed in Fig. 5.14 There were significant differences in mean, SD and CV of the velocity between wild-type and *Npc1*$^{-/-}$ untreated groups in Fig. 5.14 A, B and C. The treatment with Mig improved these three variables in velocity and the improvements in mean and CV of velocity also can be seen in the ALL treatment. However, there was no improvement observed in other treatments (ADLL and ADL).

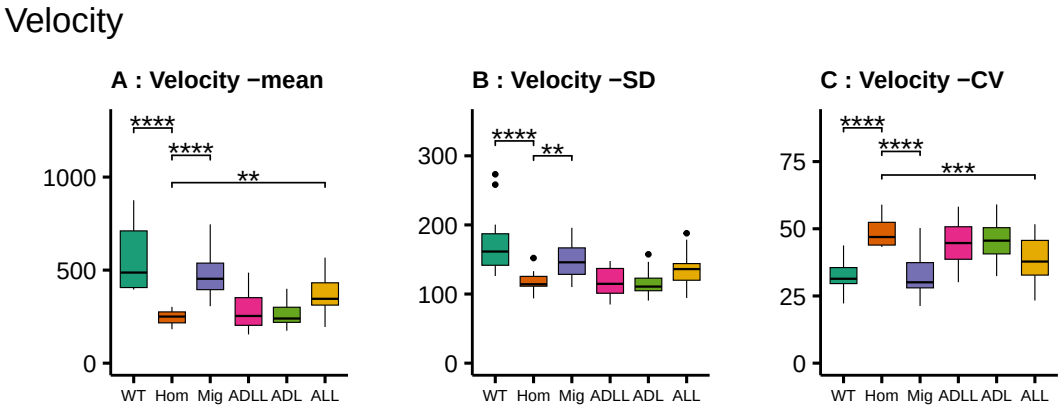


Figure 5.14: The results of group comparison in velocity.
A and D: the mean of velocity; B and E: the SD of velocity; C and F: the coefficient of variation (CV) of velocity.
WT: untreated wild type group; Hom: untreated *NPC*$^{-/-}$ group; Mig: miglustat; ADLL: acetyl-DL-leucine treated group; ADL: acetyl-D-leucine treated group; ALL: acetyl-L-leucine treated group.
The groups were analysed by one-way ANOVA with post hoc analysis (Dunnett's test). Significance levels: *=$p \leq 0.05$; **=$p \leq 0.01$; ***=$p \leq 0.001$; ****=$p \leq 0.0001$.

5.3.4 X direction variables

The variables in the X direction were explained in section 5.2.3. Fig. 5.15 shows the plot of X coordinate against time in $0.01seconds$. The direction of lines in the plot indicates the direction of walking in the walkway and it does not impact the interpretation. From the plot, there were two key observations: the time spent in a run and the smoothness of the lines between the groups were different.

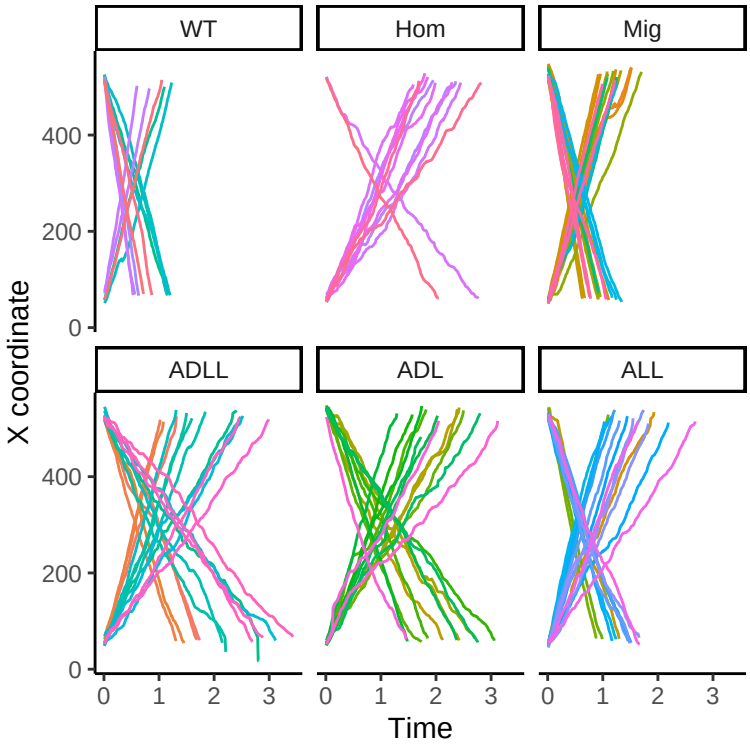


Figure 5.15: Plots of X coordinate against time.
Each line represents a run. WT: untreated wild type group; Hom: untreated $NPC^{+/-}$ group; Mig: miglustat treated group; ADLL: acetyl-DL-leucine treated group; ADL: acetyl-D-leucine treated group; ALL: acetyl-L-leucine treated group. The direction of the line simply reflects whether the run is right to left or left to right and has no intrinsic relevance to the analysis.

These observations were quantified into the slope of mean and variations (SD and CV). The results are shown in Fig. 5.16. The slope of lines in X-t graphs also reflects forward speed. The mean and variations (SD and CV) of slope refer to the differences in time spent and the smoothness of lines respectively in Fig. 5.16. The resultant observations from these variables allow for distinguishing between

WT and *Npc1* untreated groups significantly. The box plots from Mig bear the closest resemblance to the WT group in all three variable plots whilst ALL only resembles WT to a degree in mean and CV variable plots whereas the D enantiomer containing acetyl-leucine was not significantly different from untreated NPC mice.

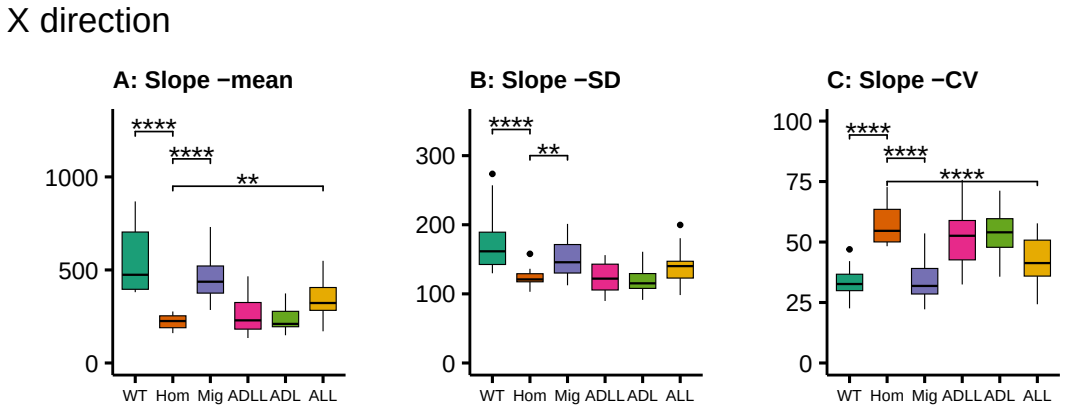


Figure 5.16: The results of group comparison in X direction variables.
A: the mean of the slope; B: the SD of the slope; C: the CV of the slope.
WT: untreated wild type group; Hom: untreated $NPC^{-/-}$ group; Mig: miglustat; ADLL: acetyl-DL-leucine treated group; ADL: acetyl-D-leucine treated group; ALL: acetyl-L-leucine treated group.
The groups were analysed by one-way ANOVA with post hoc analysis (Dunnett's test).
Significance levels: *=$p \leq 0.05$; **=$p \leq 0.01$; ***=$p \leq 0.001$; ****=$p \leq 0.0001$.

5.3.5 Y direction variables

The variables in the Y direction groups were explained in section 5.2.3. The mean of the Y coordinate did not show significant differences between groups (see Fig. 5.17 A). In terms of the SD of the Y coordinate and mean of Y distance, only mice from the Mig treated group showed significant improvements (see Fig 5.17 B and C). Mig treated mice's walking behaviour was therefore shown to be closer to that of WT mice (i.e. walking in a straight line). However, these results were not in agreement with Dr Ecem Kaya's publication [98] due to the different methodologies undertaken and will be discussed in the discussion section.

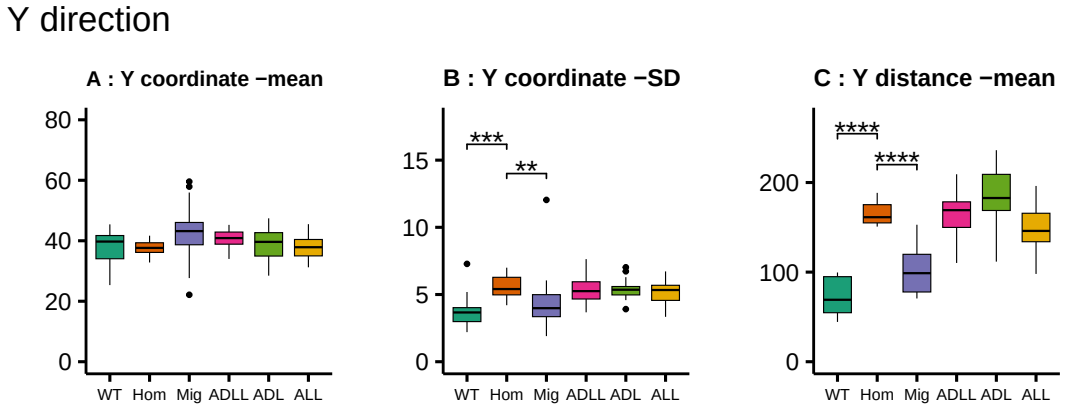


Figure 5.17: The results of group comparison in Y direction variables.
A: the mean of the Y coordinate; B: the SD of the Y coordinate. C: the mean of the Y travelled distance.
WT: untreated wild type group; Hom: untreated *NPC*$^{-/-}$ group; Mig: miglustat; ADLL: acetyl-DL-leucine treated group; ADL: acetyl-D-leucine treated group; ALL: acetyl-L-leucine treated group.
The groups were analysed by one-way ANOVA with post hoc analysis (Dunnett's test). Significance levels: *=$p \leq 0.05$; **=$p \leq 0.01$; ***=$p \leq 0.001$; ****=$p \leq 0.0001$.

Fig. 5.18 displays the results of periodic features of the Y coordinate (see section 5.2.3). The mean of cycle and amplitude shows significant differences between WT and *Npc1*$^{-/-}$ untreated groups and Mig improved these two variables (see Fig. 5.18). There was improvement observed in the mean of cycle from mice in the ALL group.

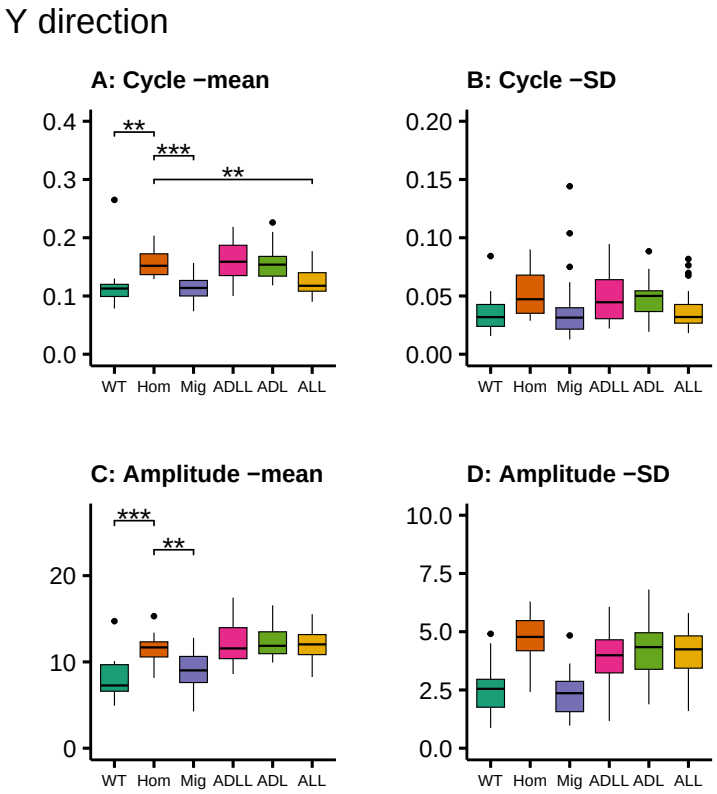


Figure 5.18: The results of group comparison in Y direction cycle and amplitude.
A: the mean of the Y coordinate cycle; B: the SD of the Y coordinate cycle; C: the mean of the Y coordinate amplitude; D: the SD of the Y coordinate amplitude.
WT: untreated wild type group; Hom: untreated $NPC^{-/-}$ group; Mig: miglustat; ADLL: acetyl-DL-leucine treated group; ADL: acetyl-D-leucine treated group; ALL: acetyl-L-leucine treated group.
The groups were analysed by one-way ANOVA with post hoc analysis (Dunnett's test). Significance levels: *=$p \leq 0.05$; **=$p \leq 0.01$; ***=$p \leq 0.001$; ****=$p \leq 0.0001$.

5.3.6 Rotating angle variables

The definition and variables related to rotating angle were explained in section 5.2.3. The results of variables in this group are demonstrated in Fig. 5.19 The mean of rotating angles in groups (see Fig. 5.19 A and B) were around 0, which implies mice were forward facing, not facing to the left or right. However, the SD of rotating angles in all treatments achieved varying degrees of significance, with Mig the most significant with p value ≤ 0.0001, and the remaining 3 treatments being less significant with p values ≤ 0.01.

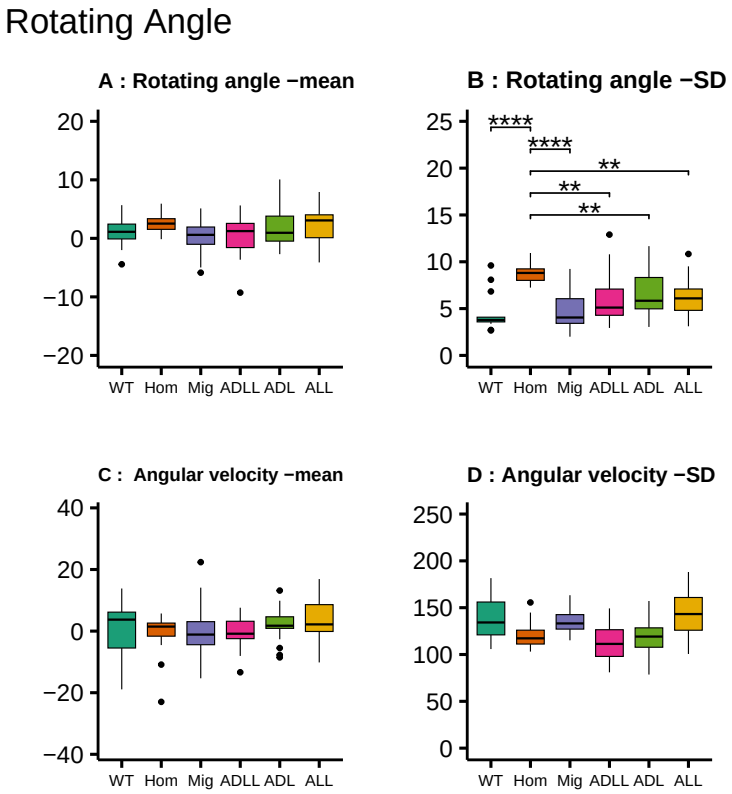


Figure 5.19: The results of group comparison in rotating angle variables.
A: the mean of the rotating angle; B: the SD of the rotating angle; C: the mean of the angular velocity; D: the SD of angular velocity.
WT: untreated wild type group; Hom: untreated *NPC*$^{-/-}$ group; Mig: miglustat; ADLL: acetyl-DL-leucine treated group; ADL: acetyl-D-leucine treated group; ALL: acetyl-L-leucine treated group.
The groups were analysed by one-way ANOVA with post hoc analysis (Dunnett's test). Significance levels: *=$p \leq 0.05$; **=$p \leq 0.01$; ***=$p \leq 0.001$; ****=$p \leq 0.0001$.

The periodic features of the rotating angle were explained in section 5.2.3 and the results are shown in Fig. 5.20. The mean and SD of cycle and amplitude shows significant differences between WT and *Npc1*$^{-/-}$ untreated groups in Fig. 5.20 A, B, C and D. Firstly, the mean of the cycle in all treatments achieved varying degrees of significance, with Mig and ALL being the most significant with p values ≤ 0.0001. Secondly, Mig and ALL can significantly improve the variation (SD) of the cycle. Finally, Mig was the only treatment beneficial to the SD of the amplitude.

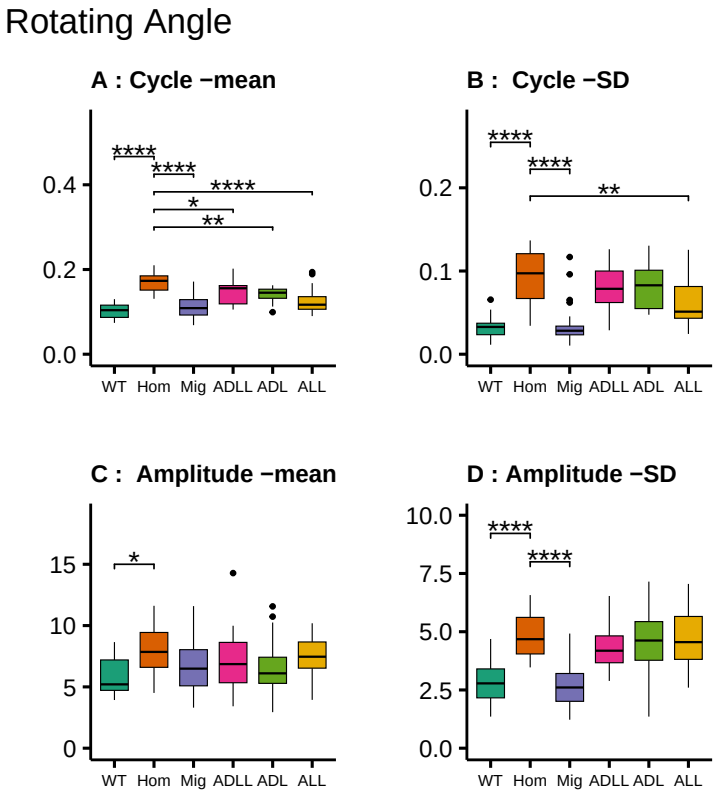


Figure 5.20: The results of group comparison in rotating angle cycle and amplitude variables.
A: the mean of the rotating angle cycle; B: the SD of the rotating angle cycle; C: the mean of the angular velocity cycle; D: the SD of angular velocity amplitude.
WT: untreated wild type group; Hom: untreated $NPC^{-/-}$ group; Mig: miglustat; ADLL: acetyl-DL-leucine treated group; ADL: acetyl-D-leucine treated group; ALL: acetyl-L-leucine treated group.
The groups were analysed by one-way ANOVA with post hoc analysis (Dunnett's test). Significance levels: *=$p \leq 0.05$; **=$p \leq 0.01$; ***=$p \leq 0.001$; ****=$p \leq 0.0001$.

5.3.7 The summary of treatments

The results were summarized in Table 5.3. The data are summarized as p values of one-way ANOVA with post hoc analysis (Dunnett's test). There were 15 out of 21 variables identified as significantly different between WT and Hom untreated mice. These are therefore regarded as relevant variables in the WPA. Looking at this in greater depth, WPA is able to describe the benefit of Mig with clarity, notwithstanding the positive therapeutic effects of ALL.

Groups	Variables	Stat	WT	Mig	ADLL	ADL	ALL
Velocity	velocity	mean	****	****	ns	ns	**
		SD	****	**	ns	ns	ns
		CV	****	****	ns	ns	***
X direction		mean	****	****	ns	ns	**
		SD	****	**	ns	ns	ns
		CV	****	****	ns	ns	****
Y direction	Y coordinate	SD	***	**	ns	ns	ns
	Y distance	mean	****	****	ns	ns	ns
	cycle	mean	**	***	ns	ns	**
	amplitude	mean	***	**	ns	ns	ns
Rotating angle	rotating angle	SD	****	****	**	**	**
	cycle	mean	****	****	*	**	****
		SD	****	****	ns	ns	**
	amplitude	mean	*	ns	ns	ns	ns
		SD	****	****	ns	ns	ns

Table 5.3: The summary of WPA results between groups.
WT: wild type group compares to *NPC* $^{-/-}$ untreated group; Mig: miglustat treated group compares to *NPC* $^{-/-}$ untreated group; ADLL: treated acetyl-DL-leucine group compares to *NPC* $^{-/-}$ untreated group; ADL: acetyl-D-leucine treated group compares to *NPC* $^{-/-}$ untreated group; ALL: acetyl-L-leucine treated group compares to *NPC* $^{-/-}$ untreated group. The results were from one-way ANOVA with post hoc analysis (Dunnett's test). Significance levels : ns: no significant; *=$p \leq 0.05$; **=$p \leq 0.01$; ***=$p \leq 0.001$; ****=$p \leq 0.0001$.

5.4 Discussion

The feasibility and potential of WPA were determined by evaluating treatments proven to improve ataxia in the *Npc1^{nih}* mouse model. WPA is further developed from the method from Dr Ecem Kaya [98], as EBGAM was limiting in showing the positive impacts from acetyl leucine analogue treatments in Chapter 4. Additionally, WPA uses the videos from the Catwalk system, which means the same data set can be analysed twice (EBGAM and WPA). The data sets are therefore consistent between the two methods and construct a more comprehensive analysis as they are based on exactly the same mice/runs. There were 21 variables proposed to be analysed initially and 15 variables were ultimately chosen based on their significance levels (p value ≤ 0.05) between WT and Hom untreated groups. EBGAM in Chapter 4 was capable of singling out Mig as the treatment with the most improvements and significant benefits in gait from Mig was also detected and confirmed using WPA.

Dr Ecem Kaya analysed the deviation between the centre of the body and a straight-line trajectory manually to determine the degree of ataxia in *Npc1^{nih}* mice. She showed ALL can reduce these deviations. Although there is no direct equivalent, a similar variable to this in WPA is the SD of the Y coordinate. This variable depicts the variation of the Y coordinate. However, while Mig lead to improvement, there did not appear to be a significant benefit from ALL. The differences in these observations are likely due to differences in methodologies undertaken. Dr Ecem Kaya manually selected the body centre of a mouse from a Catwalk heat map. The selected points were approximately corresponding to the gait cycle. This means any distinctive points were more likely to be recognized. On the other hand, WPA was able to analyse all the body centre points in an unbiased way. Therefore, the distinct points were smoothed out. For example, using Dr Ecem Kaya's method, the SD of only two Y coordinate points, 1 and 10, was computed to be 6.36, while WPA analysed all Y coordinate points between 1 and 10(inclusive), which resulted in a much smaller SD of 3.03, thereby reducing variability. The variation of the Y coordinate is not sensitive to a change in Y deviation and therefore WPA

does not depict ALL as showing improvement. However, ALL did improve other aspects of ataxia using WPA and these included the CV of the X slope, the mean of the Y coordinate cycle and the SD of the rotating angle and its mean of the cycle, confirming ALL does improve clinical signs of ataxia. These variables will be described in further detail below.

Another variable which describes the features of ataxia is the variations (SD and CV) of the X slope. Mice with ataxia have interruptions in forward speed, hence analysing these variables would allow the quantification of the consistency of forward speed. From Table 5.3, ALL has the same significance level (p value ≤ 0.0001) as Mig. This means WPA can identify the benefits to ataxia in both treatments. Rotating angles were also analysed in WPA, which captures the degree to which the head turns while mice walk. The SD of this variable was improved by all treatments with Mig ((p value ≤ 0.0001) and acetyl leucine analogues including the D-enantiomer (p value ≤ 0.01). In periodic features (Y coordinate and rotating angle), ALL achieved the most improvement among the acetyl leucine treatments and Mig can improve all periodic features except the mean of amplitude in the rotating angle. The ability of WPA to differentiate the effects of therapies can also be evaluated by using acetyl leucine analogue treatments. ADLL is a $50:50$ racemic mixture of ADL and ALL. Both the number of variables and the levels of significance are different between the three acetyl leucine groups. This gives the confidence of WPA to differentiate the therapeutic effects between racemic drugs.

All in all, WPA can detect the positive impacts of proven treatments, which overcomes the limitations of the Catwalk EBGAM analysis. The improvements from Mig can be observed in both gait and WPA and the benefits of ALL can primarily be seen in WPA. This means the specific ataxia improvements can only be seen using WPA. Therefore, it is ideal to conduct both analyses to get the full picture of differential drug actions. The findings in this chapter further reinforce the fact that Mig and AL drugs have independent mechanisms of action hence they are synergistic when combined [98].

6

General Discussion and Future Plans

In this thesis, I have developed two methods (EBGAM and WPA) to analyse gait in *Npc1*$^{-/-}$ mice. In Chapter 2, two *Npc1*$^{-/-}$ mouse models were first characterised to validate the Evidence Base Gait Analysis Method (EBGAM) that I have developed. This is the first-time gait in the NPC mouse models has been investigated in detail. With EBGAM, all variables in the Catwalk were evaluated and determined whether they are relevant to disease progression in these mouse disease models. This allowed us to select relevant variables in an unbiased way rather than selecting variables based on a hypothesis or assumptions. When comparing the two *Npc1*$^{-/-}$ mouse models 171 and 84 variables were found to be significantly changed in the *Npc1*^{nih} and *Npc1*^{nmf164} models respectively. This differential number of variables matches the severity of the two models the *Npc1*^{nih} mouse has a more severe phenotype than the *Npc1*^{nmf164} mouse. We found robust evidence to support the fact that the *Npc1*^{nmf164} mice developed slower and less severe symptoms than the *Npc1*^{nih} mice. This conclusion was based on the fact that EBGAM revealed details in the temporal changes in gait using data from the Catwalk system as the two models aged. The validation of EBGAM in Chapter 2 supported the use of this new methodology to determine if it was sensitive enough to detect the therapeutic benefits of disease-modifying therapies.

In Chapter 3, EBGAM was therefore tested to see if it could detect disease-modifying effects in *Npc1*^{nih} mice treated with the HSP70 amplifier arimoclomol and its combination with the standard-of-care drug miglustat. The results showed the time points where the effects of treatments became apparent and the variables which were differentially affected by the treatments. Moreover, the results identified not only improvements but also some negative effects on some aspects of gait with arimoclomol treatment. On the other hand, miglustat treated mice showed global benefits improving physical and coordination variable improvements beginning from 8 weeks of age and sustained to 10 weeks of age. We also explored combination therapy (arimoclomol and miglustat) that revealed miglustat can reverse the negative effects attributable to arimoclomol. These features were never identified previously. As the time frame of the study in Chapter 3 (6-10 weeks of age) was longer than in Chapter 2 (6-8 weeks of age), there were more variables identified affected by disease progression in the *Npc1*^{nih} model. These results confirmed that EBGAM is both objective and highly sensitive. With the details of gait, we can differentiate the impacts of combination therapy from the two monotherapies. This will help us to distinguish the synergistic and additive effects of combination therapy with the long-term aspiration of using this method to propose an optimal combination therapy for clinical translation in the future.

In Chapter 4, we investigated the validity and limitation of Catwalk analysis with EBGAM comparing miglustat with acetyl leucines (ADLL, ADL and ALL). Mig and acetyl leucine analogues have been shown to improve ataxia in *Npc1* mice and have different mechanisms of action (see section 1.6.1 and 1.6.3). Miglustat is a substrate reduction therapy whereas acetyl leucines improve cellular energy metabolism [98].

The first step to validating Catwalk analysis with EBGAM was to compare the results of Evidence Based Variable Analysis (EBVA) in *Npc1*^{nih} independent cohorts. We found that there are approximately 60% physical-related variables that are identified in two independent cohorts compared with approximately 80% of coordination-related variables. This is because physical-related variables were influenced by individual variability, which was reduced with the size of the sample

and varied in the two experimental cohorts used for this analysis. On the other hand, coordination-related variables are not sensitive to individual variability and remain robust even with smaller group sizes. The top 10 most common physical and coordination-related overlapping variables were selected. These variables can be used as a proxy to compare the treatment effects in any circumstance when EBVA cannot be applied (e.g., when performing single time point studies).

The second step to validating Catwalk analysis with EBGAM was to evaluate the degree of positive impacts on gait from Mig and and acetyl leucine analogues, which are both proven treatments in showing benefits to ataxia in the *Npc1*^{nih} model [70, 98] and in NPC patients [96, 139]. However, the results from EBGAM did not show definitive positive effects on gait for ALL treatments. This is because the Catwalk system generates variables based on paw signals, which ignores other essential features of body movement relating to ataxia. Therefore, this is a major limitation of using the Catwalk system as the sole method for evaluating gait is paw placement based and so another method is required in conjunction with this to measure ataxic trajectories.

As a result, Walking Path Analysis (WPA) was developed in Chapter 5. WPA is a standardized process to analyse the data collected from Catwalk raw videos using the DeepLabCut (DLC) algorithm. Three reference point body regions are highlighted on the mouse videos (base of the tail, centre of the body and nose). The X and Y coordinates of the walking paths of mice retrieved from Catwalk videos are then analysed using deep learning, DeepLabCut (DLC). WPA, therefore, quantifies how a mouse walks in a straight line by analysing the X and Y coordinates of the walking path. The dynamic movements of a mouse are also captured by the periodic variables (cycle and amplitude of the Y coordinate and the rotating angle). Initially, the system was trained using *Npc1*^{nih} videos so the system recognised the abnormal state. There were 21 variables proposed which were generated from the DLC data. Of these, 15 out of the 21 variables showed the ability to distinguish *Npc1*^{nih} mice from WT mice (Table 5.3) reliably with p value ≤ 0.05 in one-way ANOVA (Dunnett's test).

Among these 15 variables, there were two variables that are major indicators of ataxia. Firstly, the SD of the Y coordinate is similar to the deviations between the centre of the body and a straight-line trajectory, which was used in Dr Ecem Kaya's original study [98] in which she manually calculated angles from Catwalk videos. However, the findings were different due to the intricacies of the two methods (manual annotation and WPA). Secondly, the variations (SD and CV) of forward speed are another indicator of ataxia. This indicator showed that ALL and Mig had the same level of significance (p value ≤ 0.0001). This means WPA can identify the benefits of ataxia from both treatments.

Other key indicators include Rotating angle and periodic features (cycle and amplitude). These were investigated in gait analysis for the first time. Previously these features were not focused upon as most existing methods for analysing these would have been too labour-intensive and time-consuming to perform. However, with the development of WPA, this is now possible with great efficiency and analysing these has become more meaningful and feasible and is unbiased. These indicators found that Mig was the most effective treatment, and ALL was the second best. Therefore, WPA is validated to show the benefits to ataxia in two treatments with different mechanisms of action.

	Conventional methods	EBGAM	WPA
All variable analyzed (including SD variables)	No	Yes	Yes
Unique disease profile	No	Yes	Yes
Disease progression	No	Yes	Yes
Specific limb traits	No	Yes	-
Inter-limb coordinations	No	Yes	-
Vedio analysis	No	-	Yes
Body coordination	No	-	Yes
X and Y-direction variables	No	-	Yes
Angular variables	No	-	Yes

Table 6.1: Summary of the advantages of the novel methods innovated in this thesis. EBGAM: Evidence Based Gait Analysis Method; WPA: Walking Path Analysis.

To sum up, these two methods have the potential to be a game changer when analyzing gait in neurodegenerative mouse disease models, not limited to *Npc1*

models and the advances of methods (EBGAM and WPA) are summarized in Table 6.1. They can provide an unbiased, evidence based, comprehensive phenotypic report on the kinetics of clinical sign progression and provide much greater insights into variables affected by disease progression and differential responses to treatments.

6.1 Future directions

If time had allowed, I would have liked to model the effect of treating *Npc1* mice with other small molecules (e.g., cyclodextrin) and also gene therapy and their combination. Moreover, WPA could also be applied to further investigate the previously neglected features (the periodic features) in gait in the NPC mouse models. I would also have liked to compare the mouse data with human gait analysis data from healthy controls and NPC patients.

Furthermore, although complicated data analysis is required for EBGAM and WPA, the application of these methods could be developed into a user-friendly app using the R package (Shiny App) for EBGAM and WPA. This would benefit researchers who are studying neurodegenerative disease mouse models, such as Alzheimer's and Parkinson's disease, but who are not experts in this challenging area of phenotypic/behavioral research/analysis. This methodology can also be extended to analyze disease progression in neurodegenerative diseases across other models, such as *Drosophila* and *feline* models, as well as in clinical patients. Recently, wearable devices have been used to collect motor data from patients with neurodegenerative diseases on a daily basis. The large datasets obtained from this approach could benefit from the analysis process developed here and help quantify the severity of the diseases and monitor their progression and potential modification by therapies. Thus, this approach has many potential applications for a variety of clinically relevant purposes in the future.

Appendices

A
Appendix

A.1 The definition of variables and statistics

This section lists the definition of variables which are in the physical-related and coordination-related groups and explains the statistics (Cstat and Cstat_R) [147].

- **Step sequence** : For each footfall pattern category the percentage of the total number of categorized footfall patterns is given. There are 6 pre-defined footfall patterns listing as followings and these patterns are considered as normal step sequence. There are three main step orders, cruciate, alternate and rotate. They are demonstrated in Fig. A.1. The colours codes for paw are (RF : right front paw ; LF : left front paw ; RH : right hind paw ;LH : left hind paw)

  1. **Cruciate**: the priority of step sequence is front paws to hind paws.

  – Ca : RF-LF-RH-LH
  – Cb : LF-RF-LH-RH

  2. **Alternate**: the priority of step sequence is one lateral side to the other.

  – Aa : RF-RH-LF-LH

- Ab : LF-RH-RF-LH

3. **Rotate**: the step sequence is either anticlockwise from RF or counter-clockwise from LF.

- Ra : RF-LF-LH-RH
- Rb : LF-RF-RH-LH

Note : In Ca, Aa and Ra, the lowercase **a** means a step sequence begins from RH (right hind paw); in Cb, Ab and Rb, the lowercase **b** means means a step sequence begins from LF (left front paw).

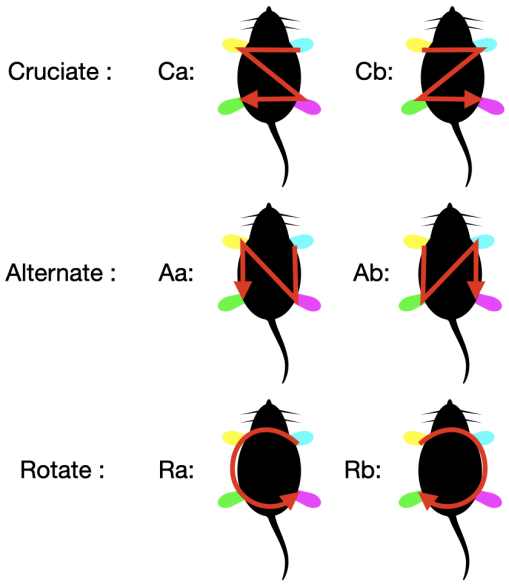


Figure A.1: Three main categories of step sequences.
Cruciate: the step sequences are S or Z shapeed.
Alternate: the step sequences are N or U shaped.
Rotate: the step sequences are counterclockwise or clockwise.

- **Base of support (BOS)** : The mean values of the length of either the front paws or the hind paws.
- **Support** : The relative duration of contact with the glass plate of all paw combinations. The combinations are: zero paw, single paw, diagonal pair of paws (RF-LH or LF-RH), lateral paws (RF-RH or LF-LH), girdle paws (RF-LF or RH-LH), three paws or four paws.

- **Phase Dispersions** : The temporal relationship between placement of two paws within a Step Cycle. It ranges from -50% to 75%. A positive Phase Dispersion value means the initial contact of the target paw occurred after the of the anchor paw (Fig A.2 A). A negative value indicates that the target paw preceded the anchor paw (Fig. A.2 B) is a simplified figure of timing view. The solid line means the ground contact (stance) of a paw and dashed line reflects the paw is on the air (swing). It shows an example of positive Phase Dispersion/Couplings (RH->LH). The Phase Dispersions/Couplings is the percentage time in which the target paw contacts the ground in a step cycle of an anchor paw. As can be seen, the stance of the anchor paw(RH) is 1 second and the time period from the beginning of the anchor paw stance to the time point when the target paw contacts the ground is 0.4 seconds. Thus, Phase Dispersion (RH->LH) is 40%. An example of negative Phase Dispersions is shown in Fig. A.2 B. The negative value reflects a target paw touching the ground before an anchor paw.

- **Couplings** : It is calculated the same way as Phase Dispersion. However, it only includes the positive values which means a target paw can never precede an anchor (Fig. A.2 A).

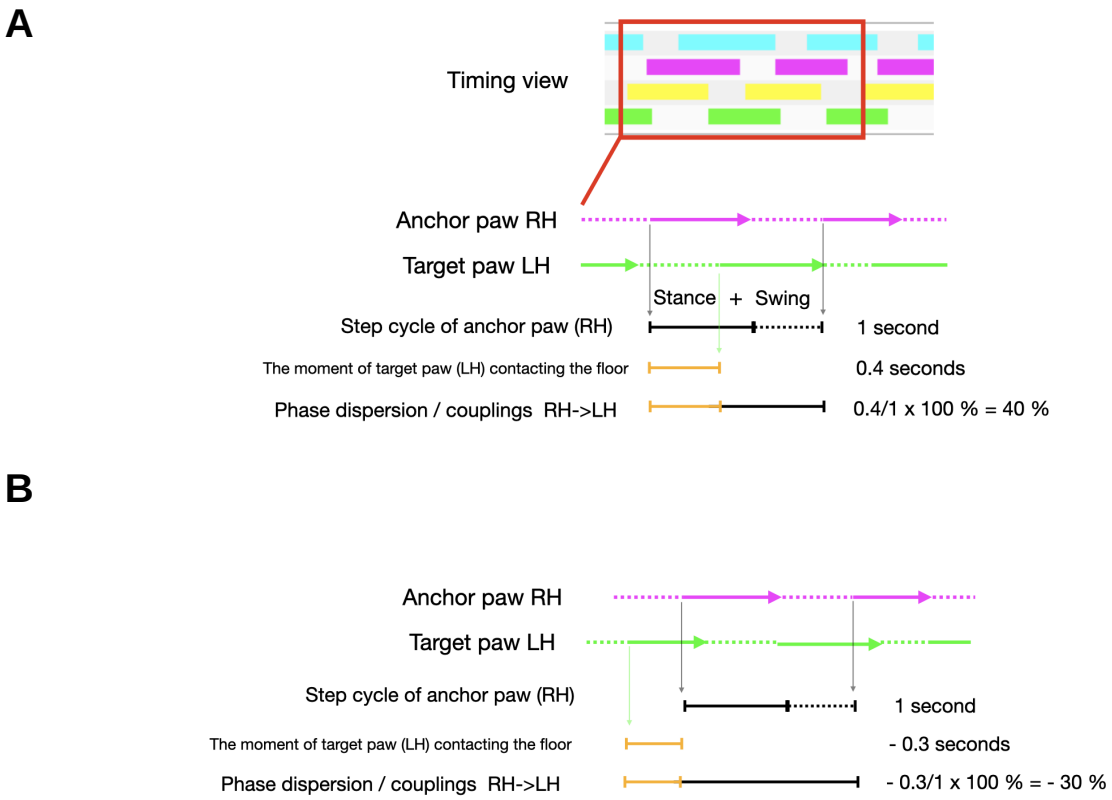


Figure A.2: Example of RH->LH Phase Dispersions and Couplings. RH (right hind paw): anchor paw; LH (left hind paw): target paw; Phase Dispersions/Couplings: the percentage of the moment of target paw touching floor in a step cycle of anchor paw. (A): example of positive Phase Dispersion; (B): example of negative Phase Dispersion.

- **Cstat Mean/ SD/ R** : The Catwalk provides circular statistics to evaluate inter-paw interactions. Phase Dispersions and Couplings can be regarded as periodic variables. 0% Phase Dispersion is equivalent to 100% in circular statistics. It is because 100% Phase Dispersion is 0% for next anchor step. The linear statistics (Mean and SD) consider Phase Dispersions and Couplings in a step-wise manner which means each step is dependent from other steps. On the other hand, circular statistics (Cstat_Mean, Cstat_SD and Cstat_R) take nearby steps into considerations. Phase Dispersions and Couplings are a cycle of 0%-100%. Cstat_Mean is the average of phase lag (the time lag between two paw touching the ground), ranging from 0 to 100. Cstat_R is the

indication of the strength of periodicity of two paw interactions in Equation (A.3). The a in the Equation (A.1) and (A.2) is phase lag. Cstat_SD is the indication of phase lags dispersion, ranging from 0 to 22.5 in Equation (A.4). If the inter-paw interaction shows a consistent periodic pattern, Cstat_R is close to 1 and Cstat_SD is close to 0.

$$X = \frac{\sum_{i=1}^{n} \cos(\frac{2\pi}{100} a_i)}{n} a = phaselag \tag{A.1}$$

$$Y = \frac{\sum_{i=1}^{n} \sin(\frac{2\pi}{100} a_i)}{n} a = phaselag \tag{A.2}$$

$$R = \sqrt{X^2 + Y^2} \tag{A.3}$$

$$SD = \frac{100}{2\pi} \sqrt{2(1 - R)} \tag{A.4}$$

- **Normal Patterns** : The number of Step Cycles that fall within one of the pre-defined footfall pattern categories.
- **Accounted Steps** : The number of steps that was considered into account to determine the footfall patterns.
- **Regularity Index (%)** : The percentage of the number of normal step sequence patterns relative to the total number of paw placements (Accounted Steps)

$$RegularityIndex = \frac{NSSP * 4}{PP} * 100$$

NSSP : The number of normal step sequence patterns. The normal step sequences are the 6 step sequences mentioned above. One step sequence patterns includes 4 steps. PP : The total number of paw placement (Accounted steps)

- **Run Duration**: The duration of the recorded run. This variable will be excluded as it can not reflect the duration of a partial run after data segmentation.
- **Run Average Speed** : The average speed of the mouse in the recorded run. This variable will be excluded as it can not reflect the duration of a partial run after data segmentation.
- **Run Maximum Variation** : The maximum variation in walking speed in the recorded run. This variable will be excluded as it can not reflect the duration of a partial run after data segmentation.
- **Body Speed** : The Body Speed of a step cycle of a specific paw is calculated by dividing the distance that the animal's body traveled from one initial contact of that paw to the next by the time to travel that distance
- **Body Speed Variation (%)** : It is calculated by dividing the absolute difference between the Body speed and the Average Speed of a run by the Average Speed.

$$BodySpeedVaration = \frac{BodySpeed - AverageSpeed}{AverageSpeed}$$

- **Other statistics : Duration**

The duration of the run on the selected steps. Which means that it only considers the selected part of the run. In the Data cleaning section 2.2.2, the non-walking part of the run is excluded. This variable can describe the duration of walking part in the run. However, it can not be used to compares between groups as the duration is covered different traveled distance.

- **Other statistics : Average Speed**

The speed of the selected steps.

- **Other statistics : Maximun Variation (%)**

The Maximum Variation in average speed of the selected steps in the data selection.

- **Cadence** : The number of step in a second.
- **Stand (s) or Stance (s)** : The duration in seconds of contact of a paw with the glass plate (Fig. A.2).
- **Stand Index** : The measure of the speed at which the paw loses contact with the glass plate. ***Note*** : it is only used for smoothly moving animal and unable to be generated when stances combined. This variable will be excluded as the steps combination is done in Data cleaning section 2.2.2
- **Single Stance** : The duration in seconds of ground contact for a single hind paw. In Fig. A.3, the solid line means the ground contact of the paw and the dashed line means the paw is in the air. The green oval area indicates the moment that right hind paw contact the ground, single stance.
- **Dual Stance** : The duration in seconds of ground contact for both hind paws. ***note*** : Dual stance is used for gait analysis in pain models.
  - **Initial Dual stance** : The duration of the first contralateral hind paw contact the ground within the stance of the other hind paw. In Fig. A.3, the blue oval area is the period of first left hind paw contact the ground within a step cycle of right hind paw, which is Initial Dual Stance.
  - **Terminal Dual Stance** : The duration of the second contralateral hind paw contact the ground within the stance of the other hind paw. In Fig. A.3, the yellow oval area is the period of second left hind paw contact the ground within a step cycle of right hind paw, which is Terminal Dual Stance.
- **Swing (s)** : The duration in seconds of no contact of a paw. Figure A.2

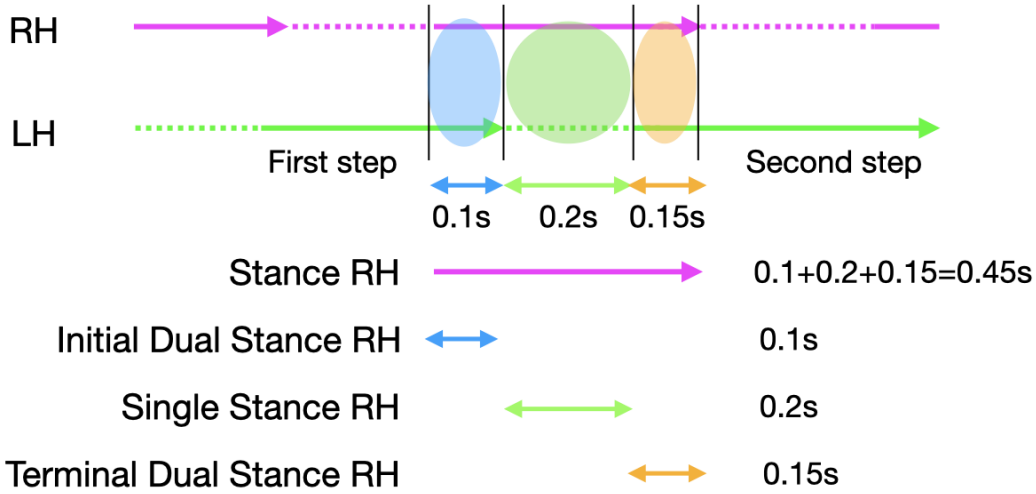


Figure A.3: Example of stance variables.

- **Swing Speed** : The speed of the paw during Swing.

$$SwingSpeed = \frac{StrideLength}{Swing}$$

- **Stride Length** : The distance between successive placements of the same paw. Calculation of Stride Length is based on the difference of X and Y coordinates between two successive placements considering Pythagoras's theorem.

- **Step Cycle (s)** : The duration in seconds between two consecutive initial Contacts of the same paw. Fig. A.2

$$StepCycle = Stand + Swing$$

- **Duty Cycle (%)** : The percentage of Stand in a step cycle. Fig. A.2

A.2 The categories of variables in the Catwalk system

The following tables display five categories of variables in the Catwalk system. There are 495 variables in total. Out of these, 245 variables (107 physical-related and 138 coordination related) are relevant to the analysis. The colours indicate different groups. Red: Description; orange: physical-related; yellow: intensity-related; green: coordination-related; blue: indices; purple: other variable.

Table A.1: The catergories of variables.

Experiment	LF_Stand_(s)_SD	FP_SingleStance_(s)_Mean
Group	LF_Swing_(s)_Mean	FP_SingleStance_(s)_SD
Group_Type	LF_Swing_(s)_SD	FP_InitialDualStance_(s)_Mean
Group_Description	LF_SwingSpeed_(cm/s)_Mean	FP_InitialDualStance_(s)_SD
Animal	LF_SwingSpeed_(cm/s)_SD	FP_TerminalDualStance_(s)_Mean
Time_Point	LF_StrideLength_(cm)_Mean	FP_TerminalDualStance_(s)_SD
Time_Point_Description	LF_StrideLength_(cm)_SD	FP_BodySpeed_(cm/s)_Mean
Trial	LF_StepCycle_(s)_Mean	FP_BodySpeed_(cm/s)_SD
Trial_Description	LF_StepCycle_(s)_SD	FP_BodySpeedVariation_(%)_Mean
NumberOfRunsUsedForCalculatingTrialStatistics	LF_DutyCycle_(%)_Mean	FP_BodySpeedVariation_(%)_SD
RF_Stand_(s)_Mean	LF_DutyCycle_(%)_SD	HP_Stand_(s)_Mean
RF_Stand_(s)_SD	LF_SingleStance_(s)_Mean	HP_Stand_(s)_SD
RF_Swing_(s)_Mean	LF_SingleStance_(s)_SD	HP_Swing_(s)_Mean
RF_Swing_(s)_SD	LF_InitialDualStance_(s)_Mean	HP_Swing_(s)_SD
RF_SwingSpeed_(cm/s)_Mean	LF_InitialDualStance_(s)_SD	HP_SwingSpeed_(cm/s)_Mean
RF_SwingSpeed_(cm/s)_SD	LF_TerminalDualStance_(s)_Mean	HP_SwingSpeed_(cm/s)_SD
RF_StrideLength_(cm)_Mean	LF_TerminalDualStance_(s)_SD	HP_StrideLength_(cm)_Mean
RF_StrideLength_(cm)_SD	LF_BodySpeed_(cm/s)_Mean	HP_StrideLength_(cm)_SD
RF_StepCycle_(s)_Mean	LF_BodySpeed_(cm/s)_SD	HP_StepCycle_(s)_Mean
RF_StepCycle_(s)_SD	LF_BodySpeedVariation_(%)_Mean	HP_StepCycle_(s)_SD
RF_DutyCycle_(%)_Mean	LF_BodySpeedVariation_(%)_SD	HP_DutyCycle_(%)_Mean
RF_DutyCycle_(%)_SD	LH_Stand_(s)_Mean	HP_DutyCycle_(%)_SD
RF_SingleStance_(s)_Mean	LH_Stand_(s)_SD	HP_SingleStance_(s)_Mean
RF_SingleStance_(s)_SD	LH_Swing_(s)_Mean	HP_SingleStance_(s)_SD
RF_InitialDualStance_(s)_Mean	LH_Swing_(s)_SD	HP_InitialDualStance_(s)_Mean
RF_InitialDualStance_(s)_SD	LH_SwingSpeed_(cm/s)_Mean	HP_InitialDualStance_(s)_SD
RF_TerminalDualStance_(s)_Mean	LH_SwingSpeed_(cm/s)_SD	HP_TerminalDualStance_(s)_Mean
RF_TerminalDualStance_(s)_SD	LH_StrideLength_(cm)_Mean	HP_TerminalDualStance_(s)_SD
RF_BodySpeed_(cm/s)_Mean	LH_StrideLength_(cm)_SD	HP_BodySpeed_(cm/s)_Mean
RF_BodySpeed_(cm/s)_SD	LH_StepCycle_(s)_Mean	HP_BodySpeed_(cm/s)_SD
RF_BodySpeedVariation_(%)_Mean	LH_StepCycle_(s)_SD	HP_BodySpeedVariation_(%)_Mean
RF_BodySpeedVariation_(%)_SD	LH_DutyCycle_(%)_Mean	HP_BodySpeedVariation_(%)_SD
RH_Stand_(s)_Mean	LH_DutyCycle_(%)_SD	BOS_FrontPaws_Mean_(cm)
RH_Stand_(s)_SD	LH_SingleStance_(s)_Mean	BOS_HindPaws_Mean_(cm)
RH_Swing_(s)_Mean	LH_SingleStance_(s)_SD	OtherStatistics_Average_Speed_Mean
RH_Swing_(s)_SD	LH_InitialDualStance_(s)_Mean	OtherStatistics_Average_Speed_SD
RH_SwingSpeed_(cm/s)_Mean	LH_InitialDualStance_(s)_SD	OtherStatistics_Maximum_Variation_(%)_Mean
RH_SwingSpeed_(cm/s)_SD	LH_TerminalDualStance_(s)_Mean	OtherStatistics_Maximum_Variation_(%)_SD
RH_StrideLength_(cm)_Mean	LH_TerminalDualStance_(s)_SD	RF_MaxContactAt_(%)_Mean
RH_StrideLength_(cm)_SD	LH_BodySpeed_(cm/s)_Mean	RF_MaxContactAt_(%)_SD
RH_StepCycle_(s)_Mean	LH_BodySpeed_(cm/s)_SD	RF_MaxContactArea_(cm²)_Mean
RH_StepCycle_(s)_SD	LH_BodySpeedVariation_(%)_Mean	RF_MaxContactArea_(cm²)_SD
RH_DutyCycle_(%)_Mean	LH_BodySpeedVariation_(%)_SD	RF_MaxContactMaxIntensity_Mean
RH_DutyCycle_(%)_SD	FP_Stand_(s)_Mean	RF_MaxContactMaxIntensity_SD
RH_SingleStance_(s)_Mean	FP_Stand_(s)_SD	RF_MaxContactMeanIntensity_Mean
RH_SingleStance_(s)_SD	FP_Swing_(s)_Mean	RF_MaxContactMeanIntensity_SD
RH_InitialDualStance_(s)_Mean	FP_Swing_(s)_SD	RF_PrintLength_(cm)_Mean
RH_InitialDualStance_(s)_SD	FP_SwingSpeed_(cm/s)_Mean	RF_PrintLength_(cm)_SD
RH_TerminalDualStance_(s)_Mean	FP_SwingSpeed_(cm/s)_SD	RF_PrintWidth_(cm)_Mean
RH_TerminalDualStance_(s)_SD	FP_StrideLength_(cm)_Mean	RF_PrintWidth_(cm)_SD
RH_BodySpeed_(cm/s)_Mean	FP_StrideLength_(cm)_SD	RF_PrintArea_(cm²)_Mean
RH_BodySpeed_(cm/s)_SD	FP_StepCycle_(s)_Mean	RF_PrintArea_(cm²)_SD
RH_BodySpeedVariation_(%)_Mean	FP_StepCycle_(s)_SD	RF_MaxIntensityAt_(%)_Mean
RH_BodySpeedVariation_(%)_SD	FP_DutyCycle_(%)_Mean	RF_MaxIntensityAt_(%)_SD
LF_Stand_(s)_Mean	FP_DutyCycle_(%)_SD	RF_MaxIntensity_Mean

Table A.2: continued to Table A.1

RF__MaxIntensity__SD	LF__MaxContactMaxIntensity__Mean	LH__ToeSpread__(cm)__SD
RF__MinIntensity__Mean	LF__MaxContactMaxIntensity__SD	LH__IntermediateToeSpread__(cm)__Mean
RF__MinIntensity__SD	LF__MaxContactMeanIntensity__Mean	LH__IntermediateToeSpread__(cm)__SD
RF__MeanIntensity__Mean	LF__MaxContactMeanIntensity__SD	LH__ManualPrintLength__(cm)__Mean
RF__MeanIntensity__SD	LF__PrintLength__(cm)__Mean	LH__ManualPrintLength__(cm)__SD
RF__MeanIntensityOfThe15MostIntensePixels__Mean	LF__PrintLength__(cm)__SD	LH__PawAngleBodyAxis__(°)__Mean
RF__MeanIntensityOfThe15MostIntensePixels__SD	LF__PrintWidth__(cm)__Mean	LH__PawAngleBodyAxis__(°)__SD
RF__ToeSpread__(cm)__Mean	LF__PrintWidth__(cm)__SD	LH__PawAngleMovementVector__(°)__Mean
RF__ToeSpread__(cm)__SD	LF__PrintArea__(cm²)__Mean	LH__PawAngleMovementVector__(°)__SD
RF__IntermediateToeSpread__(cm)__Mean	LF__PrintArea__(cm²)__SD	FP__MaxContactAt__(%)__Mean
RF__IntermediateToeSpread__(cm)__SD	LF__MaxIntensityAt__(%)__Mean	FP__MaxContactAt__(%)__SD
RF__ManualPrintLength__(cm)__Mean	LF__MaxIntensityAt__(%)__SD	FP__MaxContactArea__(cm²)__Mean
RF__ManualPrintLength__(cm)__SD	LF__MaxIntensity__Mean	FP__MaxContactArea__(cm²)__SD
RF__PawAngleBodyAxis__(°)__Mean	LF__MaxIntensity__SD	FP__MaxContactMaxIntensity__Mean
RF__PawAngleBodyAxis__(°)__SD	LF__MinIntensity__Mean	FP__MaxContactMaxIntensity__SD
RF__PawAngleMovementVector__(°)__Mean	LF__MinIntensity__SD	FP__MaxContactMeanIntensity__Mean
RF__PawAngleMovementVector__(°)__SD	LF__MeanIntensity__Mean	FP__MaxContactMeanIntensity__SD
RH__MaxContactAt__(%)__Mean	LF__MeanIntensity__SD	FP__PrintLength__(cm)__Mean
RH__MaxContactAt__(%)__SD	LF__MeanIntensityOfThe15MostIntensePixels__Mean	FP__PrintLength__(cm)__SD
RH__MaxContactArea__(cm²)__Mean	LF__MeanIntensityOfThe15MostIntensePixels__SD	FP__PrintWidth__(cm)__Mean
RH__MaxContactArea__(cm²)__SD	LF__ToeSpread__(cm)__Mean	FP__PrintWidth__(cm)__SD
RH__MaxContactMaxIntensity__Mean	LF__ToeSpread__(cm)__SD	FP__PrintArea__(cm²)__Mean
RH__MaxContactMaxIntensity__SD	LF__IntermediateToeSpread__(cm)__Mean	FP__PrintArea__(cm²)__SD
RH__MaxContactMeanIntensity__Mean	LF__IntermediateToeSpread__(cm)__SD	FP__MaxIntensityAt__(%)__Mean
RH__MaxContactMeanIntensity__SD	LF__ManualPrintLength__(cm)__Mean	FP__MaxIntensityAt__(%)__SD
RH__PrintLength__(cm)__Mean	LF__ManualPrintLength__(cm)__SD	FP__MaxIntensity__Mean
RH__PrintLength__(cm)__SD	LF__PawAngleBodyAxis__(°)__Mean	FP__MaxIntensity__SD
RH__PrintWidth__(cm)__Mean	LF__PawAngleBodyAxis__(°)__SD	FP__MinIntensity__Mean
RH__PrintWidth__(cm)__SD	LF__PawAngleMovementVector__(°)__Mean	FP__MinIntensity__SD
RH__PrintArea__(cm²)__Mean	LF__PawAngleMovementVector__(°)__SD	FP__MeanIntensity__Mean
RH__PrintArea__(cm²)__SD	LH__MaxContactAt__(%)__Mean	FP__MeanIntensity__SD
RH__MaxIntensityAt__(%)__Mean	LH__MaxContactAt__(%)__SD	FP__MeanIntensityOfThe15MostIntensePixels__Mean
RH__MaxIntensityAt__(%)__SD	LH__MaxContactArea__(cm²)__Mean	FP__MeanIntensityOfThe15MostIntensePixels__SD
RH__MaxIntensity__Mean	LH__MaxContactArea__(cm²)__SD	FP__ToeSpread__(cm)__Mean
RH__MaxIntensity__SD	LH__MaxContactMaxIntensity__Mean	FP__ToeSpread__(cm)__SD
RH__MinIntensity__Mean	LH__MaxContactMaxIntensity__SD	FP__IntermediateToeSpread__(cm)__Mean
RH__MinIntensity__SD	LH__MaxContactMeanIntensity__Mean	FP__IntermediateToeSpread__(cm)__SD
RH__MeanIntensity__Mean	LH__MaxContactMeanIntensity__SD	FP__ManualPrintLength__(cm)__Mean
RH__MeanIntensity__SD	LH__PrintLength__(cm)__Mean	FP__ManualPrintLength__(cm)__SD
RH__MeanIntensityOfThe15MostIntensePixels__Mean	LH__PrintLength__(cm)__SD	FP__PawAngleBodyAxis__(°)__Mean
RH__MeanIntensityOfThe15MostIntensePixels__SD	LH__PrintWidth__(cm)__Mean	FP__PawAngleBodyAxis__(°)__SD
RH__ToeSpread__(cm)__Mean	LH__PrintWidth__(cm)__SD	FP__PawAngleMovementVector__(°)__Mean
RH__ToeSpread__(cm)__SD	LH__PrintArea__(cm²)__Mean	FP__PawAngleMovementVector__(°)__SD
RH__IntermediateToeSpread__(cm)__Mean	LH__PrintArea__(cm²)__SD	HP__MaxContactAt__(%)__Mean
RH__IntermediateToeSpread__(cm)__SD	LH__MaxIntensityAt__(%)__Mean	HP__MaxContactAt__(%)__SD
RH__ManualPrintLength__(cm)__Mean	LH__MaxIntensityAt__(%)__SD	HP__MaxContactArea__(cm²)__Mean
RH__ManualPrintLength__(cm)__SD	LH__MaxIntensity__Mean	HP__MaxContactArea__(cm²)__SD
RH__PawAngleBodyAxis__(°)__Mean	LH__MaxIntensity__SD	HP__MaxContactMaxIntensity__Mean
RH__PawAngleBodyAxis__(°)__SD	LH__MinIntensity__Mean	HP__MaxContactMaxIntensity__SD
RH__PawAngleMovementVector__(°)__Mean	LH__MinIntensity__SD	HP__MaxContactMeanIntensity__Mean
RH__PawAngleMovementVector__(°)__SD	LH__MeanIntensity__Mean	HP__MaxContactMeanIntensity__SD
LF__MaxContactAt__(%)__Mean	LH__MeanIntensity__SD	HP__PrintLength__(cm)__Mean
LF__MaxContactAt__(%)__SD	LH__MeanIntensityOfThe15MostIntensePixels__Mean	HP__PrintLength__(cm)__SD
LF__MaxContactArea__(cm²)__Mean	LH__MeanIntensityOfThe15MostIntensePixels__SD	HP__PrintWidth__(cm)__Mean
LF__MaxContactArea__(cm²)__SD	LH__ToeSpread__(cm)__Mean	HP__PrintWidth__(cm)__SD

Table A.3: continued to Table A.1

HP__PrintArea_(cm²)__Mean	PhaseDispersions_RF->RH_SD	Couplings_LF->LH_SD
HP__PrintArea_(cm²)__SD	PhaseDispersions_RF->RH_CStat_Mean	Couplings_LF->LH_CStat_Mean
HP__MaxIntensityAt_(%)__Mean	PhaseDispersions_RF->RH_CStat_SD	Couplings_LF->LH_CStat_SD
HP__MaxIntensityAt_(%)__SD	PhaseDispersions_RF->RH_CStat_R	Couplings_LF->LH_CStat_R
HP__MaxIntensity__Mean	PhaseDispersions_LF->LH_Mean	Couplings_RH->RF_Mean
HP__MaxIntensity__SD	PhaseDispersions_LF->LH_SD	Couplings_RH->RF_SD
HP__MinIntensity__Mean	PhaseDispersions_LF->LH_CStat_Mean	Couplings_RH->RF_CStat_Mean
HP__MinIntensity__SD	PhaseDispersions_LF->LH_CStat_SD	Couplings_RH->RF_CStat_SD
HP__MeanIntensity__Mean	PhaseDispersions_LF->LH_CStat_R	Couplings_RH->RF_CStat_R
HP__MeanIntensity__SD	Couplings_RF->LH_Mean	Couplings_LH->LF_Mean
HP__MeanIntensityOfThe15MostIntensePixels__Mean	Couplings_RF->LH_SD	Couplings_LH->LF_SD
HP__MeanIntensityOfThe15MostIntensePixels__SD	Couplings_RF->LH_CStat_Mean	Couplings_LH->LF_CStat_Mean
HP__ToeSpread_(cm)__Mean	Couplings_RF->LH_CStat_SD	Couplings_LH->LF_CStat_SD
HP__ToeSpread_(cm)__SD	Couplings_RF->LH_CStat_R	Couplings_LH->LF_CStat_R
HP__IntermediateToeSpread_(cm)__Mean	Couplings_LF->RH_Mean	Support__Zero_(%)
HP__IntermediateToeSpread_(cm)__SD	Couplings_LF->RH_SD	Support__Single_(%)
HP__ManualPrintLength_(cm)__Mean	Couplings_LF->RH_CStat_Mean	Support__Diagonal_(%)
HP__ManualPrintLength_(cm)__SD	Couplings_LF->RH_CStat_SD	Support__Girdle_(%)
HP__PawAngleBodyAxis_(°)__Mean	Couplings_LF->RH_CStat_R	Support__Lateral_(%)
HP__PawAngleBodyAxis_(°)__SD	Couplings_LH->RF_Mean	Support__Three_(%)
HP__PawAngleMovementVector_(°)__Mean	Couplings_LH->RF_SD	Support__Four_(%)
HP__PawAngleMovementVector_(°)__SD	Couplings_LH->RF_CStat_Mean	OtherStatistics_Sciatic_Functional_Index_Mean
PrintPositions_RightPaws_Mean_(cm)	Couplings_LH->RF_CStat_SD	OtherStatistics_Sciatic_Functional_Index_SD
PrintPositions_LeftPaws_Mean_(cm)	Couplings_LH->RF_CStat_R	OtherStatistics_Peroneal_Functional_Index_Mean
StepSequence_NumberOfPatterns	Couplings_RH->LF_Mean	OtherStatistics_Peroneal_Functional_Index_SD
StepSequence_CA_(%)	Couplings_RH->LF_SD	OtherStatistics_Posterior_Tibial_Functional_Index_Mean
StepSequence_CB_(%)	Couplings_RH->LF_CStat_Mean	OtherStatistics_Posterior_Tibial_Functional_Index_SD
StepSequence_AA_(%)	Couplings_RH->LF_CStat_SD	OtherStatistics_RM_(%)
StepSequence_AB_(%)	Couplings_RH->LF_CStat_R	OtherStatistics_RK_(%)
StepSequence_RA_(%)	Couplings_LH->RH_Mean	OtherStatistics_LM_(%)
StepSequence_RB_(%)	Couplings_LH->RH_SD	OtherStatistics_LK_(%)
StepSequence_RegularityIndex_(%)	Couplings_LH->RH_CStat_Mean	OtherStatistics_NO_(%)
OtherStatistics_NumberOfSteps	Couplings_LH->RH_CStat_SD	OtherStatistics_AB_(%)
OtherStatistics_Cadence	Couplings_LH->RH_CStat_R	OtherStatistics_TA_(%)
PhaseDispersions_RF->LH_Mean	Couplings_LF->RF_Mean	OtherStatistics_GT_(%)
PhaseDispersions_RF->LH_SD	Couplings_LF->RF_SD	Run_Duration_(s)_Mean
PhaseDispersions_RF->LH_CStat_Mean	Couplings_LF->RF_CStat_Mean	Run_Duration_(s)_SD
PhaseDispersions_RF->LH_CStat_SD	Couplings_LF->RF_CStat_SD	Run_Average_Speed_(cm/s)_Mean
PhaseDispersions_RF->LH_CStat_R	Couplings_LF->RF_CStat_R	Run_Average_Speed_(cm/s)_SD
PhaseDispersions_LF->RH_Mean	Couplings_RH->LH_Mean	Run_Maximum_Variation_(%)_Mean
PhaseDispersions_LF->RH_SD	Couplings_RH->LH_SD	Run_Maximum_Variation_(%)_SD
PhaseDispersions_LF->RH_CStat_Mean	Couplings_RH->LH_CStat_Mean	RF_StandIndex_Mean
PhaseDispersions_LF->RH_CStat_SD	Couplings_RH->LH_CStat_SD	RF_StandIndex_SD
PhaseDispersions_LF->RH_CStat_R	Couplings_RH->LH_CStat_R	RH_StandIndex_Mean
PhaseDispersions_LH->RH_Mean	Couplings_RF->LF_Mean	RH_StandIndex_SD
PhaseDispersions_LH->RH_SD	Couplings_RF->LF_SD	LF_StandIndex_Mean
PhaseDispersions_LH->RH_CStat_Mean	Couplings_RF->LF_CStat_Mean	LF_StandIndex_SD
PhaseDispersions_LH->RH_CStat_SD	Couplings_RF->LF_CStat_SD	LH_StandIndex_Mean
PhaseDispersions_LH->RH_CStat_R	Couplings_RF->LF_CStat_R	LH_StandIndex_SD
PhaseDispersions_LF->RF_Mean	Couplings_RF->RH_Mean	FP_StandIndex_Mean
PhaseDispersions_LF->RF_SD	Couplings_RF->RH_SD	FP_StandIndex_SD
PhaseDispersions_LF->RF_CStat_Mean	Couplings_RF->RH_CStat_Mean	HP_StandIndex_Mean
PhaseDispersions_LF->RF_CStat_SD	Couplings_RF->RH_CStat_SD	HP_StandIndex_SD
PhaseDispersions_LF->RF_CStat_R	Couplings_RF->RH_CStat_R	OtherStatistics_Duration_Mean
PhaseDispersions_RF->RH_Mean	Couplings_LF->LH_Mean	OtherStatistics_Duration_SD

References

[1] J. Paul Luzio, Paul R. Pryor, and Nicholas A. Bright. "Lysosomes: fusion and function". In: *Nature Reviews Molecular Cell Biology* 8.8 (2007), pp. 622–632.

[2] Stanley Ching-Cheng Huang et al. "Cell-Intrinsic Lysosomal Lipolysis Is Essential for Alternative Activation of Macrophages". In: *Nature Immunology* 15.9 (Sept. 2014), pp. 846–855. DOI: 10.1038/ni.2956. pmid: 25086775.

[3] Mireille Ouimet et al. "Autophagy Regulates Cholesterol Efflux from Macrophage Foam Cells via Lysosomal Acid Lipase". In: *Cell Metabolism* 13.6 (June 8, 2011), pp. 655–667. DOI: 10.1016/j.cmet.2011.03.023. pmid: 21641547.

[4] Sarah R. Hanson, Michael D. Best, and Chi-Huey Wong. "Sulfatases: Structure, Mechanism, Biological Activity, Inhibition, and Synthetic Utility". In: *Angewandte Chemie (International Ed. in English)* 43.43 (Nov. 5, 2004), pp. 5736–5763. DOI: 10.1002/anie.200300632. pmid: 15493058.

[5] M. Sardiello et al. "Sulfatases and Sulfatase Modifying Factors: An Exclusive and Promiscuous Relationship". In: *Human Molecular Genetics* 14.21 (Nov. 1, 2005), pp. 3203–3217. DOI: 10.1093/hmg/ddi351. pmid: 16174644.

[6] Yuuki Fujiwara, Keiji Wada, and Tomohiro Kabuta. "Lysosomal Degradation of Intracellular Nucleic Acids-Multiple Autophagic Pathways". In: *Journal of Biochemistry* 161.2 (Feb. 1, 2017), pp. 145–154. DOI: 10.1093/jb/mvw085. pmid: 28039390.

[7] Carmine Settembre et al. "Signals from the lysosome: a control centre for cellular clearance and energy metabolism". In: *Nature Reviews. Molecular Cell Biology* 14.5 (2013), pp. 283–296.

[8] Purvi C. Trivedi, Jordan J. Bartlett, and Thomas Pulinilkunnil. "Lysosomal Biology and Function: Modern View of Cellular Debris Bin". In: *Cells* 9.5 (May 4, 2020), E1131. DOI: 10.3390/cells9051131. pmid: 32375321.

[9] Michela Palmieri et al. "Characterization of the CLEAR network reveals an integrated control of cellular clearance pathways". In: *Human Molecular Genetics* 20.19 (2011), pp. 3852–3866.

[10] Diego L. Medina et al. "Lysosomal calcium signalling regulates autophagy through calcineurin and TFEB". In: *Nature Cell Biology* 17.3 (2015), pp. 288–299.

[11] Giancarlo Parenti, Generoso Andria, and Andrea Ballabio. "Lysosomal storage diseases: from pathophysiology to therapy". In: *Annual Review of Medicine* 66 (2015), pp. 471–486.

[12] Andrea Ballabio and Juan S. Bonifacino. "Lysosomes as dynamic regulators of cell and organismal homeostasis". In: *Nature Reviews Molecular Cell Biology* 21.2 (2020), pp. 101–118.

[13] D. Höglinger et al. "NPC1 regulates ER contacts with endocytic organelles to mediate cholesterol egress". In: *Nature Communications* 10.1 (2019), p. 4276.

[14] Yvette C. Wong et al. "Regulation and Function of Mitochondria–Lysosome Membrane Contact Sites in Cellular Homeostasis". In: *Trends in cell biology* 29.6 (2019), pp. 500–513.

[15] Agnès Chapel et al. "An extended proteome map of the lysosomal membrane reveals novel potential transporters". In: *Molecular & cellular proteomics: MCP* 12.6 (2013), pp. 1572–1588.

[16] Michael Schwake, Bernd Schröder, and Paul Saftig. "Lysosomal Membrane Proteins and Their Central Role in Physiology". In: *Traffic* 14.7 (2013), pp. 739–748.

[17] Haigang Ren and Guanghui Wang. "Autophagy and Lysosome Storage Disorders". In: Springer, 2020, pp. 87–102.

[18] Frances M. Platt, Barry Boland, and Aarnoud C. van der Spoel. "The cell biology of disease: lysosomal storage disorders: the cellular impact of lysosomal dysfunction". In: *The Journal of Cell Biology* 199.5 (2012), pp. 723–734.

[19] Peter G. Pentchev. "Niemann–Pick C research from mouse to gene". In: *Biochimica et Biophysica Acta (BBA) - Molecular and Cell Biology of Lipids* 1685.1 (2004), pp. 3–7.

[20] Marie T. Vanier. "Niemann-Pick diseases". In: *Handbook of Clinical Neurology* 113 (2013), pp. 1717–1721.

[21] R. O. Brady et al. "The metabolism of sphingomyelin. II. Evidence of an enzymatic deficiency in Niemann-Pick diseae". In: *Proceedings of the National Academy of Sciences of the United States of America* 55.2 (1966), pp. 366–369.

[22] Mark L. Schultz, Kelsey L. Krus, and Andrew P. Lieberman. "Lysosome and endoplasmic reticulum quality control pathways in Niemann-Pick type C disease". In: *Brain research* 1649.Pt B (2016), pp. 181–188.

[23] George A. Diaz et al. "One-Year Results of a Clinical Trial of Olipudase Alfa Enzyme Replacement Therapy in Pediatric Patients with Acid Sphingomyelinase Deficiency". In: *Genetics in Medicine* 23.8 (Aug. 2021), pp. 1543–1550. DOI: 10.1038/s41436-021-01156-3. URL: https://linkinghub.elsevier.com/retrieve/pii/S1098360021050620 (visited on 11/03/2022).

[24] *Olipudase Alfa - Sanofi - AdisInsight*. URL: https://adisinsight.springer.com/drugs/800011964 (visited on 11/03/2022).

[25] Marc Patterson. "Niemann-Pick Disease Type C". In: 1993. URL: http://www.ncbi.nlm.nih.gov/books/NBK1296/.

[26] Marie T. Vanier. "Niemann-Pick disease type C". In: *Orphanet Journal of Rare Diseases* 5 (2010), p. 16.

[27] Judith Storch and Zhi Xu. "Niemann-Pick C2 (NPC2) and Intracellular Cholesterol Trafficking". In: *Biochimica Et Biophysica Acta* 1791.7 (July 2009), pp. 671–678. DOI: 10.1016/j.bbalip.2009.02.001. pmid: 19232397.

[28] Emyr Lloyd-Evans and Frances M. Platt. "Lipids on Trial: The Search for the Offending Metabolite in Niemann-Pick Type C Disease". In: *Traffic* 11.4 (Mar. 10, 2010), pp. 419–428. (Visited on 11/03/2022).

[29] Rodney E. Infante et al. "Purified NPC1 Protein. I. Binding of Cholesterol and Oxysterols to a 1278-Amino Acid Membrane Protein". In: *The Journal of Biological Chemistry* 283.2 (Jan. 11, 2008), pp. 1052–1063. DOI: 10.1074/jbc.M707943200. pmid: 17989073.

[30] Frances M. Platt. "Sphingolipid lysosomal storage disorders". In: *Nature* 510.7503 (2014), pp. 68–75.

[31] Simon Wheeler and Dan J. Sillence. "Niemann–Pick type C disease: cellular pathology and pharmacotherapy". In: *Journal of Neurochemistry* 153.6 (2020), pp. 674–692.

[32] Marie T. Vanier. "Complex lipid trafficking in Niemann-Pick disease type C". In: *Journal of Inherited Metabolic Disease* 38.1 (2015), pp. 187–199.

[33] Ettore Salsano et al. "Vertical supranuclear gaze palsy in Niemann-Pick type C disease". In: *Neurological Sciences: Official Journal of the Italian Neurological Society and of the Italian Society of Clinical Neurophysiology* 33.6 (2012), pp. 1225–1232.

[34] Dominika Sitarska and Agnieszka Ługowska. "Laboratory diagnosis of the Niemann-Pick type C disease: an inherited neurodegenerative disorder of cholesterol metabolism". In: *Metabolic Brain Disease* 34.5 (2019), pp. 1253–1260.

[35] Olivier Bonnot et al. "Psychiatric and neurological symptoms in patients with Niemann-Pick disease type C (NP-C): Findings from the International NPC Registry". In: *The World Journal of Biological Psychiatry: The Official Journal of the World Federation of Societies of Biological Psychiatry* 20.4 (2019), pp. 310–319.

[36] I. A. Auer et al. "Paired Helical Filament Tau (PHFtau) in Niemann-Pick Type C Disease Is Similar to PHFtau in Alzheimer's Disease". In: *Acta Neuropathologica* 90.6 (1995), pp. 547–551. DOI: 10.1007/BF00318566. pmid: 8615074.

[37] Valentina Pallottini and Frank W. Pfrieger. "Understanding and Treating Niemann–Pick Type C Disease: Models Matter". In: *International Journal of Molecular Sciences* 21.23 (Nov. 26, 2020), p. 8979. DOI: 10.3390/ijms21238979. URL: https://www.mdpi.com/1422-0067/21/23/8979 (visited on 10/28/2022).

[38] Maximilian J. Feldman, Brenton C. Poirier, and B. Markus Lange. "Misexpression of the Niemann-Pick Disease Type C1 (NPC1)-like Protein in Arabidopsis Causes Sphingolipid Accumulation and Reproductive Defects". In: *Planta* 242.4 (Oct. 2015), pp. 921–933. DOI: 10.1007/s00425-015-2322-4. pmid: 26007685.

[39] Krishnamurthy Malathi et al. "Mutagenesis of the Putative Sterol-Sensing Domain of Yeast Niemann Pick C-related Protein Reveals a Primordial Role in Subcellular Sphingolipid Distribution". In: *The Journal of Cell Biology* 164.4 (Feb. 16, 2004), pp. 547–556. DOI: 10.1083/jcb.200310046. pmid: 14970192.

[40] Gert de Voer, Dorien Peters, and Peter E. M. Taschner. "Caenorhabditis Elegans as a Model for Lysosomal Storage Disorders". In: *Biochimica et Biophysica Acta (BBA) - Molecular Basis of Disease* 1782.7 (July 1, 2008), pp. 433–446. DOI: 10.1016/j.bbadis.2008.04.003. URL: https://www.sciencedirect.com/science/article/pii/S0925443908000938 (visited on 11/03/2022).

[41] E. Thomas Danielsen et al. "A Drosophila Genome-Wide Screen Identifies Regulators of Steroid Hormone Production and Developmental Timing". In: *Developmental Cell* 37.6 (June 20, 2016), pp. 558–570. DOI: 10.1016/j.devcel.2016.05.015. pmid: 27326933.

[42] Sophie Louwette et al. "NPC1 Defect Results in Abnormal Platelet Formation and Function: Studies in Niemann-Pick Disease Type C1 Patients and Zebrafish". In: *Human Molecular Genetics* 22.1 (Jan. 1, 2013), pp. 61–73. DOI: 10.1093/hmg/dds401. pmid: 23010472.

[43] Tyler Schwend et al. "Requirement of Npc1 and Availability of Cholesterol for Early Embryonic Cell Movements in Zebrafish[S]". In: *Journal of Lipid Research* 52.7 (July 1, 2011), pp. 1328–1344. DOI: 10.1194/jlr.M012377. URL: https://www.sciencedirect.com/science/article/pii/S0022227520370279 (visited on 11/03/2022).

[44] Cathrine K. Fog and Thomas Kirkegaard. "Animal models for Niemann-Pick type C: implications for drug discovery & development". In: *Expert Opinion on Drug Discovery* 14.5 (2019), pp. 499–509.

[45] Charles H. Vite et al. "Clinical, Electrophysiological, and Serum Biochemical Measures of Progressive Neurological and Hepatic Dysfunction in Feline Niemann-Pick Type C Disease". In: *Pediatric Research* 64.5 (Nov. 2008), pp. 544–549. DOI: 10.1203/PDR.0b013e318184d2ce. pmid: 18614965.

[46] M. Kuwamura et al. "Type C Niemann-Pick Disease in a Boxer Dog". In: *Acta Neuropathologica* 85.3 (1993), pp. 345–348. DOI: 10.1007/BF00227733. pmid: 8460536.

[47] Shernae A. Woolley et al. "Molecular Basis for a New Bovine Model of Niemann-Pick Type C Disease". In: *PloS One* 15.9 (2020), e0238697. DOI: 10.1371/journal.pone.0238697. pmid: 32970694.

[48] Yee Ting Lee et al. "Mouse Models of Atherosclerosis: A Historical Perspective and Recent Advances". In: *Lipids in Health and Disease* 16 (Jan. 17, 2017), p. 12. DOI: 10.1186/s12944-016-0402-5. pmid: 28095860. URL: https://www.ncbi.nlm.nih.gov/pmc/articles/PMC5240327/ (visited on 11/03/2022).

[49] S. K. Loftus et al. "Murine Model of Niemann-Pick C Disease: Mutation in a Cholesterol Homeostasis Gene". In: *Science (New York, N.Y.)* 277.5323 (July 11, 1997), pp. 232–235.

[50] P. G. Pentchev et al. "A lysosomal storage disorder in mice characterized by a dual deficiency of sphingomyelinase and glucocerebrosidase". eng. In: *Biochimica Et Biophysica Acta* 619.3 (Sept. 1980), pp. 669–679. DOI: 10.1016/0005-2760(80)90116-2.

[51] S. Miyawaki et al. "Sphingomyelinosis, a New Mutation in the Mouse: A Model of Niemann-Pick Disease in Humans". In: *Journal of Heredity* 73.4 (June 26, 1982), pp. 257–263. URL: https://eurekamag.com/research/044/377/044377882.php (visited on 11/03/2022).

[52] Xuefen Xie et al. "Amino acid substitution in NPC1 that abolishes cholesterol binding reproduces phenotype of complete NPC1 deficiency in mice". In: *Proceedings of the National Academy of Sciences* 108.37 (2011), pp. 15330–15335.

[53] Walter D. Park et al. "Identification of 58 Novel Mutations in Niemann-Pick Disease Type C: Correlation with Biochemical Phenotype and Importance of PTC1-like Domains in NPC1". In: *Human Mutation* 22.4 (2003), pp. 313–325. (Visited on 11/03/2022).

[54] Marta Gómez-Grau et al. "New murine Niemann-Pick type C models bearing a pseudoexon-generating mutation recapitulate the main neurobehavioural and molecular features of the disease". In: *Scientific Reports* 7.1 (2017), p. 41931.

[55] Jorge L. Rodriguez-Gil et al. "Genetic Background Modifies Phenotypic Severity and Longevity in a Mouse Model of Niemann-Pick Disease Type C1". In: *Disease Models & Mechanisms* (Jan. 1, 2020), p. dmm.042614. DOI: 10.1242/dmm.042614. URL: https://journals.biologists.com/dmm/article/doi/10.1242/dmm.042614/267160/Genetic-background-modifies-phenotypic-severity (visited on 11/03/2022).

[56] Matthew J. Elrick et al. "Conditional Niemann-Pick C Mice Demonstrate Cell Autonomous Purkinje Cell Neurodegeneration". In: *Human Molecular Genetics* 19.5 (Mar. 1, 2010), pp. 837–847. DOI: 10.1093/hmg/ddp552. URL: https://academic.oup.com/hmg/article-lookup/doi/10.1093/hmg/ddp552 (visited on 11/02/2022).

[57] Ting Yu et al. "Temporal and Cell-Specific Deletion Establishes That Neuronal Npc1 Deficiency Is Sufficient to Mediate Neurodegeneration". In: *Human Molecular Genetics* 20.22 (Nov. 15, 2011), pp. 4440–4451. DOI: 10.1093/hmg/ddr372. URL: https://academic.oup.com/hmg/article-lookup/doi/10.1093/hmg/ddr372 (visited on 11/03/2022).

[58] Ting Yu and Andrew P. Lieberman. "Npc1 Acting in Neurons and Glia Is Essential for the Formation and Maintenance of CNS Myelin". In: *PLoS Genetics* 9.4 (Apr. 11, 2013). Ed. by Kasturi Haldar, e1003462. DOI: 10.1371/journal.pgen.1003462. URL: https://dx.plos.org/10.1371/journal.pgen.1003462 (visited on 11/03/2022).

[59] PETER G. Pentchev et al. "Immunological and Catalytic Quantitation of Splenic Glucocerebrosidase from the Three Clinical Forms of Gaucher Disease." In: *American journal of human genetics* 35.4 (1983), p. 621.

[60] P. G. Pentchev et al. "The Cholesterol Storage Disorder of the Mutant BALB/c Mouse. A Primary Genetic Lesion Closely Linked to Defective Esterification of Exogenously Derived Cholesterol and Its Relationship to Human Type C Niemann-Pick Disease." In: *Journal of Biological Chemistry* 261.6 (1986), pp. 2772–2777.

[61] Robert A. Maue et al. “A novel mouse model of Niemann-Pick type C disease carrying a D1005G-Npc1 mutation comparable to commonly observed human mutations”. In: *Human Molecular Genetics* 21.4 (2012), pp. 730–750.

[62] David Smith et al. “Beneficial Effects of Anti-Inflammatory Therapy in a Mouse Model of Niemann-Pick Disease Type C1”. In: *Neurobiology of Disease* 36.2 (Nov. 2009), pp. 242–251. pmid: 19632328.

[63] Mark E. Gelsthorpe et al. “Niemann-Pick type C1 I1061T mutant encodes a functional protein that is selected for endoplasmic reticulum-associated degradation due to protein misfolding”. In: *The Journal of Biological Chemistry* 283.13 (2008), pp. 8229–8236.

[64] Naoe Nakasone et al. “Endoplasmic reticulum-associated degradation of Niemann-Pick C1: evidence for the role of heat shock proteins and identification of lysine residues that accept ubiquitin”. In: *The Journal of Biological Chemistry* 289.28 (2014), pp. 19714–19725.

[65] Andrew B. Munkacsi et al. “Normalization of Hepatic Homeostasis in the Npc1nmf164 Mouse Model of Niemann-Pick Type C Disease Treated with the Histone Deacetylase Inhibitor Vorinostat”. In: *The Journal of Biological Chemistry* 292.11 (2017), pp. 4395–4410.

[66] EMA. *EU/3/06/351*. European Medicines Agency. Sept. 17, 2018. URL: https://www.ema.europa.eu/en/medicines/human/orphan-designations/eu306351 (visited on 11/03/2022).

[67] Mercè Pineda, Mark Walterfang, and Marc C. Patterson. “Miglustat in Niemann-Pick Disease Type C Patients: A Review”. In: *Orphanet Journal of Rare Diseases* 13 (Aug. 15, 2018), p. 140. pmid: 30111334.

[68] F. M. Platt et al. “N-Butyldeoxynojirimycin Is a Novel Inhibitor of Glycolipid Biosynthesis”. In: *The Journal of Biological Chemistry* 269.11 (Mar. 18, 1994), pp. 8362–8365. pmid: 8132559.

[69] A. Treiber, O. Morand, and M. Clozel. “The Pharmacokinetics and Tissue Distribution of the Glucosylceramide Synthase Inhibitor Miglustat in the Rat”. In: *Xenobiotica* 37.3 (Mar. 1, 2007), pp. 298–314. pmid: 17624027.

[70] G. D’Arcangelo et al. “Miglustat Reverts the Impairment of Synaptic Plasticity in a Mouse Model of NPC Disease”. In: *Neural Plasticity* 2016 (2016), p. 3830424.

[71] Mylvaganam Jeyakumar et al. “Storage Solutions: Treating Lysosomal Disorders of the Brain”. In: *Nature Reviews. Neuroscience* 6.9 (Sept. 2005), pp. 713–725.

[72] M. Zervas et al. “Critical role for glycosphingolipids in Niemann-Pick disease type C”. In: *Current biology: CB* 11.16 (2001), pp. 1283–1287.

[73] Katherine A. Lyseng-Williamson. “Miglustat: A Review of Its Use in Niemann-Pick Disease Type C”. In: *Drugs* 74.1 (Jan. 2014), pp. 61–74. (Visited on 11/02/2022).

[74] Marc C. Patterson et al. “Treatment outcomes following continuous miglustat therapy in patients with Niemann-Pick disease Type C: a final report of the NPC Registry”. In: *Orphanet Journal of Rare Diseases* 15.1 (2020), p. 104.

[75] Tatiana Remenova et al. “A double-blind, randomized, placebo-controlled trial studying the effects of Saccharomyces boulardii on the gastrointestinal tolerability, safety, and pharmacokinetics of miglustat”. In: *Orphanet Journal of Rare Diseases* 10.1 (2015), p. 81.

[76] Ulrika Andersson et al. “N-Butyldeoxygalactonojirimycin: A More Selective Inhibitor of Glycosphingolipid Biosynthesis than N-butyldeoxynojirimycin, in Vitro and in Vivo”. In: *Biochemical Pharmacology* 59.7 (Apr. 1, 2000), pp. 821–829. (Visited on 11/03/2022).

[77] Pierre Déchelotte. “Type 1 Gaucher’s disease in the adult. Nutritional management during initiation of treatment with miglustat”. In: *Presse medicale (Paris, France* 33.7 (Apr. 1, 2004), pp. 494–496. pmid: 15105774.

[78] Nadia Belmatoug et al. “Gastrointestinal Disturbances and Their Management in Miglustat-Treated Patients”. In: *Journal of Inherited Metabolic Disease* 34.5 (Oct. 2011), pp. 991–1001. pmid: 21779792.

[79] McCormack Paul L and Karen L Goa. *Miglustat | SpringerLink*. 2003. URL: https://link.springer.com/article/10.2165/00003495-200363220-00006#citeas (visited on 11/02/2022).

[80] Merit E. Cudkowicz et al. “Arimoclomol at Dosages up to 300 Mg/Day Is Well Tolerated and Safe in Amyotrophic Lateral Sclerosis”. In: *Muscle & Nerve: Official Journal of the American Association of Electrodiagnostic Medicine* 38.1 (2008), pp. 837–844.

[81] Cathrine K. Fog et al. “The Heat Shock Protein Amplifier Arimoclomol Improves Refolding, Maturation and Lysosomal Activity of Glucocerebrosidase”. In: *eBioMedicine* 38 (Dec. 1, 2018), pp. 142–153. (Visited on 11/01/2022).

[82] Linda Ingemann and Thomas Kirkegaard. “Lysosomal Storage Diseases and the Heat Shock Response: Convergences and Therapeutic Opportunities”. In: *Journal of Lipid Research* 55.11 (Nov. 2014), pp. 2198–2210. pmid: 24837749.

[83] Thomas Kirkegaard et al. “Heat Shock Protein-Based Therapy as a Potential Candidate for Treating the Sphingolipidoses”. In: *Science Translational Medicine* 8.355 (Sept. 7, 2016), 355ra118. pmid: 27605553.

[84] Thomas Kirkegaard et al. “Hsp70 Stabilizes Lysosomes and Reverts Niemann-Pick Disease-Associated Lysosomal Pathology”. In: *Nature* 463.7280 (Jan. 28, 2010), pp. 549–553. pmid: 20111001.

[85] Rocio Gomez-Pastor, Eileen T. Burchfiel, and Dennis J. Thiele. “Regulation of Heat Shock Transcription Factors and Their Roles in Physiology and Disease”. In: *Nature Reviews Molecular Cell Biology* 19.1 (1 Jan. 2018), pp. 4–19. (Visited on 11/03/2022).

[86] Peizhen Song et al. “Individual bile acids have differential effects on bile acid signaling in mice”. In: *Toxicology and Applied Pharmacology* 283.1 (2015), pp. 57–64.

[87] Eugene D. Carstea et al. “Niemann-Pick C1 Disease Gene: Homology to Mediators of Cholesterol Homeostasis”. In: *Science* 277.5323 (1997), pp. 228–231.

[88] Nina H. Pipalia et al. "Histone Deacetylase Inhibitors Correct the Cholesterol Storage Defect in Most Niemann-Pick C1 Mutant Cells". In: *Journal of Lipid Research* 58.4 (Apr. 1, 2017), pp. 695–708. pmid: 28193631. (Visited on 11/03/2022).

[89] Andrea Dardis et al. "Molecular Genetics of Niemann–Pick Type C Disease in Italy: An Update on 105 Patients and Description of 18 NPC1 Novel Variants". In: *Journal of Clinical Medicine* 9.3 (3 Mar. 2020), p. 679. DOI: 10.3390/jcm9030679. URL: https://www.mdpi.com/2077-0383/9/3/679 (visited on 11/03/2022).

[90] H. Runz. "Niemann-Pick Type C Disease Gene Variation Database". In: *Schneider, AR, Stichling, F., Hoffmann, M., Scheler, R., Arnold, JC, &* (2009).

[91] Mhoriam Ahmed et al. *Amplifying the Heat Shock Response Ameliorates Pathology in Mouse and Human Models of ALS and FTD.* preprint. In Review, Jan. 29, 2021. DOI: 10.21203/rs.3.rs-152813/v1. URL: https://www.researchsquare.com/article/rs-152813/v1 (visited on 11/03/2022).

[92] Mhoriam Ahmed et al. "Targeting Protein Homeostasis in Sporadic Inclusion Body Myositis". In: *Science Translational Medicine* 8.331 (Mar. 23, 2016), 331ra41–331ra41. DOI: 10.1126/scitranslmed.aad4583. URL: https://www.science.org/doi/abs/10.1126/scitranslmed.aad4583 (visited on 11/03/2022).

[93] Eugen Mengel et al. "Efficacy and Safety of Arimoclomol in Niemann-Pick Disease Type C: Results from a Double-Blind, Randomised, Placebo-Controlled, Multinational Phase 2/3 Trial of a Novel Treatment". In: *Journal of Inherited Metabolic Disease* 44.6 (Nov. 2021), pp. 1463–1480. DOI: 10.1002/jimd.12428. pmid: 34418116.

[94] Marc C. Patterson et al. "Validation of the 5-Domain Niemann-Pick Type C Clinical Severity Scale". In: *Orphanet Journal of Rare Diseases* 16.1 (Dec. 2021), p. 79. DOI: 10.1186/s13023-021-01719-2. URL: https://ojrd.biomedcentral.com/articles/10.1186/s13023-021-01719-2 (visited on 11/03/2022).

[95] Nicolas Vibert and Pierre-Paul Vidal. "*In Vitro* Effects of Acetyl- DL -Leucine (Tanganil®) on Central Vestibular Neurons and Vestibulo-Ocular Networks of the Guinea-Pig: Effects of Isoleucine on Vestibulo-Ocular Networks". In: *European Journal of Neuroscience* 13.4 (Feb. 2001), pp. 735–748. DOI: 10.1046/j.0953-816x.2000.01447.x. URL: http://doi.wiley.com/10.1046/j.0953-816x.2000.01447.x (visited on 11/03/2022).

[96] Tatiana Bremova et al. "Acetyl-dl-leucine in Niemann-Pick type C: A case series". In: *Neurology* 85.16 (2015), pp. 1368–1375.

[97] Mario Cortina-Borja et al. "Annual severity increment score as a tool for stratifying patients with Niemann-Pick disease type C and for recruitment to clinical trials". In: *Orphanet Journal of Rare Diseases* 13 (2018), p. 143.

[98] Ecem Kaya et al. "Acetyl-leucine slows disease progression in lysosomal storage disorders". In: *Brain Communications* 3.1 (2021), fcaa148.

[99] Lisa Günther et al. "N-Acetyl-L-leucine Accelerates Vestibular Compensation after Unilateral Labyrinthectomy by Action in the Cerebellum and Thalamus". In: *PloS One* 10.3 (2015), e0120891.

[100] Tatiana Bremova-Ertl et al. "Efficacy and safety of N-acetyl-l-leucine in Niemann–Pick disease type C". In: *Journal of Neurology* 269.3 (2022), pp. 1651–1662.

[101] Justyna R. Sarna et al. "Patterned Purkinje Cell Degeneration in Mouse Models of Niemann-Pick Type C Disease". In: *The Journal of Comparative Neurology* 456.3 (Feb. 10, 2003), pp. 279–291. DOI: 10.1002/cne.10522. URL: https://onlinelibrary.wiley.com/doi/10.1002/cne.10522 (visited on 11/02/2022).

[102] A. Bozkurt et al. "CatWalk gait analysis in assessment of functional recovery after sciatic nerve injury". In: *Journal of Neuroscience Methods* 173.1 (2008), pp. 91–98.

[103] Gheorghita Isvoranu, Emilia Manole, and Monica Neagu. "Gait Analysis Using Animal Models of Peripheral Nerve and Spinal Cord Injuries". In: *Biomedicines* 9.8 (2021), p. 1050.

[104] Xiao Hong Wang et al. "Quantitative assessment of gait and neurochemical correlation in a classical murine model of Parkinson's disease". In: *BMC neuroscience* 13 (2012), p. 142.

[105] João Casaca-Carreira et al. "Coexistence of Gait Disturbances and Chorea in Experimental Huntington's Disease". In: *Behavioural Neurology* 2015 (2015), p. 970204.

[106] E. Caballero-Garrido et al. "Characterization of long-term gait deficits in mouse dMCAO, using the CatWalk system". In: *Behavioural Brain Research* 331 (2017), pp. 282–296.

[107] Mei Chen et al. "Study of the association between gait variability and gene expressions in a mouse model of transient focal ischemic stroke". In: *International Journal of Neuroscience* 130.1 (2020), pp. 52–63.

[108] R. W. Sperry. "Cerebral regulation of motor coordination in monkeys following multiple transection of sensorimotor cortex". In: *Journal of Neurophysiology* 10.4 (1947), pp. 275–294.

[109] L. de Medinaceli, W. J. Freed, and R. J. Wyatt. "An index of the functional condition of rat sciatic nerve based on measurements made from walking tracks". In: *Experimental Neurology* 77.3 (1982), pp. 634–643.

[110] D. M. Basso, M. S. Beattie, and J. C. Bresnahan. "A sensitive and reliable locomotor rating scale for open field testing in rats". In: *Journal of Neurotrauma* 12.1 (1995), pp. 1–21.

[111] F. P. Hamers et al. "Automated quantitative gait analysis during overground locomotion in the rat: its application to spinal cord contusion and transection injuries". In: *Journal of Neurotrauma* 18.2 (2001), pp. 187–201.

[112] Frank Hamers, Guido Koopmans, and Elbert Joosten. "CatWalk-Assisted Gait Analysis in the Assessment of Spinal Cord Injury". In: *Journal of Neurotrauma* 23 (2006).

[113] Halil Kara et al. "Comparison of a manual walking platform and the CatWalk gait analysis system in a rat osteoarthritis model". In: *Advances in Clinical and Experimental Medicine: Official Organ Wroclaw Medical University* 30.9 (2021), pp. 949–956.

[114] Ivanna K. Timotius et al. "Systematic data analysis and data mining in CatWalk gait analysis by heat mapping exemplified in rodent models for neurodegenerative diseases". In: *Journal of Neuroscience Methods* 326 (2019), p. 108367.

[115] Elisabeth A. Kappos et al. "Validity and reliability of the CatWalk system as a static and dynamic gait analysis tool for the assessment of functional nerve recovery in small animal models". In: *Brain and Behavior* 7.7 (2017), e00723.

[116] Elisavet I. Kyriakou et al. "Automated quantitative analysis to assess motor function in different rat models of impaired coordination and ataxia". In: *Journal of Neuroscience Methods* 268 (2016), pp. 171–181.

[117] Samuel T. Crowley, Kazunori Kataoka, and Keiji Itaka. "Combined CatWalk Index: an improved method to measure mouse motor function using the automated gait analysis system". In: *BMC research notes* 11.1 (2018), p. 263.

[118] Annemarie Zimprich et al. "Analysis of locomotor behavior in the German Mouse Clinic". In: *Journal of Neuroscience Methods* 300 (2018), pp. 77–91.

[119] Marianne Huebner, Werner Vach, and Saskia le Cessie. "A systematic approach to initial data analysis is good research practice". In: *The Journal of Thoracic and Cardiovascular Surgery* 151.1 (2016), pp. 25–27.

[120] Willians Fernando Vieira et al. "Gait analysis correlates mechanical hyperalgesia in a model of streptozotocin-induced diabetic neuropathy: A CatWalk dynamic motor function study". In: *Neuroscience Letters* 736 (2020), p. 135253.

[121] David Smith et al. "Beneficial effects of anti-inflammatory therapy in a mouse model of Niemann-Pick disease type C1". In: *Neurobiology of Disease* 36.2 (2009), pp. 242–251.

[122] N. Shen and J. Zhu. "Application of Sciatic Functional Index in Nerve Functional Assessment". In: *Microsurgery* 16.8 (1995), pp. 552–555. DOI: 10.1002/micr.1920160809. pmid: 8538433.

[123] RStudio Team. *RStudio : Integrated Development for R.RStudio, PBC, Boston, MA*. 2020.

[124] Ulrik Lyngs. *oxforddown: An Oxford University Thesis Template for R Markdown*. https://github.com/ulyngs/oxforddown. 2019. DOI: 10.5281/zenodo.3484682.

[125] Kyle B. Martin et al. "Identification of Novel Pathways Associated with Patterned Cerebellar Purkinje Neuron Degeneration in Niemann-Pick Disease, Type C1". In: *International Journal of Molecular Sciences* 21.1 (Dec. 31, 2019), p. 292. DOI: 10.3390/ijms21010292. URL: https://www.mdpi.com/1422-0067/21/1/292.

[126] Ian M. Williams et al. "Improved neuroprotection using miglustat, curcumin and ibuprofen as a triple combination therapy in Niemann-Pick disease type C1 mice". In: *Neurobiology of Disease* 67 (2014), pp. 9–17.

[127] Eriola Hoxha et al. "Purkinje Cell Signaling Deficits in Animal Models of Ataxia". In: *Frontiers in Synaptic Neuroscience* 10 (Apr. 26, 2018), p. 6. DOI: 10.3389/fnsyn.2018.00006. pmid: 29760657. URL: https://www.ncbi.nlm.nih.gov/pmc/articles/PMC5937225/.

[128] Johannes Heinzel et al. "Use of the CatWalk gait analysis system to assess functional recovery in rodent models of peripheral nerve injury – a systematic review". In: *Journal of Neuroscience Methods* 345 (2020), p. 108889.

[129] Huanwen Chen et al. "Establishing a reliable gait evaluation method for rodent studies". In: *Journal of Neuroscience Methods* 283 (2017), pp. 92–100.

[130] S. K. Loftus et al. "Murine model of Niemann-Pick C disease: mutation in a cholesterol homeostasis gene". In: *Science (New York, N.Y.)* 277.5323 (1997), pp. 232–235.

[131] Juan F. Calderón and Andrés D. Klein. "Controversies on the Potential Therapeutic Use of Rapamycin for Treating a Lysosomal Cholesterol Storage Disease". In: *Molecular Genetics and Metabolism Reports* 15 (May 12, 2018), pp. 135–136. DOI: 10.1016/j.ymgmr.2018.05.001. pmid: 30023307. URL: https://www.ncbi.nlm.nih.gov/pmc/articles/PMC6047216/ (visited on 11/04/2022).

[132] F. M. Platt et al. "N-butyldeoxygalactonojirimycin inhibits glycolipid biosynthesis but does not affect N-linked oligosaccharide processing". In: *The Journal of Biological Chemistry* 269.43 (1994), pp. 27108–27114.

[133] Marc C. Patterson et al. "Long-term miglustat therapy in children with Niemann-Pick disease type C". eng. In: *Journal of Child Neurology* 25.3 (Mar. 2010), pp. 300–305. DOI: 10.1177/0883073809344222.

[134] M. Pineda et al. "Miglustat in patients with Niemann-Pick disease Type C (NP-C): a multicenter observational retrospective cohort study". eng. In: *Molecular Genetics and Metabolism* 98.3 (Nov. 2009), pp. 243–249. DOI: 10.1016/j.ymgme.2009.07.003.

[135] James E. Wraith et al. "Miglustat in adult and juvenile patients with Niemann-Pick disease type C: long-term data from a clinical trial". eng. In: *Molecular Genetics and Metabolism* 99.4 (Apr. 2010), pp. 351–357. DOI: 10.1016/j.ymgme.2009.12.006.

[136] Thomas Kirkegaard et al. "Heat shock protein-based therapy as a potential candidate for treating the sphingolipidoses". In: *Science Translational Medicine* 8.355 (2016), 355ra118.

[137] Eugen Mengel et al. "Efficacy and safety of arimoclomol in Niemann-Pick disease type C: Results from a double-blind, randomised, placebo-controlled, multinational phase 2/3 trial of a novel treatment". In: *Journal of Inherited Metabolic Disease* 44.6 (2021), pp. 1463–1480.

[138] Mark Zervas et al. "Critical Role for Glycosphingolipids in Niemann-Pick Disease Type C". In: *Current Biology* 11.16 (Aug. 21, 2001), pp. 1283–1287. URL: https://www.cell.com/current-biology/abstract/S0960-9822(01)00396-7 (visited on 10/11/2022).

[139] Dominika Sitarska, Anna Tylki-Szymańska, and Agnieszka Ługowska. "Treatment Trials in Niemann-Pick Type C Disease". In: *Metabolic Brain Disease* 36.8 (Dec. 2021), pp. 2215–2221. DOI: 10.1007/s11011-021-00842-0.

[140] Roman Schniepp et al. "Acetyl-DL-leucine improves gait variability in patients with cerebellar ataxia-a case series". In: *Cerebellum & Ataxias* 3 (2016), p. 8.

[141] Michael Strupp et al. "Effects of acetyl-DL-leucine in patients with cerebellar ataxia: a case series". In: *Journal of Neurology* 260.10 (2013), pp. 2556–2561.

[142] Marc C. Patterson et al. "Long-term Survival Outcomes of Patients with Niemann-Pick Disease Type C Receiving Miglustat Treatment: A Large Retrospective Observational Study". In: *Journal of Inherited Metabolic Disease* 43.5 (Sept. 2020), pp. 1060–1069.

[143] Grant C. Churchill et al. "Acetylation turns leucine into a drug by membrane transporter switching". In: *Scientific Reports* 11 (2021), p. 15812.

[144] Tanmay Nath et al. "Using DeepLabCut for 3D markerless pose estimation across species and behaviors". In: *Nature Protocols* 14.7 (2019), pp. 2152–2176.

[145] Alexander Mathis et al. "DeepLabCut: markerless pose estimation of user-defined body parts with deep learning". In: *Nature Neuroscience* 21.9 (2018), pp. 1281–1289.

[146] Marwick Ben. *Testing Coefficients of Variation from Multiple Samples*. Jan. 7, 2019. URL: https://cran.r-project.org/web/packages/cvequality/vignettes/how_to_test_CVs.html (visited on 11/20/2022).

[147] *CatWalk XT Version 10.6 Reference Manual*. 2015.